NAVAL POSTGRADUATE SCHOOL
Monterey, California

THESIS

SENSITIVITY OF THE STEADY-STATE
KALMAN FILTERS TO STABILITY DERIVATIVES
VARIATIONS IN AN INERTIAL NAVIGATION SYSTEM

by

Jose Augusto Matallana R.

September 1980

Thesis Advisor: Daniel J. Collins

Approved for public release; distribution unlimited

REPORT DOCUMENTATION PAGE		READ INSTRUCTIONS BEFORE COMPLETING FORM
1. REPORT NUMBER	2. GOVT ACCESSION NO. AD-A096 393	3. RECIPIENT'S CATALOG NUMBER
4. TITLE (and Subtitle) Sensitivity of the Steady-State Kalman Filters to Stability Derivatives Variations in an Inertial Navigation System.		5. TYPE OF REPORT & PERIOD COVERED Master's Thesis; September 1980
		6. PERFORMING ORG. REPORT NUMBER
7. AUTHOR(s) Jose Augusto Matallana R.		8. CONTRACT OR GRANT NUMBER(s)
9. PERFORMING ORGANIZATION NAME AND ADDRESS Naval Postgraduate School Monterey, California 93940		10. PROGRAM ELEMENT, PROJECT, TASK AREA & WORK UNIT NUMBERS
11. CONTROLLING OFFICE NAME AND ADDRESS Naval Postgraduate School Monterey, California 93940		12. REPORT DATE September 1980
		13. NUMBER OF PAGES 102
14. MONITORING AGENCY NAME & ADDRESS(if different from Controlling Office) Naval Postgraduate School Monterey, California 93940		15. SECURITY CLASS. (of this report) Unclassified
		15a. DECLASSIFICATION/DOWNGRADING SCHEDULE

16. DISTRIBUTION STATEMENT (of this Report)

Approved for public release; distribution unlimited

17. DISTRIBUTION STATEMENT (of the abstract entered in Block 20, if different from Report)

Approved for public release; distribution unlimited

18. SUPPLEMENTARY NOTES

19. KEY WORDS (Continue on reverse side if necessary and identify by block number)

Inertial Navigation System (INS)
Steady-State Kalman Filter (SKF)
Stability Derivatives (SD)

20. ABSTRACT (Continue on reverse side if necessary and identify by block number)

In a tactical missile with mid-course guidance, an Inertial Navigation System (INS) is required. Strapdown INS using Steady-State Kalman Filters (SKF) as estimators has been suggested and this kind of INS is considered to be easier and cheaper to implement than the gimbaled INS.

This thesis investigates one aspect of the INS problem: The sensitivity of the SKF to inaccuracies in the filter parameters such

as the stability derivatives. The analysis has been performed by
varying each of the flight parameters over a given range and noting
the effect on the accuracy of the filter. The great advantage
of the analysis in the sensitivity of rms estimate errors to
inaccuracies in the stabiltiy derivatives is that it points out
clearly which derivatives are worthy of detailed accurate
determination and which are not.

2

Sensitivity of the Steady-State
Kalman Filters to Stability Derivatives
Variations in an Inertial Navigation System

by

Jose Augusto Matallana R.
Lieutenant, Colombian Navy

Submitted in partial fulfillment of the
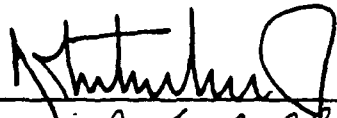requirements for the degree of

MASTER OF SCIENCE IN ELECTRICAL ENGINEERING

from the

NAVAL POSTGRADUATE SCHOOL
September 1980

Author _____

Approved by: _____
                                        Thesis Advisor

_____
                                        Second Reader

_____
Chairman, Department of Electrical Engineering

_____
Dean of Science and Engineering

3

ABSTRACT

In a tactical missile with mid-course guidance, an
Inertial Navigation System (INS) is required. Strapdown INS
using Steady-State Kalman Filters (SKF) as estimators has
been suggested and this kind of INS is considered to be
easier and cheaper to implement than the gimbaled INS.

This thesis investigates one aspect of the INS problem:
The sensitivity of the SKF to inaccuracies in the filter
parameters such as the stability derivatives. The analysis
has been performed by varying each of the flight parameters
over a given range and noting the effect on the accuracy of
the filter. The great advantage of the analysis in the
sensitivity of rms estimate errors to inaccuracies in the
stability derivatives is that it points out clearly which
derivatives are worthy of detailed accurate determination and
which are not.

TABLE OF CONTENTS

6

LIST OF FIGURES

7

8

9

ACKNOWLEDGEMENT

I would like to express my gratitude to Dr. D. J. Collins for his assistance, guidance and continuous encouragement which he provided during the pursuit of this study. To my wife I would like to offer my thanks and love for her patience, understanding and fortitude during a time which tested both of us.

JOSE A MATALLANA

I. INTRODUCTION

In a typical tactical missile trajectory, standoff (or mid-course) guidance is required when the missile is launched at such long ranges from the target that either the missile seeker cannot detect the target or, if it can, the information is of such poor quality that is unusable. The mid-course guidance law usually consists of some pre-programed strategy such as to maintain the launch heading, constant altitude and speed. Mid-course guidance is primarily an inertial instrumentation problem. Typical sensors onboard missiles consist of three rate gyros (pitch, yaw and roll), accelerometers, sometimes magnetic compass and some kind of altimeter. Additional state information can be provided by the seeker. A radar seeker could provide range and range rate.

Here is considered the problem of using steady-state Kalman Filters as part of a navigation system, where the two estimators together (longitudinal and lateral estimators), constitute a strapdown system that does not use accelerometers or gimbaled gyros. Strapdown Inertial Navigation Systems (INS) using Steady-State Kalman Filters (SKF) as estimators have been considered as cheaper and easier to implement than the gimbaled INS. The sensors used in this analysis are: pitch and roll rate gyros, altimeter and magnetic compass. Since constant gain estimators have been

suggested as easier and cheaper to implement, the analysis is confined to the SKF.

This work has been motivated by the idea given in Ref. [4], where the author discusses in detail the configuration of such a navigation system as described before, but the problem is presented as a particular application in the INS of the DC-8 airplane. For convenience the model used here essentially is the same as Ref. [4] in lieu of a missile. This was done in order to eliminate classification problems.

This thesis investigates only one aspect of the INS problem. That aspect is the sensitivity of the Kalman Filter to inaccuracies in the filter parameters or variation between the filter model and the plant model. These differences can be due to either inaccuracies as indicated or to a normal variation in the flight parameters due to different flight regimes. One result of this is the sensitivity of rms estimate errors to inaccuracies or differences in the stability derivatives.

The work was begun by reproducing the results given in Ref. [4] with the correct implementation of the dynamics in the filter parameters (i.e., X_u, Y_v, etc.) over a given range and noting the effect on the accuracy of the filter.

II. STOCHASTIC MODELS AND ESTIMATION

A. KALMAN FILTER

The Kalman Filter is widely documented and no attempt at a development of general theory has been made in this work. A brief description has been included in order to establish the particular formulation used. For a more complete development one is referred to Ref [1].

1. Linear Dynamic System

The formulation used employs state-space notation which offers the advantage of mathematical and notational convenience. Consider the linear time invariant system (system and measurement models) given by equation (1), where x represents the states of the system; z is the

$$\dot{x} = Fx + \Gamma w \tag{1-a}$$

$$z = Hx + v \tag{1-b}$$

measurement vector; F is the system matrix; Γ is the driving noise coefficient matrix; H describes the relationship between the states and the measurement; w and v are independent, zero-mean white gaussian noise process with covariance matrices Q and R respectively, that in mathematical terms are given by:

$$E(w(t)w^T(\tau)) = Q(t)\delta(t-\tau), \; E(w(t)) = 0 \tag{2-a}$$

$$E(v(t)v^T(\tau)) = R(t)\delta(t-\tau), \; E(v(t)) = 0 \tag{2-b}$$

13

2. Continuous Time Kalman Filter

A continuous time Kalman Filter is described by equation (3), where $\hat{x}$ is the state estimate; K is a matrix of constant filter gains. The implementation of the System Model and the Kalman Filter is shown in block diagram in Figure 1.

$$\dot{\hat{x}} = F\hat{x} + K(z-H\hat{x}) \tag{3}$$
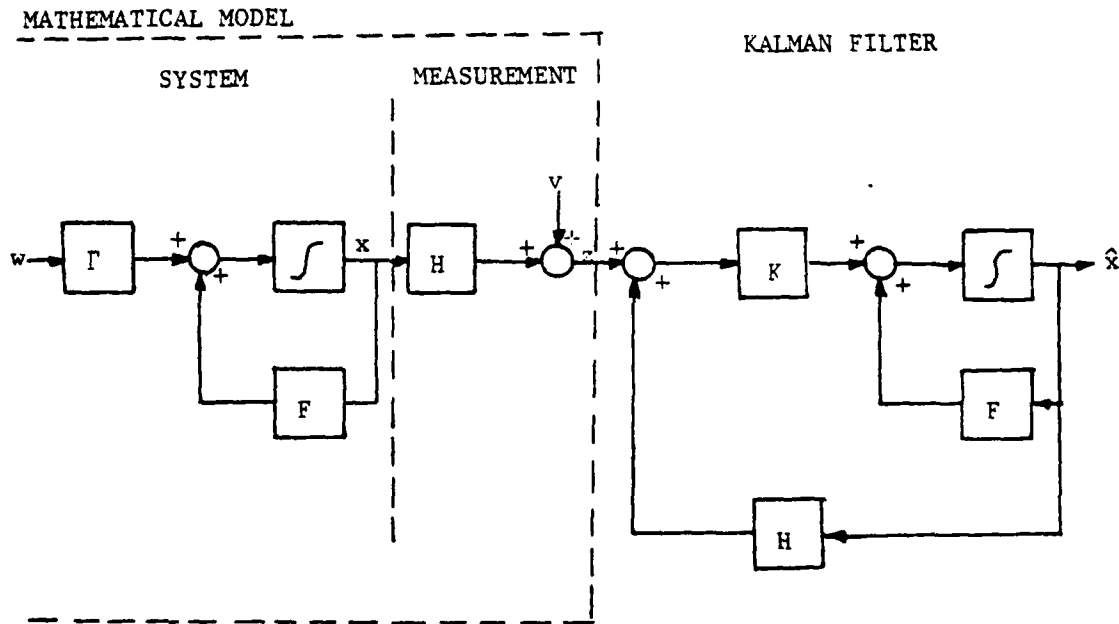
Figure 1

System Model and Kalman Filter

The estimate error is defined by equation (4) as,

$$\tilde{x} \overset{\Delta}{=} \hat{x} - x \tag{4}$$

and the differential equation for $\tilde{x}$ is given by

$$\dot{\tilde{x}} = (F-KH)x - \Gamma w + Kv \tag{5}$$

The differential equations for the state of a linear system driven by white noise can be expressed as

$$\begin{bmatrix} \dot{\tilde{x}} \\ \dot{x} \end{bmatrix} = \begin{bmatrix} F-KH & 0 \\ 0 & F \end{bmatrix} \begin{bmatrix} \tilde{x} \\ x \end{bmatrix} + \begin{bmatrix} Kv-\Gamma w \\ \Gamma w \end{bmatrix} \tag{6}$$

The covariance of the estimate-error, designated P, is given by equation (7). It provides a statistical measure of the uncertainty in x.

$$P = E[\tilde{x}\tilde{x}^T] \tag{7}$$

The diagonal elements of the covariance matrix are the mean square errors in the knowledge of the state variables. Also, the trace of P is the mean square length of the vector $\tilde{x}$. The off diagonal terms of P are indicators of cross-correlation between the elements of $\tilde{x}$. The covariance matrix P is obtained by solving the linear Lyapunov equation given by

15

$$P = (F-KH)P + P(F-KH)^T + \Gamma Q\Gamma^T + KRK^T \tag{8}$$

The eigenvalues of the filter are the roots of equation (9).

$$|SI - F + KH| = 0 \tag{9}$$

B. STATE AUGMENTATION AND SHAPING FILTERS

When the system random disturbances are correlated in time, i.e., colored noise, it is necessary to use their power spectral density data in order to develop a mathematical model that produces an output which duplicates the noise characteristics [Ref. 2]. Correlated random noises are taken to be state variables of a fictitious linear time invariant system (generally called a shaping filter) which is itself excited by white gaussian noise. Such a model is given by equation (10), where the subscript f, denotes filter and n, is a nonwhite, i.e., time-correlated, gaussian noise. The filter output is used to drive the system as show in Fig. 2.

$$\dot{x}_f = F_f x_f + \Gamma_f w \tag{10-a}$$

$$n = H_f x_f \tag{10-b}$$

The dimension of the state vector (1) is increased by including the disturbances as well as a description of the system dynamics behavior in appropriate rows of an enlarged F matrix, this is called state vector augmentation.

16
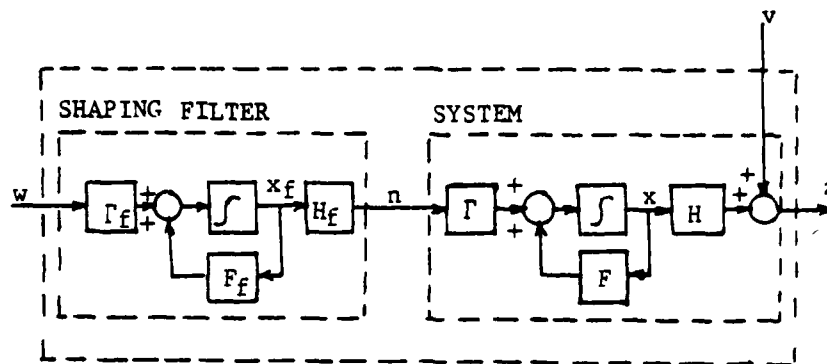
Figure 2
Shaping filter generating driving noise.
Conformation of the Augmented System.

The augmented state equation is given by

$$
\begin{bmatrix} \dot{x} \\ \hline \dot{x}_f \end{bmatrix} = \begin{bmatrix} F & | & \Gamma H_f \\ \hline 0 & | & F_f \end{bmatrix} \begin{bmatrix} x \\ \hline x_f \end{bmatrix} + \begin{bmatrix} 0 \\ \hline \Gamma_f \end{bmatrix} w
$$

(11)

The associated measurement equation given by equation (12)

$$
z = \begin{bmatrix} H & | & 0 \end{bmatrix} \begin{bmatrix} x \\ \hline x_f \end{bmatrix} + v
$$

(12)

C. SENSITIVITY TO PARAMETER VARIATION

Observing the structure of the Kalman Filter illustrated
in Figure 1; the filter contains an exact model of the system

17

dynamics. The filter gain matrix is calculated using the parameters of the exact model of the dynamics.

1. Incorrect Implementation of Dynamics

The analysis of how the error covariance behaves when the gain matrix is computed using wrong values of F matrix, i.e., varying parameters due to different flight conditions, is quite well explained in Reference [1]. Figure 3 shows the block diagram for the system model and the Kalman Filter, where the quantities K* and F* represent the gain matrix and the system dynamics implemented in the filter.
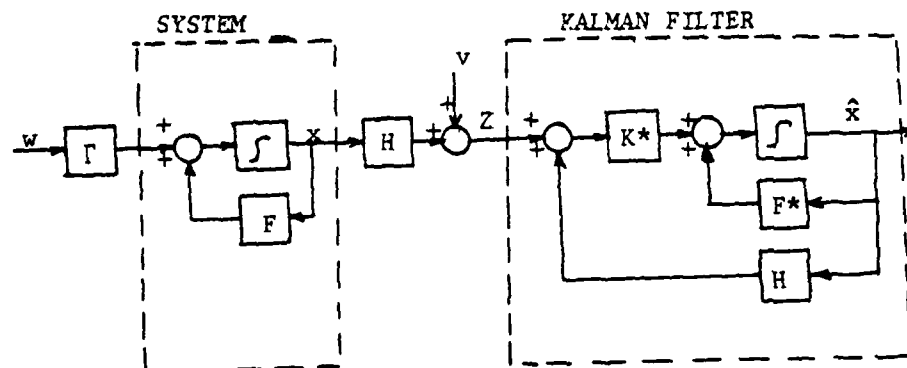
Figure 3

Block diagram of the System Model and Kalman Filter with incorrect implementation of dynamics.

18

The equation for the estimate is given by

$$\dot{\hat{x}} = F^*\hat{x} + K^*(z - H\hat{x}) \tag{13}$$

The error in the estimate given by (14)

$$\dot{\tilde{x}} = (F^* - K^*H)\tilde{x} + \Delta Fx - \Gamma w + K^*v \tag{14}$$

where

$$\Delta F \overset{\Delta}{=} F^* - F$$

The differential equations for the states of a linear system driven by white gaussian noise given previously by equation (6) becomes now

$$\begin{bmatrix} \dot{\tilde{x}} \\ \dot{x} \end{bmatrix} = \begin{bmatrix} F^* - K^*H & \Delta F \\ 0 & F \end{bmatrix} \begin{bmatrix} \tilde{x} \\ x \end{bmatrix} + \begin{bmatrix} K^*v - \Gamma w \\ \Gamma w \end{bmatrix} \tag{15}$$

Letting x' be the augmented state vector, $x' \overset{\Delta}{=} \begin{bmatrix} \tilde{x} \\ x \end{bmatrix}$, where the covariance matrix of x' is given by:

$$E(x'x'^T) = \begin{bmatrix} P & V^T \\ V & U \end{bmatrix} \tag{16}$$

where

$$P \triangleq E(\tilde{x}\tilde{x}^T), \quad V \triangleq E(x\tilde{x}^T), \quad U \triangleq E(xx^T)$$

The quantity of interest is P, the covariance of x.

The error sensitivity equations are given by

$$\dot{P} = (F^* - K^*H)P + P(F^* - K^*H)^T + \Delta FV$$
$$+ V^T \Delta F^T + \Gamma Q \Gamma^T + K^* R K^{*T} \qquad (17\text{-}a)$$

$$\dot{V} = FV + V(F^* - K^*H)^T + U\Delta F^T - \Gamma Q \Gamma^T \qquad (17\text{-}b)$$

$$\dot{U} = FU + UF^T + \Gamma Q \Gamma^T \qquad (17\text{-}c)$$

with initial conditions

$$P(0) = -V(0) = U(0) = E(x(0)x(0)^T)$$

when the actual system dynamics are faithfully reproduced in the filter, i.e., $F = F^*$, $\Delta F = 0$, the equation (17) reduces to the linear Lyapunov equation given by equation (8).

D. MODAL COORDINATES TRANSFORMATION

The representation of the system given by equation (1) is not unique. Considering an alternative linear transformation of the states given in references [3] and [4] , let $x = T\xi$, where ξ represents the transformation of the states and T is the transformation matrix with the columns formed by the

eigenvectors of the system matrix F (for a complex eigenvalue, the first column is the real part and the second column is the imaginary part of the eigenvector). The similarity transformation of equation (1) is given by

$$\xi = A\xi + Bw \qquad \qquad (18\text{-}a)$$

$$z = C\xi + v \qquad \qquad (18\text{-}b)$$

where

$$A = T^{-1}FT, \quad B = T^{-1}\Gamma, \quad C = HT$$

A case of particular interest (canonical form) occurs when the resulting A matrix is diagonal (the eigenvalues of the F matrix form the diagonal). The design of the estimator in modal coordinates is analogous to using transfer functions in partial fraction form. The canonical form is more informative than the transfer frunction method, since observability and controllability can be obtained by inspection.

E. SOLUTION OF THE KALMAN FILTER WITH A PRESCRIBED DEGREE OF STABILITY

The Kalman Filter designed with constant gain (SKF) and used as an observer will diverge if there are undisturbed, neutrally stable (UNS) modes in the system model. In references [4] and [5] the authors presented the idea of

destabilization of the system model (1), the amount of destabilization can be varied until the resulting suboptimal observer has a specified degree of stability. The method presented in Ref. [4] refers only to destabilizing the UNS modes in the system model, that method is called "modal destabilization" (MDS). The gains of the filter are constrained so that

$$Re(Si) \overset{\cdot}{\geq} -\sigma, \quad i = 1,2,\ldots.n \tag{19}$$

where Re (Si) indicates "real part of (Si)," $S_1,\ldots.Sn$ are the eigenvalues of the filter, i.e., the roots of equation (9) and σ is a specified positive number.

The original system is destabilized in accordance with equation (20), where F' is the resultant destabilized matrix, E the destabilization matrix (diagonal) and T is the modal transformation matrix (eigenvector matrix). The matrix F' is used in order to calculate the modified gains of the filter (suboptimal gains).

$$F' = F + TET^{-1} \tag{20}$$

This method avoids the divergence of the steady-state Kalman Filter with a slight decrease in estimation accuracy.

22

III. DYNAMIC AND MEASUREMENT SYSTEM MODELS

A. REFERENCE AXIS SYSTEM

The Reference Axis System in a missile is centered on the c.g. and fixed on the body as follows:

> X axis, called the roll axis, forwards, along the axis of symmetry.
>
> Y axis, called the pitch axis, outwards and to the right if viewing the missile from behind.
>
> Z axis, called the yaw axis, downwards in the plane of symmetry to form a right-handed orthogonal system with the other two.

The symbols from Appendix A define the forces and moments acting on the missile, the linear and angular velocities, and the moments of inertia; those quantities are shown in Figure 4.
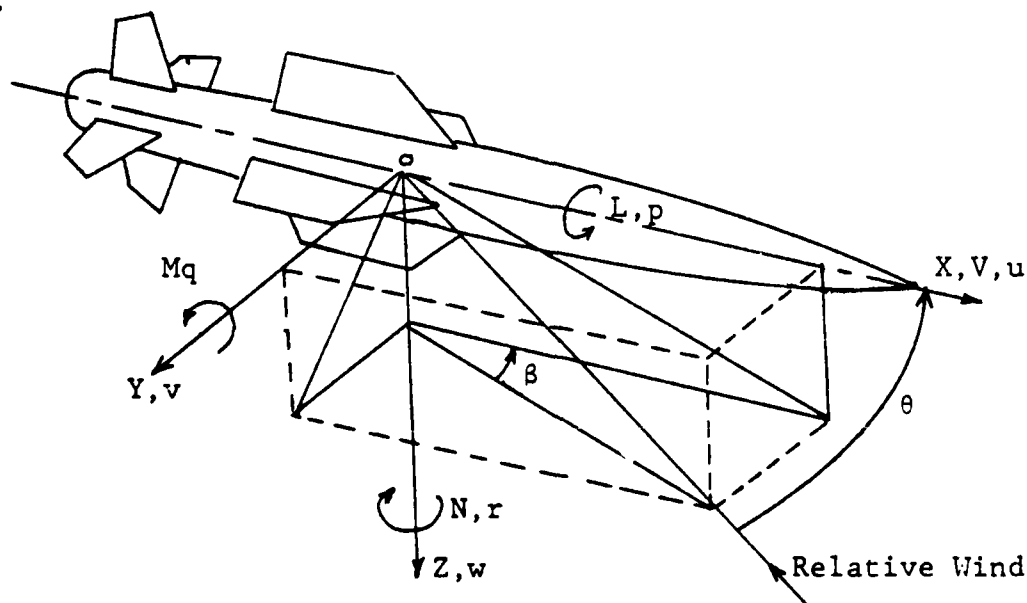
Figure 4
Reference Axis System

B. MISSILE EQUATIONS OF MOTION

The equations of motion used in the present study in order to represent the missile dynamics are quite well defined in Reference [7]. A linear dynamical model of the missile based on the rigid body approximation is appropriate.

1. Longitudinal Motion

The longitudinal motions of a missile are modeled by a fifth-order system given by equation (21), where the state variables are u, velocity along the X axis; w, velocity along the Z axis; q, pitch rate, θ, pitch angle and h, altitude.

$$
\begin{bmatrix} \dot{u} \\ \dot{w} \\ \dot{q} \\ \dot{\theta} \\ \dot{h} \end{bmatrix} = \begin{bmatrix} Xw & Xw & 0 & -g & 0 \\ Zw & Zw & V & 0 & 0 \\ Mu+M\dot{w}Zu & Mw+M\dot{w}Zw & Mq+MwV & 0 & 0 \\ 0 & 0 & 1 & 0 & 0 \\ 0 & -1 & 0 & V & 0 \end{bmatrix} \begin{bmatrix} u \\ w \\ q \\ \theta \\ h \end{bmatrix} \quad (21)
$$

2. Lateral Motion

The lateral motions of a missile are modeled by a fifth-order system given by equation (22), where the state variables defined are; β sideslip angle; r yaw rate; p roll rate; ϕ roll angle; ψ heading angle.

24

$$
\begin{bmatrix} \dot{\beta} \\ \dot{r} \\ \dot{p} \\ \dot{\phi} \\ \dot{\psi} \end{bmatrix} = \begin{bmatrix} Y_v & -1 & 0 & g/V & 0 \\ N_\beta^1 & N_r^1 & N_p^1 & 0 & 0 \\ L_\beta^1 & L_r^1 & L_p^1 & 0 & 0 \\ 0 & 0 & 1 & 0 & 0 \\ 0 & 1 & 0 & 0 & 0 \end{bmatrix} \begin{bmatrix} \beta \\ r \\ p \\ \phi \\ \psi \end{bmatrix} \tag{22}
$$

C. MODEL

The aerodynamic data used in the present study is given in Appendix B [Ref 9]. Essentially the models and noise dynamics are those of reference [4].

1. Longitudinal Motion Estimation

The main disturbance inputs are the two wind velocities u_g and w_g. Under the particular flight conditions, the turbulance represented by the fluctuating parts of u_g and w_g are color noise. They are modeled by first-order shaping filters with white gaussian noise inputs as given in equation (10). The resultant linear model is given by equation (23) [Ref 8].

$$
\begin{bmatrix} \dot{u}_g \\ \dot{w}_g \end{bmatrix} = \begin{bmatrix} -0.413 & 0 \\ 0 & -0.853 \end{bmatrix} \begin{bmatrix} u_g \\ w_g \end{bmatrix} + \begin{bmatrix} 0.413 & 0 \\ 0 & 0.853 \end{bmatrix} \begin{bmatrix} \mu_u \\ \mu_w \end{bmatrix}
$$

$$\tag{23}$$

The numerical data for the longitudinal dimensional derivatives was used in equation (21), the resultant model is

given by equation (24), that corresponds to the state vector augmentation given by equation (11). Units are scaled with u, w, u_g and w_g in units of 10 ft/s, q in units of 0.01 rad/s.

$$
\begin{bmatrix} \dot{u} \\ \dot{w} \\ \dot{q} \\ \dot{\theta} \\ \dot{h} \\ \dot{u}_g \\ \dot{w}_g \end{bmatrix} = \begin{bmatrix} -0.015 & 0.004 & 0 & -0.0322 & 0 & -0.015 & 0.004 \\ -0.074 & -0.806 & 0.824 & 0 & 0 & -0.074 & -0.806 \\ -0.749 & -10.7 & -1.344 & 0 & 0 & 0.749 & -10.7 \\ 0 & 0 & 1 & 0 & 0 & 0 & 0 \\ 0 & -0.1 & 0 & 0.0824 & 0 & 0 & 0 \\ 0 & 0 & 0 & 0 & 0 & -0.413 & 0 \\ 0 & 0 & 0 & 0 & 0 & 0 & -0.853 \end{bmatrix} \begin{bmatrix} u \\ w \\ q \\ \theta \\ h \\ u_g \\ w_g \end{bmatrix} + \begin{bmatrix} 0 & 0 \\ 0 & 0 \\ 0 & 0 \\ 0 & 0 \\ 0 & 0 \\ 0.413 & 0 \\ 0 & 0.853 \end{bmatrix} \begin{bmatrix} \mu_u \\ \mu_w \end{bmatrix}
$$

(24)

θ in units of 0.01 rad., and h in units of 100 ft.

The measurement model given by equation (25) assumes a rate gyro in order to measure z_q and a barometric altimeter in order to measure z_h.

$$
\begin{bmatrix} z_q \\ z_h \end{bmatrix} = \begin{bmatrix} 0 & 0 & 1 & 0 & 0 & 0 & 0 \\ 0 & 0 & 0 & 0 & 1 & 0 & 0 \end{bmatrix} \begin{bmatrix} u \\ w \\ q \\ \theta \\ h \\ u_g \\ w_g \end{bmatrix} + \begin{bmatrix} 1 & 0 \\ 0 & 1 \end{bmatrix} \begin{bmatrix} v_q \\ v_h \end{bmatrix}
$$

(25)

2. Lateral Motion Estimation

The main disturbance input is lateral wind v_g. The turbulence represented by the fluctuating part of v_g is color noise, it is modeled as a first-order shaping filter with white gaussian noise input as given in equation (10). The resulting shaping filter is as given by equation (26) and taken from Reference [4].

$$\dot{\beta}_g = -0.853\beta_g + 0.853\mu$$

where   (26)

$$\beta_g = v_g/V$$

The numerical data for the lateral dimensional derivatives was used in equation (22) to obtain the equation (27). This corresponds to the state vector augmentation given by equation (11).

$$\begin{bmatrix} \dot{\beta} \\ \dot{r} \\ \dot{p} \\ \dot{\phi} \\ \dot{\psi} \\ \dot{\beta}_g \end{bmatrix} = \begin{bmatrix} -0.0868 & -1 & 0 & 0.03907 & 0 & -0.0868 \\ 2.14 & -0.228 & -0.0204 & 0 & 0 & 2.14 \\ -4.41 & 0.334 & -1.181 & 0 & 0 & -4.41 \\ 0 & 0 & 1 & 0 & 0 & 0 \\ 0 & 1 & 0 & 0 & 0 & 0 \\ 0 & 0 & 0 & 0 & 0 & -0.853 \end{bmatrix} \begin{bmatrix} \beta \\ r \\ p \\ \phi \\ \psi \\ \beta_g \end{bmatrix} + \begin{bmatrix} 0 \\ 0 \\ 0 \\ 0 \\ 0 \\ 0.853 \end{bmatrix} \mu$$

(27)

The measurement model given by equation (28), represents the situation where the measurement z_p is taking with a roll-rate gyro and the measurement z_ψ using a magnetic compass.

$$\begin{bmatrix} z_p \\ z_\psi \end{bmatrix} = \begin{bmatrix} 0 & 0 & 1 & 0 & 0 & 0 \\ 0 & 0 & 0 & 0 & 1 & 0 \end{bmatrix} \begin{bmatrix} \beta \\ r \\ p \\ \phi \\ \psi \\ \beta_g \end{bmatrix} + \begin{bmatrix} 1 & 0 \\ 0 & 1 \end{bmatrix} \begin{bmatrix} v_p \\ v_\psi \end{bmatrix} \qquad (28)$$

28

IV. ANALYSIS

A. THE SIMULATION

A computer program was developed in order to solve the sensitivity equations given by equation (17). Basically, the program was used to handle a set of 105 linear differential equations in the longitudinal case and 78 in the lateral. The principle program output is the time history of the P matrix and the square root of its diagonal elements (the rms estimate errors).

The Kalman Filter computer program was the primary tool used in computing the gains. The program was developed at the Massachusetts Institute of Technology [Ref. 10] and adapted for use at the Naval Postgraduate School. A second computer program composed at Stanford University, OPTSYS 4 Computer Program [Ref. 11], which utilizes several options of the Kalman Filter, was also implemented in this analysis. In particular, the suboptimal filter using the modal destabilization (MDS) design option was required for the lateral case.

B. THE RESULTS

As the problem is described, the results are presented in two parts, the longitudinal and the lateral case.

Initially both models given by equations (24) and (27) were modified in order to include another state in each of them, the perturbed position. The resultant observers were

tested, but in both cases they were unstable.

1. Longitudinal Motion Estimation Analysis

A steady-state Kalman Filter was designed [Ref. 4] and used as a constant gain state estimator (equation (3)).

The first step in this analysis was to reproduce the results for the case of exact implementation of dynamics in the calculation of the Kalman gain matrix. That analysis was done using the M.I.T. Kalman Filter Computer Program [Ref. 10]. The results are shown below:

Filter gain matrix K.

0.059	0.060
0.264	-0.161
3.517	0.040
0.001	-0.080
0.013	0.136
-0.011	0.035
-1.288	0.128

Filter Eigenvalues

$-0.310 \pm j0.411$
-0.429
-0.178
-0.261
$-0.063 \pm j0.0743$

rms estimate errors

$\bar{u} = 2.090$ ft/s	$\bar{\theta} = 0.317$ deg
$\bar{w} = 5.102$ ft/s	$\bar{h} = 8.2$ i5 Γt
$\bar{q} = 0.416$ deg/s	$\bar{u}_g = 4.776$ ft/s
	$\bar{w}_g = 5.701$ ft/s

30

These results are essentially identical to those of Ref. [4].

The next objective was to consider the incorrect implementation of dynamics in the Kalman Filter, in order to study the sensitivity of rms estimate errors to inaccuracies in the stability derivatives. The numerical variation of the parameters were considered individually in order to establish the F* matrix to be used in equation (17) and also for finding the filter gain matrix K* to be implemented in the same equation. For each variation of the parameter under observation it was necessary to run the M.I.T. Computer Program [Ref. 10] in order to find the matrix of gains K* and then to run the sensitivity covariance program in order to study the propagation of the estimate errors.

The results are shown in Tables 1-8 and Figures 5-40. In the Tables, the true value of each parameter is marked with an asterisk. The description of the results are:

Xu. The dimensional variation of X force with forward speed (u) has a nominal value of -0.015. This quantity was changed in a range of ±20%. The behavior of the rms estimate errors are presented in Table 1. From that it can be seen that any numerical variation of Xu derivative does not cause significant changes in the nominal values of the rms estimate errors of the states, $\bar{w}$, $\bar{q}$, $\bar{\theta}$, $\bar{u}_g$ and $\bar{w}_g$. For the states $\bar{u}$ and $\bar{h}$ the results are shown in Figures 5-6 respectively, with some effect, but not significant for positive variation of Xu.

31

<u>Xw</u>. The dime. ional variation of X force with downward speed (w) has a nominal value of 0.004. As before, the numerical variation was performed in a range of $\pm 20\%$. The behavior of the rms estimate errors were tabulated in Table 2. Checking the results there is no variation in the nominal values of rms estimate errors of the states, $\bar{w}$, $\bar{q}$, $\bar{\theta}$, $\bar{u}_g$ and $\bar{w}_g$, for any of the changes made in Xw derivative. The variations in the estimate errors for $\bar{u}$ and $\bar{h}$ are indicated in Figures 7 and 8 respectively. Increasing the value of Xw the $\bar{u}$ error decreases but $\bar{h}$ increases, while taking smaller values of the parameter, the effect is contrary. Those changes in the rms errors are considered not important.

<u>Zu</u>. The dimensional variation of Z force caused by a change in forward speed (u) has a nominal value of -0.074. The effects of changing its design value was observed in a range of 20% and its result condensed in Table 3 as well as in Figures 9-14. All the rms errors show some degree of sensitivity except $\bar{q}$. The most important changes occur in $\bar{u}$, $\bar{\theta}$, and $\bar{h}$ errors and the large variation in $\bar{u}$ can begin to be important in terms of accuracy in radial position.

<u>Zw</u>. The dimensional variation of Z force with downward speed (w) has a nominal value of -0.806. The results for this case are presented in Table 4 and Figures 15-20. Again, the variation in the value of Zw was made in a range of $\pm 20\%$. All the rms estimate errors show a large degree of

sensitivity and it can be considered that any numerical variation of Z_w beyond $\pm$ 2% is critical and unacceptable.

$\underline{Mu}$. The dimensional variation of M moment caused by a change in forward speed (u) has a nominal value of -0.000786. The value of Mu was changed in a range of 20% and the results are given in Table 5 as well as Figures 21-26. Any variation in Mu quantity does not cause important changes in the value of the rms estimate errors of the states, $\bar{q}$, $\bar{u}_g$ and $\bar{w}_g$. For For the states $\bar{u}$, $\bar{w}$, $\bar{\theta}$, and $\bar{h}$, the variation in the errors can be considered with some significant effect for large deviations of Mu value, i.e., more than $\pm$10%.

$\underline{Mw}$. The dimensional variation of M moment with speed (w) has a nominal value of -0.0111. Its numerical variation was taken in a range of $\pm$10%. From Table 6 and Figures 27-32, it can be seen that any alteration in the true value of Mw is reflected with a strong effect on all the rms estimate errors. This derivative can be considered the most critical in the longitudinal motion estimation case.

$\underline{Mq}$. The dimensional variation of pitching moment with pitch rate (q) has a nominal value of -0.924. The results are given in Table 7 and Figures 33 and 34 for a range of $\pm$20% in the numerical variation of Mq. The sensitivity of the rms estimate errors due to changes in this parameter is minimum for all the states.

33

$\overset{\bullet}{M w}$. The dimensional variation of pitching moment
with rate of change of downward speed ($\overset{\bullet}{w}$) has a nominal value
of -0.00051. Table 8 and Figures 35-40 presents the infor-
mation about the changes of the rms estimate errors in a
range of $\pm 20\%$ in the variation of $M\overset{\bullet}{w}$ derivative. All the
errors show some degree of sensitivity and with more than $\pm 2\%$
in the alteration of the $M\overset{\bullet}{w}$ value, the variation in the errors
begins to be significant.

2. Lateral Motion Estimation Analysis

The dynamic system (equation (27)) and measurement
models (equation (28)) were transformed into modal coordin-
ates in accordance with equation (18). This was done using
the OPTSYS 4 Computer Program [Ref. 11]; the results are
given below:

$$
\begin{bmatrix}
\overset{\bullet}{\xi}D1 \\
\overset{\bullet}{\xi}D2 \\
\overset{\bullet}{\xi}R \\
\overset{\bullet}{\xi}S \\
\overset{\bullet}{\xi}H \\
\overset{\bullet}{\xi}vg
\end{bmatrix}
=
\begin{bmatrix}
-0.119 & 1.490 & 0 & 0 & 0 & 0 \\
-1.490 & -0.119 & 0 & 0 & 0 & 0 \\
0 & 0 & -1.254 & 0 & 0 & 0 \\
0 & 0 & 0 & -0.0041 & 0 & 0 \\
0 & 0 & 0 & 0 & 0 & 0 \\
0 & 0 & 0 & 0 & 0 & -0.853
\end{bmatrix}
\begin{bmatrix}
\xi D1 \\
\xi D2 \\
\xi R \\
\xi S \\
\xi H \\
\xi vg
\end{bmatrix}
+
\begin{bmatrix}
-1.702 \\
-0.610 \\
-5.106 \\
-0.004 \\
0 \\
3.788
\end{bmatrix}
[\mu]
$$

(29)

$$
\begin{bmatrix} z_p \\ z_\psi \end{bmatrix} = \begin{bmatrix} 1 & 0 & -0.782 & 0 & 1 & -0.605 \\ 0.276 & 0.295 & -0.008 & 0.995 & 1 & 0.162 \end{bmatrix} \begin{bmatrix} \xi_{D1} \\ \xi_{D2} \\ \xi_R \\ \xi_S \\ \xi_H \\ \xi_{v_g} \end{bmatrix} + \begin{bmatrix} 1 & 0 & v_p \\ 0 & 1 & v_\psi \end{bmatrix} \quad (30)
$$

These results are identical to those given in Ref. [4]. In the same reference the author gives a complete analysis of controllability and observability using the results given in equations (29) and (30). From these can be seen that the spiral mode ξ_S has its eigenvalue close to the origin and it is almost undisturbed by the process noise; also it is unobservable with the measurement z_p. Using a steady-state Kalman Filter as an observer fail to estimate the heading mode ξ_H and its estimation of the spiral mode ξ_S is too slow. The next objective was to take the SKF and to consider the situation of parameter variations in the dynamic implemented in the filter. With the true values of the F matrix implemented in the filter the results are shown below:

Filter Gain Matrix K

0.051	-0.967
-1.536	0.411
2.695	-0.004
0.386	-0.789
-0.005	0.906
-1.713	0.655

Filter Eigenvalues

    -2.350 $\pm$ j2.594
    -0.624 $\pm$ j0.492
    -0.00125
     0.0

rms Estimate Errors

$V\bar{\beta}$ = 3.329   ft/s
$\bar{r}$ = 0.244   deg/s
$\bar{p}$ = 0.377   deg/s
$\bar{\phi}$ = 0.222   deg
$\bar{\psi}$ = 0.214   deg
$V\beta g$ = 5.506   ft/s

These results are essentially identical to those
from Ref. [4]. The filter was found to be stable but with a
narrow margin of stability. Any attempt to change parameters
resulted in a failure of the estimator due to divergence with
the most minimum variation (i.e., $\pm$1%) of any of the para-
meters. This result complements the analysis given previously
[Ref. 4] and it shows definitely that it is impossible to use
the SKF as an estimator for the lateral motion with the actual
configuration of the model given by equations (27) and (28).

    The alternative solution was to design a suboptimal
observer (MDS) with the constrain (19) as given in Ref. [4],
σ = 0.029 and using equation (20) in the MDS option the
computer program OPTSYS 4 [Ref. 11]. The results are:

36

Filter Gain Matrix K

-0.073	-0.871
-1.560	0.430
2.731	-0.033
0.339	-0.753
-0.033	0.928
-1.622	0.585

Filter Eigenvalues

$-2.350 \pm j2.589$

$-0.624 \pm j0.492$

$-0.0291 + j0.005$

rms Estimate Errors

$V\bar{\beta} = 3.799$ ft/s

$\bar{r} = 0.245$ deg/s

$\bar{p} = 0.379$ deg/s

$\bar{\phi} = 0.226$ deg

$\bar{\psi} = 0.216$ deg

$V\bar{\beta}g = 5.712$ ft/s

These results are essentially identical to those from Ref. [4].

The sensitivity of the lateral rms estimate errors due to inaccuracies in the stability derivatives was studied using the suboptimal filter (MDS) design and following the same procedure explained before for the longitudinal case. The results are shown in Tables 9-15 and Figures 41-76. The results are described in detail as follows:

$\underline{Yv}$. The dimensional variation of Y force with side velocity (v) has a nominal value of -.0868. This value was changed in a range of $\pm 20\%$ and the results appear in Table 9 and Figures 41-44. $\bar{r}$, $\bar{p}$, $\bar{\psi}$, and $\overline{V\beta}g$ show almost no sensitivity to the variation in Yv parameter, $\overline{V\beta}$ changes but it can be considered of secondary importance. The most sensitivity change occurs in $\bar{\phi}$ and it begins to be important for a variation of $\pm 5\%$ in Yv value.

$\underline{N_\beta'}$. The dimensional variation of yawing moment about Z axis with sideslip angle (β) has a nominal value of 2.14. Table 10 and Figures 45-50 give the results for a variation of N_β' derivative in a range of $\pm 10\%$. All the rms estimate errors except $\bar{\psi}$ present strong sensitivity, especially $\overline{V\beta}$ and $\bar{\phi}$. With a variation of more than $\pm 1\%$ the estimation of these errors begin to show large values and the filter takes a long time to reach the steady state value (more than 150 s). For that reason, any variation in the true value of N_β' with the purpose of implementation in a Kalman Filter as an estimator must be considered unacceptable.

$\underline{N_r'}$. The dimensional variation of yawing moment about Z axis with yaw rate (r) has a nominal value of -0.228. In a range of $\pm 20\%$ the variation of N_r' value was performed and the results tabulated in Table 11 as well as the important variations registered in Figures 51-54. The effects on sensitivity of all the rms estimate errors are secondary and

there is no important alteration in their values due to large variations in the N_r' parameter.

$N\dot{p}$. The dimensional variation of yawing moment about $\dot{Z}$ axis with roll rate (p) has a nominal value of -0.0204. This number was changed in a range of $\pm 20\%$ and the results observed are given in Table 12 and Figures 55-60. $\bar{r}$, $\bar{p}$, $\bar{\psi}$, and $V\bar{\beta}g$ rms errors do not present any important variation. The sensitivity in rms estimate error is observed in $V\bar{\beta}$ and $\bar{\phi}$, in particular. For the last one, the change is too large for a variation of 5% in the value of the parameter.

$L\beta$. The dimensional variation of rolling moment about X axis with sideslip angle (β) has a nominal value of -4.41. Its variation was given just in a margin of $\pm 10\%$ because with larger changes the estimator starts to diverge. The results obtained are given in Table 13 and Figures 60-66. All the rms estimate errors show some degree of sensitivity due to the variation in L_β' parameter and with 1% of change some of the errors like $V\bar{\beta}$ and $\bar{\phi}$ present very large variations. For that reason this derivative must be considered critical in the implementation of the Kalman Filter as an estimator.

L_r'. The dimensional variation of rolling moment about X axis with yaw rate (r) has a nominal value of -0.334. The results presented in Table 14 and Figures 67-72 are the product of the observation for the variation of the parameter L_r' in a range of $\pm 10\%$ and it can be considered as the most

39

important stability derivative for the lateral model, because the dynamics implemented in the filter does not allow any variation of its true value, otherwise, the estimation of the errors becomes to be too large and probably the filter can diverge. In other words, the sensitivity of the estimator to any variation in L_r' value is extremely critical.

$\underline{L_p}$. The dimensional variation of rolling moment about X axis with roll rate has a nominal value of -1.204. The behavior of the rms estimate errors were observed taking a variation of $\pm 10\%$ of the L_p parameter and they are given in Table 15 and Figures 73-76. V_β and $\bar{r}$ are the variables that present some degree of sensitivity in the increment of their rms estimate errors, respectively, and they begin to be important with a variation of more than $\pm 5\%$ of the L_p true value.

U RMS ESTIMATE ERROR VS XU
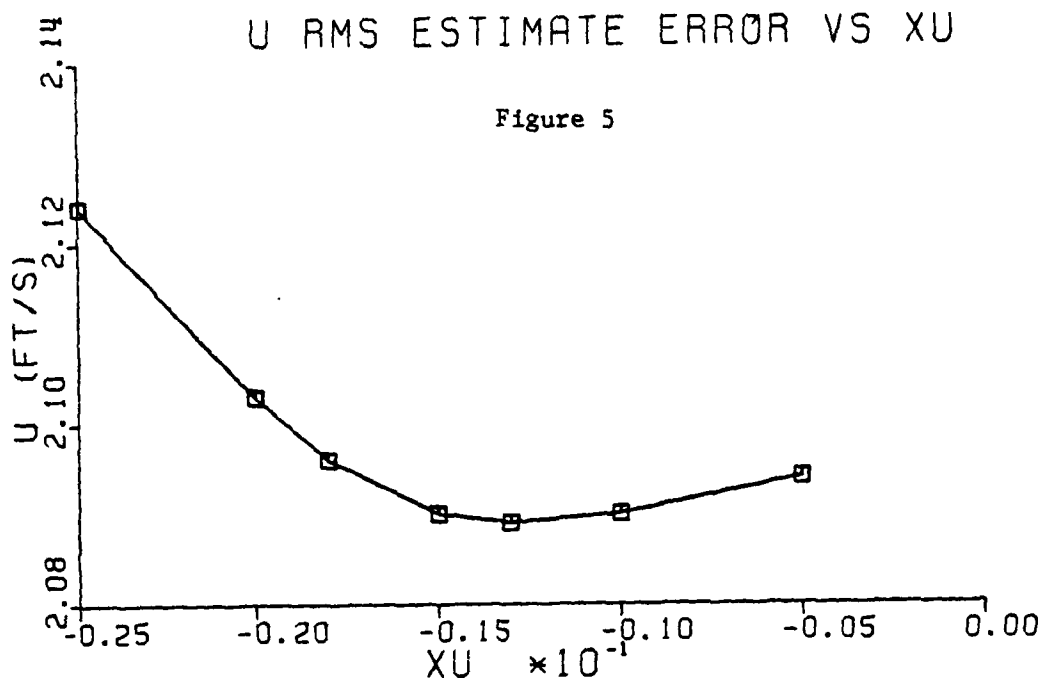
Figure 5

Figures 5 & 6. Sensitivity of $\bar{u}$ and $\bar{h}$ rms estimate errors vs variation in Xu stability derivative

H RMS ESTIMATE ERROR VS XU

Figure 6

U RMS ESTIMATE ERROR VS XW

Figure 7

Figures 7 & 8. Sinsitivity of $\bar{u}$ and $\bar{h}$ rms estimate errors vs variation in Xw stability derivative.

H RMS ESTIMATE ERROR VS XW

Figure 8

U RMS ESTIMATE ERROR VS ZU
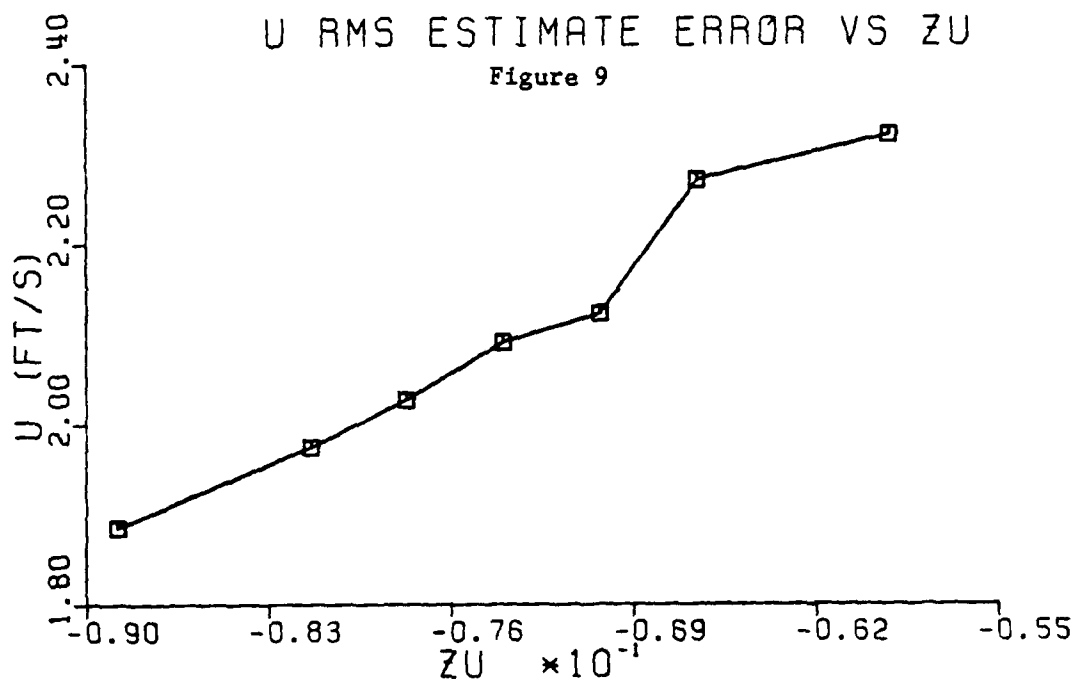
Figure 9

Figures 9 & 10. Sensitivity of $\bar{u}$ and $\bar{w}$ rms estimate errors vs variation in Zu stability derivative.

W RMS ESTIMATE ERROR VS ZU

Figure 10

43

H RMS ESTIMATE ERROR VS ZU

Figure 11

Figures 11 & 12. Sensitivity of $\bar{h}$ and $\bar{\theta}$ rms estimate errors vs variation in Zu stability derivative.

THETA RMS ESTIMATE ERROR VS ZU

Figure 12

WG RMS ESTIMATE ERROR VS ZU

Figure 13

Figures 13 & 14. Sensitivity of $\bar{w}_g$ and $\bar{u}_g$ rms estimate errors vs variation of Zu stability derivative.

UG RMS ESTIMATE ERROR VS ZU

Figure 14

U RMS ESTIMATE ERROR VS ZW

Figure 15

Figures 15 & 16. Sensitivity of $\bar{u}$ and $\bar{w}$ rms estimate errors vs variation in Zw stability derivative.

W RMS ESTIMATE ERROR VS ZW

Figure 16

Q RMS ESTIMATE ERROR VS ZW
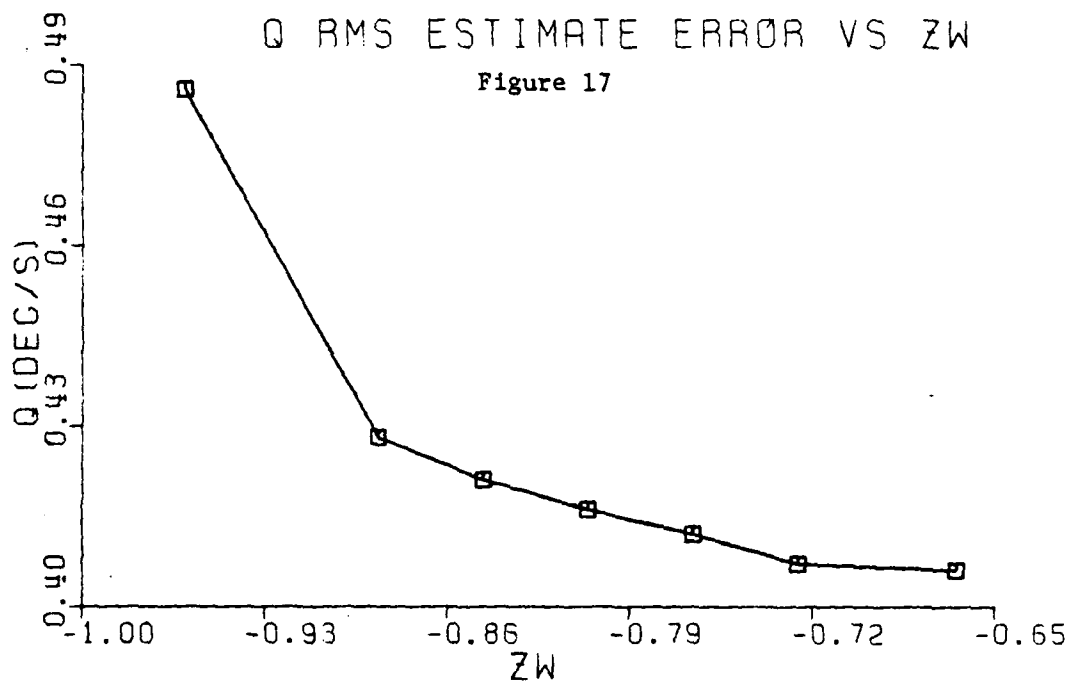
Figure 17

Figures 17 & 18. Sensitivity of $\bar{q}$ and $\bar{\theta}$ rms estimate errors vs variation in Zw stability derivative.

THETA RMS ESTIMATE ERROR VS ZW

Figure 18

47

H RMS ESTIMATE ERROR VS ZW
Figure 19
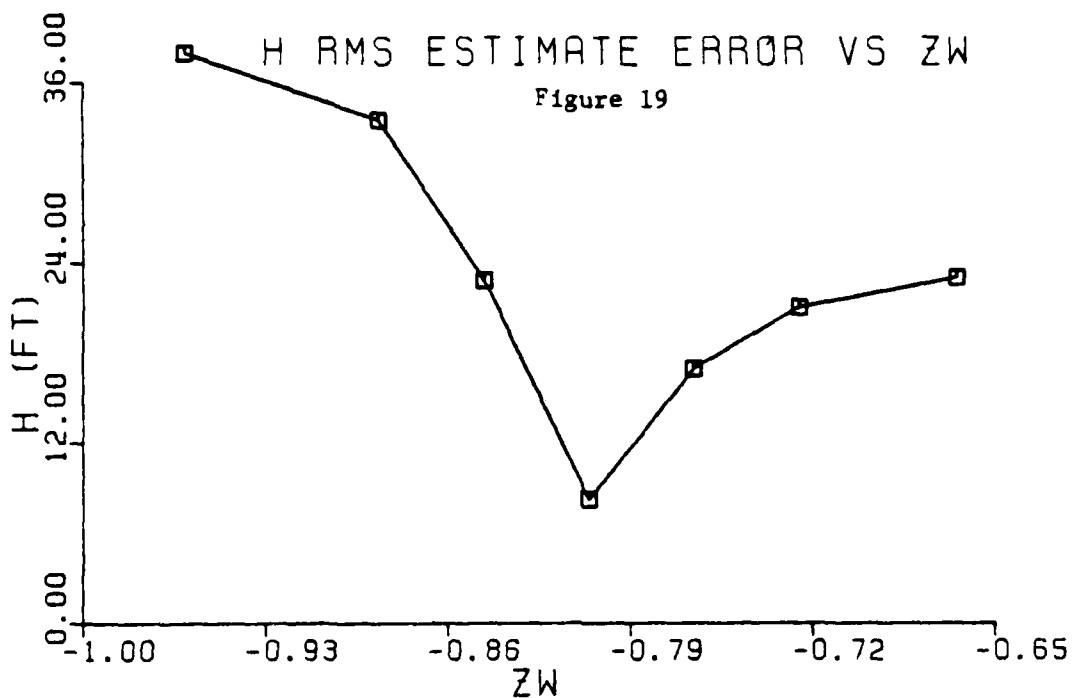
Figures 19 & 20. Sensitivity of $\bar{h}$ and $\bar{u}_g$ rms estimate errors vs variation in Zw stability derivative.

UG RMS ESTIMATE ERROR VS ZW
Figure 20
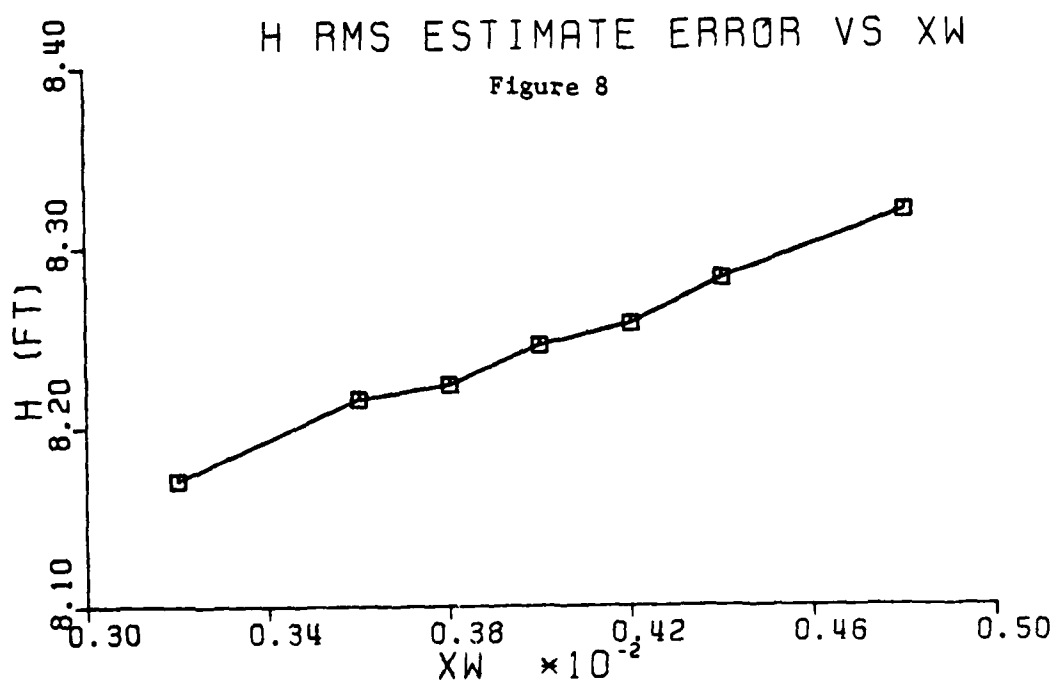
48

U RMS ESTIMATE ERROR VS MU
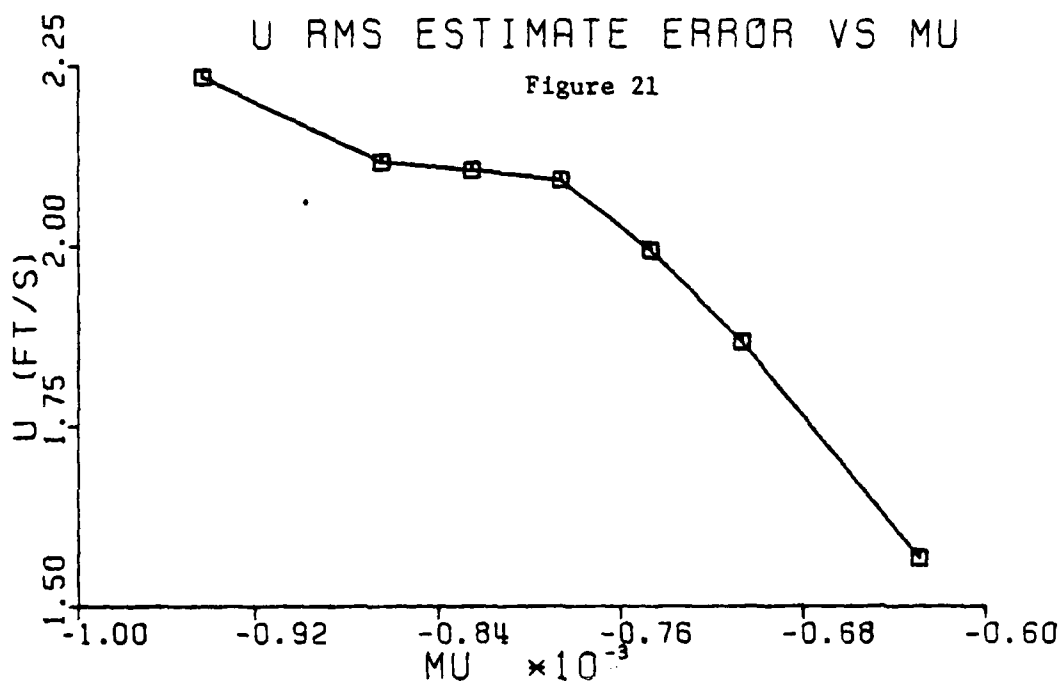
Figure 21

Figures 21 & 22. Sensitivity of $\bar{u}$ and $\bar{w}$ rms estimate errors vs variation in M_u stability derivate.

W RMS ESTIMATE ERROR VS MU

Figure 22

49

THETA RMS ESTIMATE ERROR VS MU
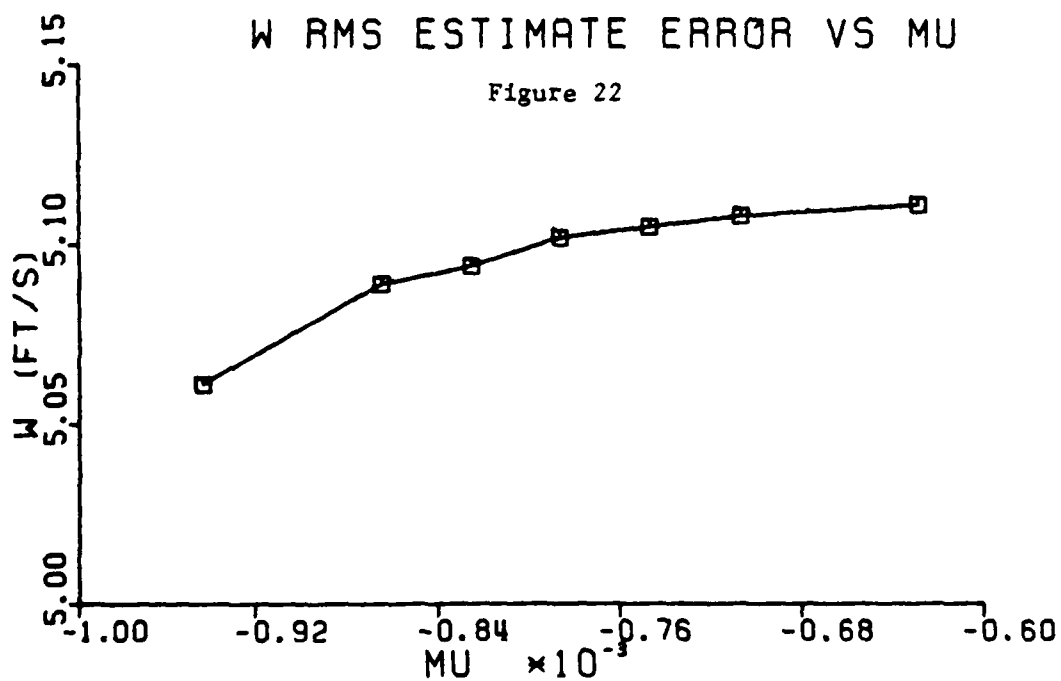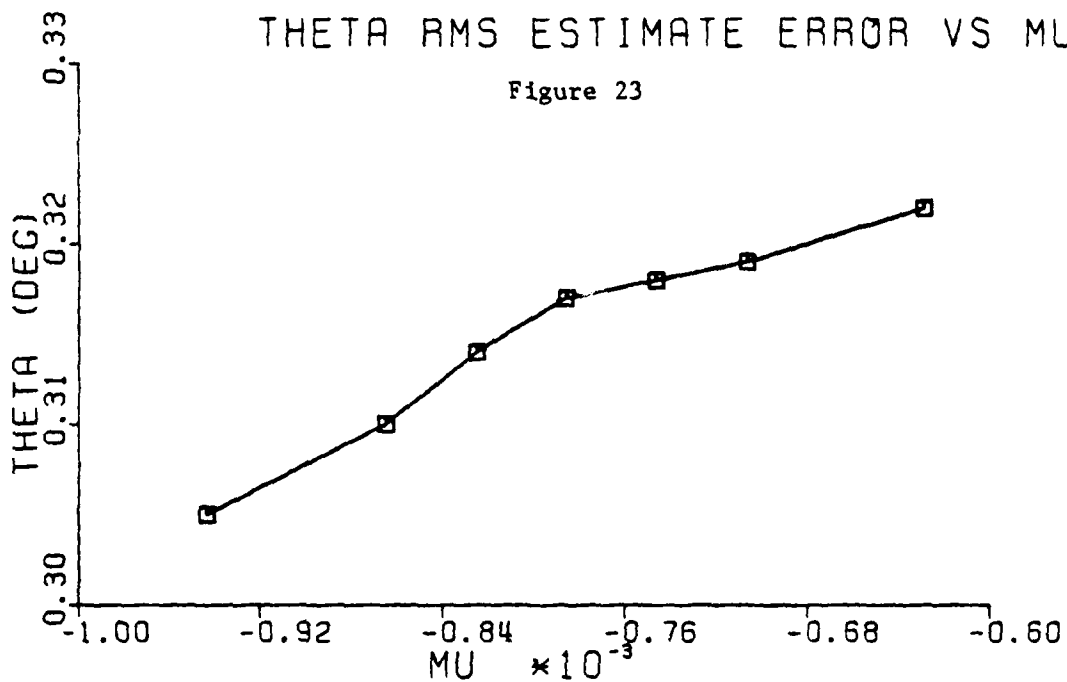
Figure 23

Figures 23 & 24. Sensitivity of $\bar{\theta}$ and $\bar{h}$ rms estimate errors vs variation in Mu stability derivative.

H RMS ESTIMATE ERROR VS MU

Figure 24

WG RMS ESTIMATE ERROR VS MU
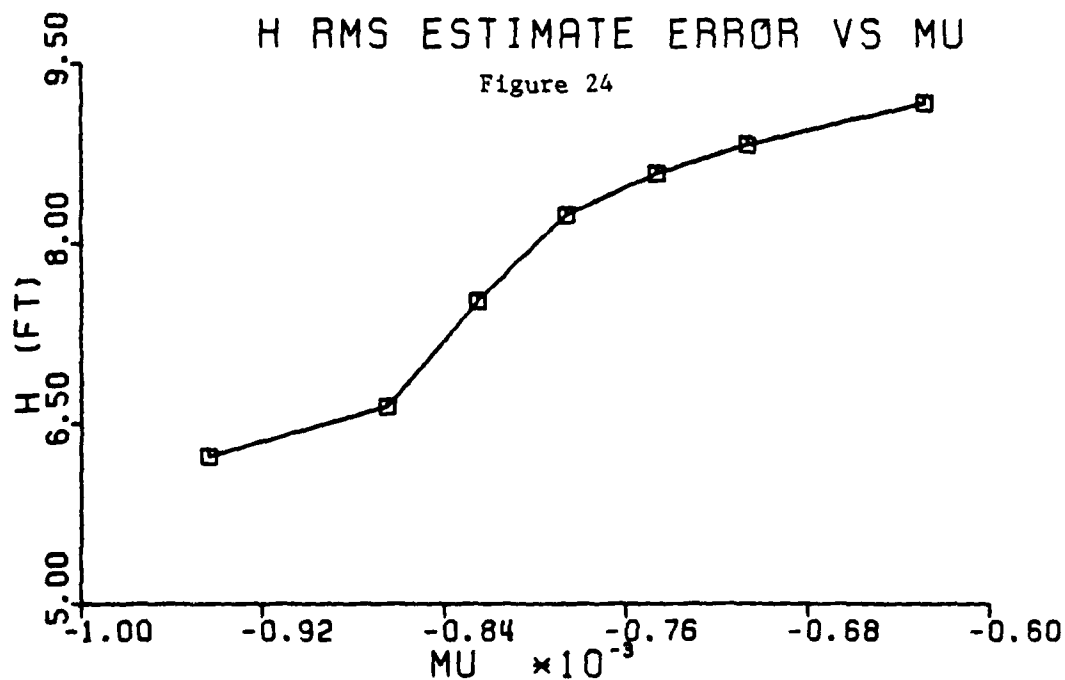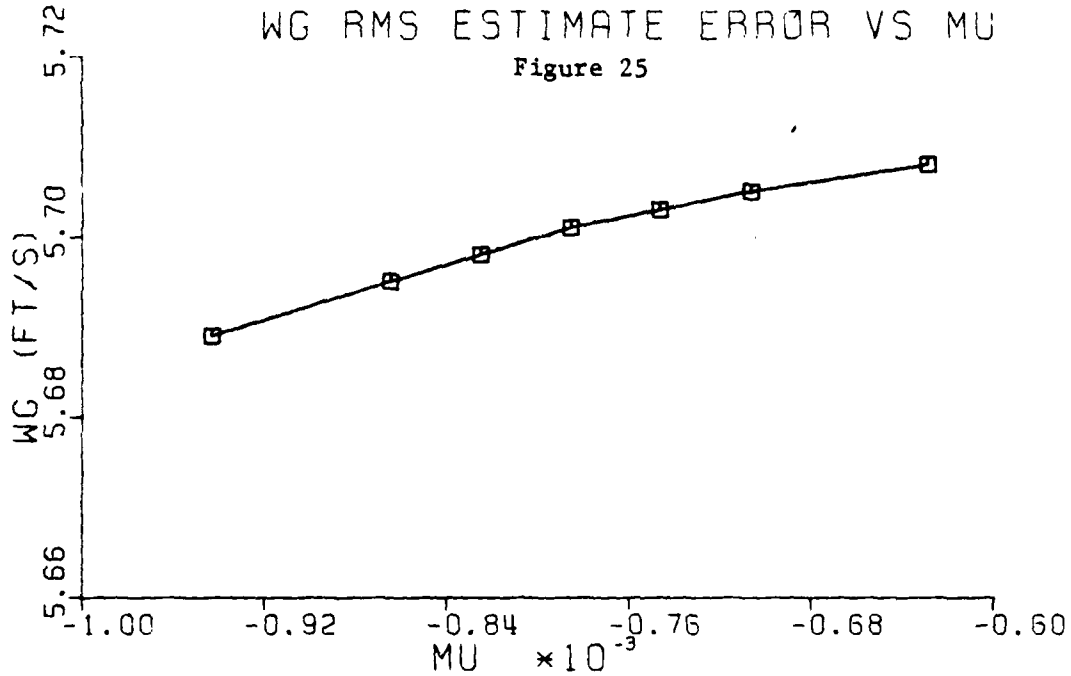
Figure 25

Figures 25 & 26. Sensitivity of $\bar{w}_g$ and $\bar{u}_g$ rms estimate errors vs variation in Mu stability derivative.

UG RMS ESTIMATE ERROR VS MU

Figure 26

51

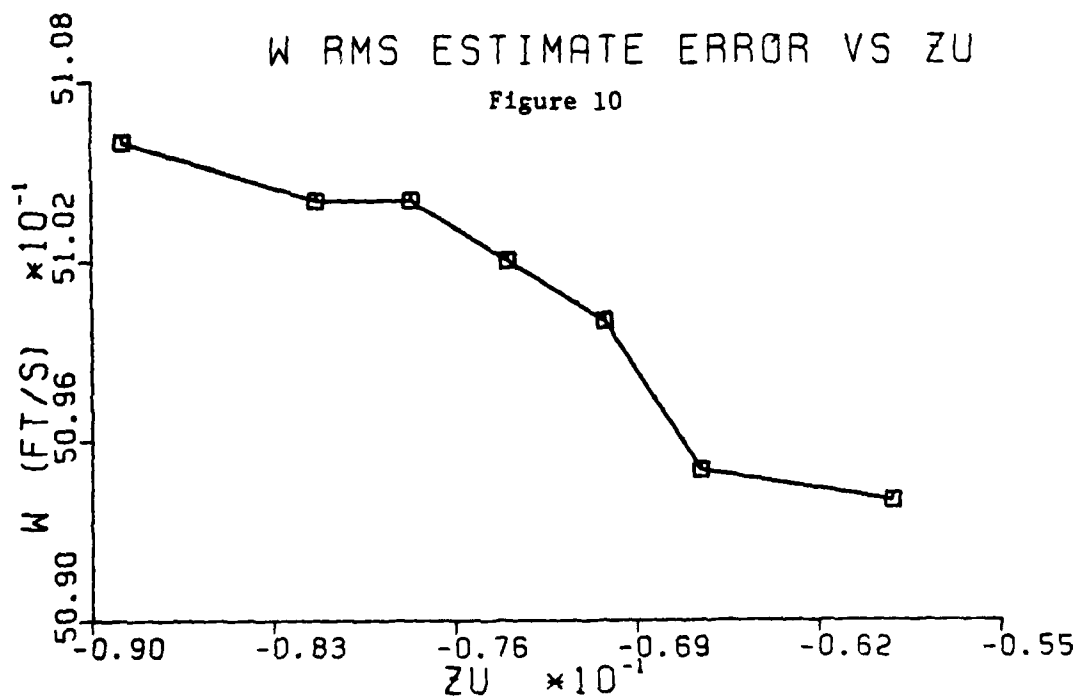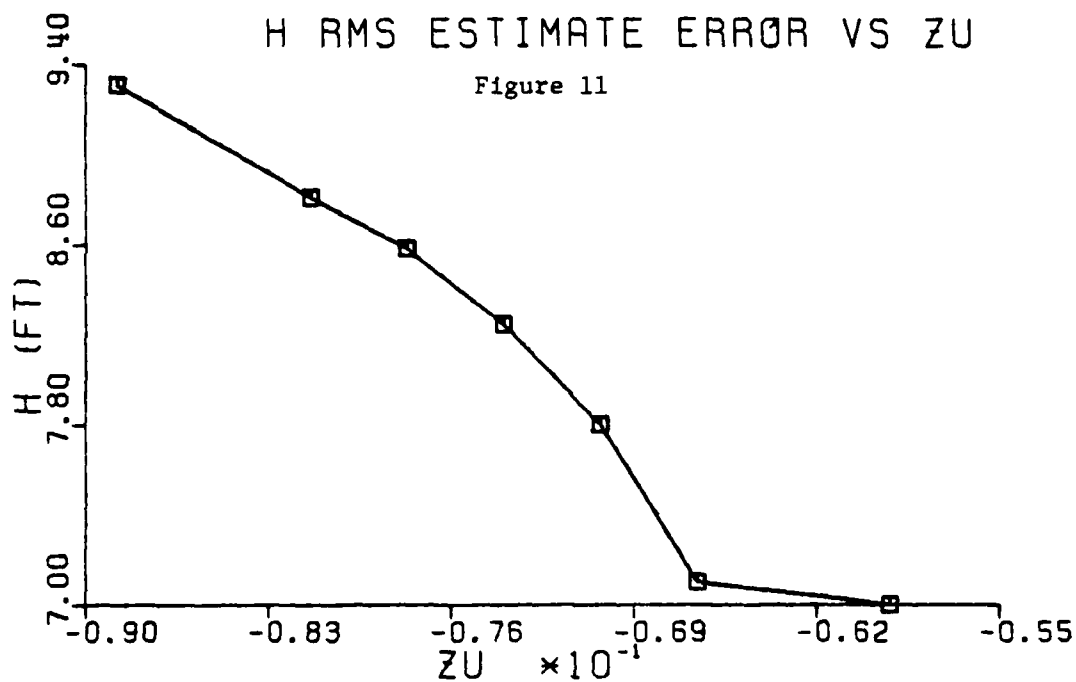**U RMS ESTIMATE ERROR VS MW**
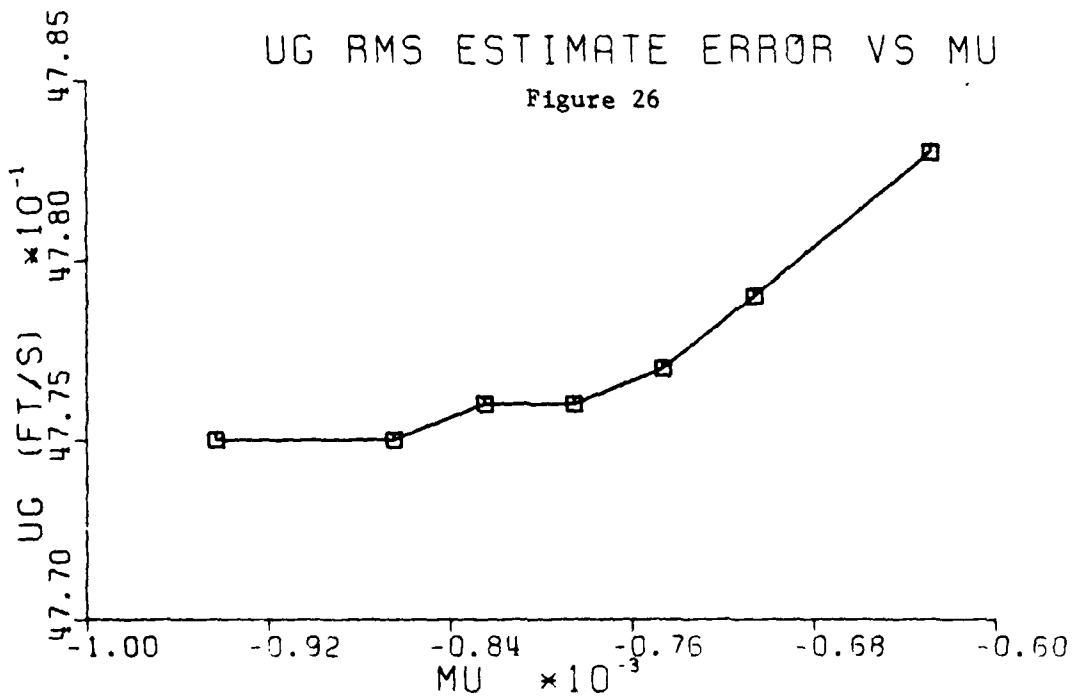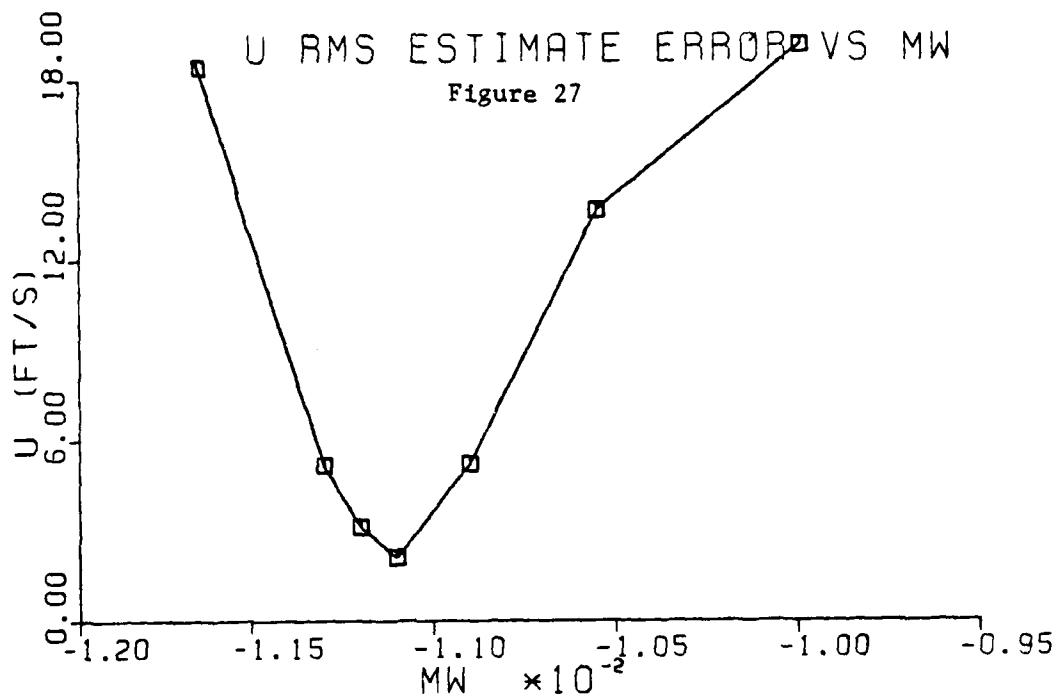
Figure 27

Figures 27 & 28. Sensitivity of $\bar{u}$ and $\bar{w}$ rms estimate errors vs variation in Mw stability derivative.

W RMS ESTIMATE ERROR VS MW

Figure 28

52

Q RMS ESTIMATE ERROR VS MW

Figure 29

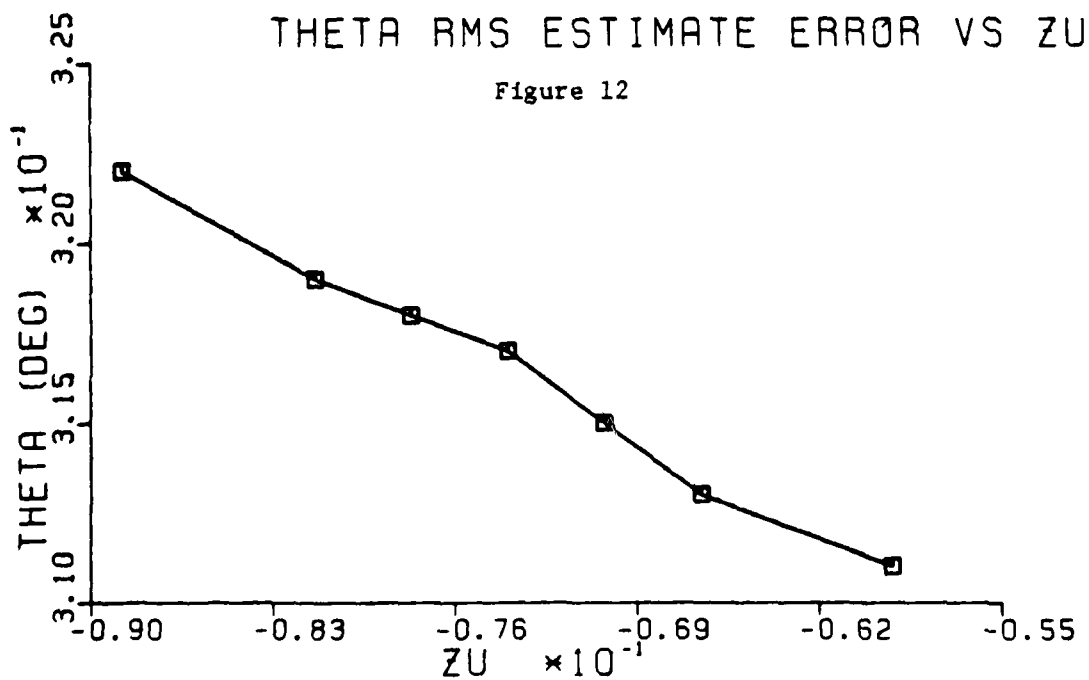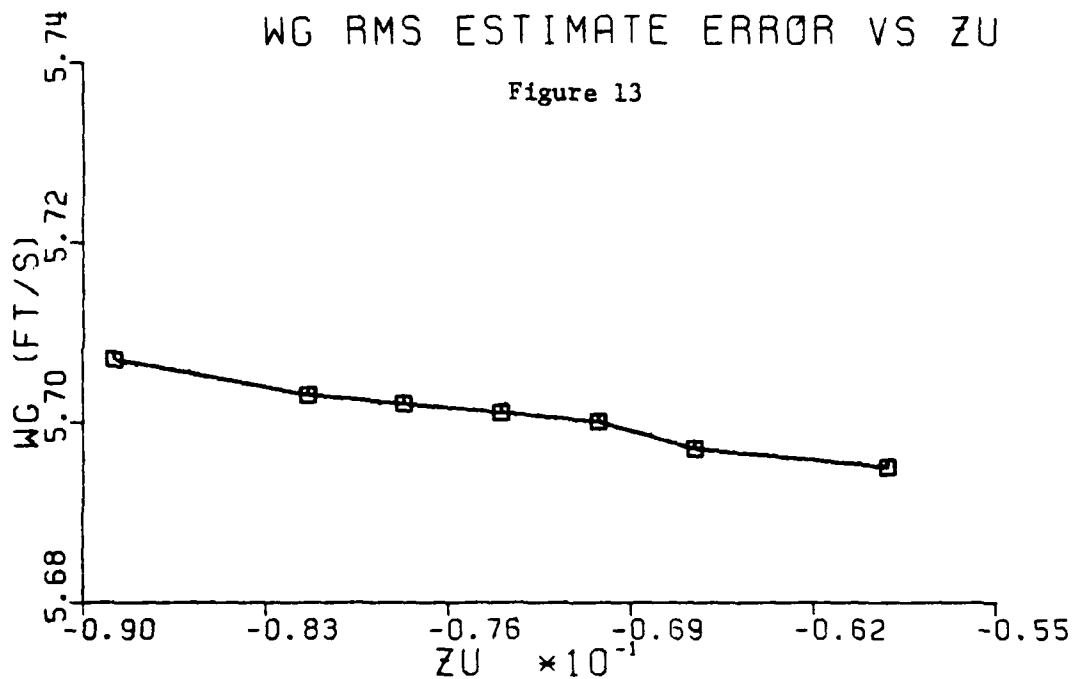# THETA RMS ESTIMATE ERROR VS MW
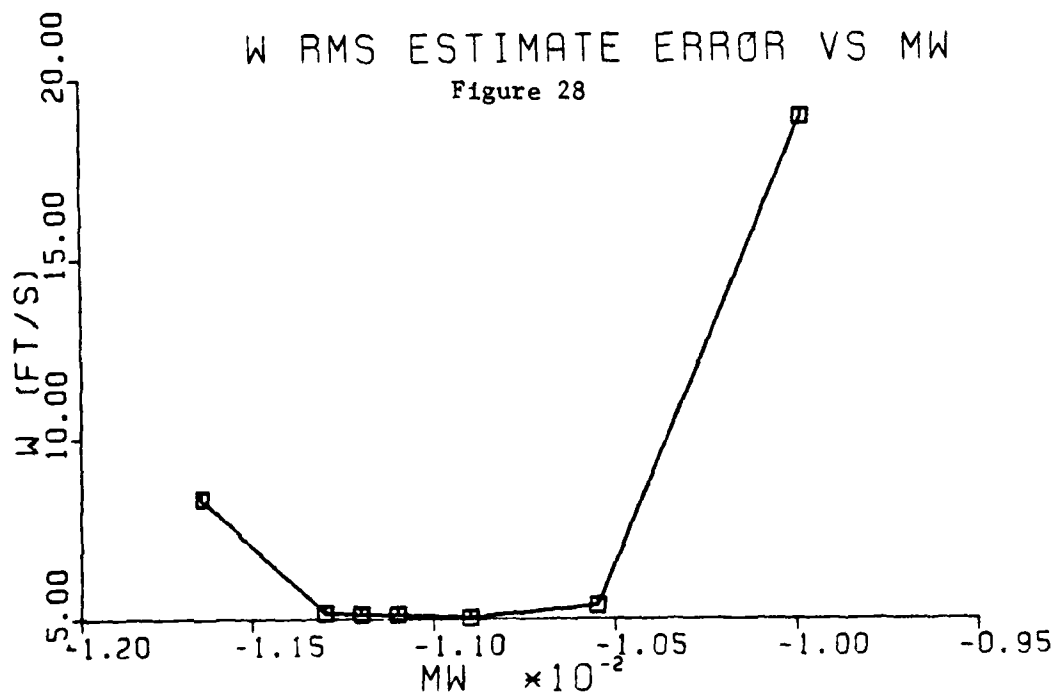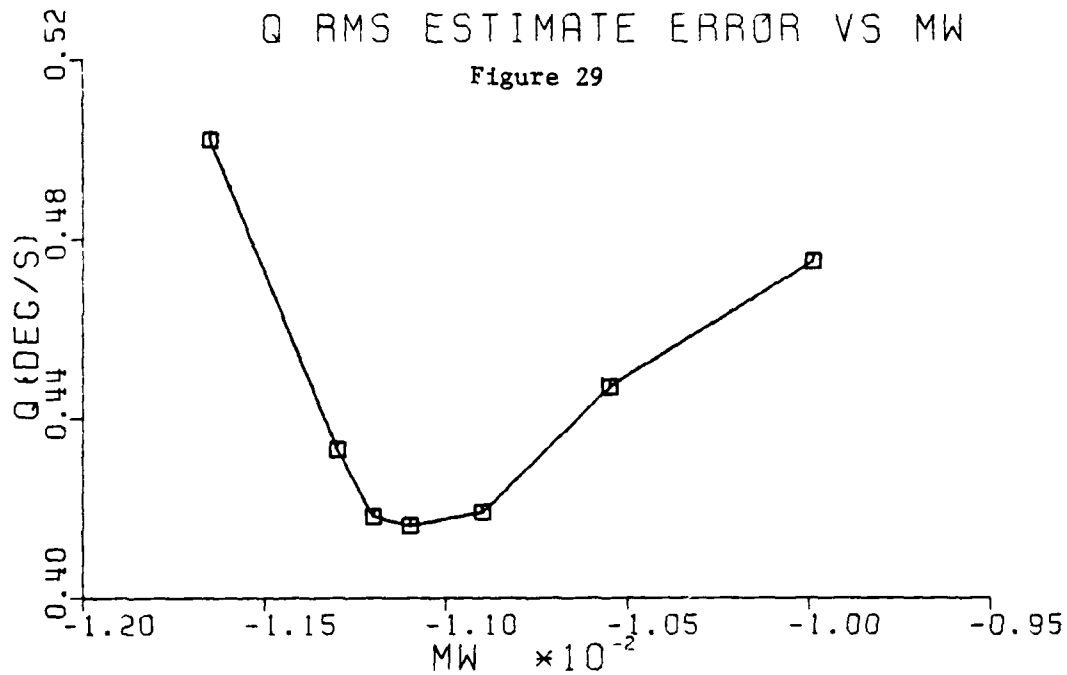
Figures 29 & 30. Sensitivity of $\bar{q}$ and $\bar{\theta}$ rms estimate errors vs variation in Mw stability derivative.

Figure 30

H RMS ESTIMATE ERROR VS MW
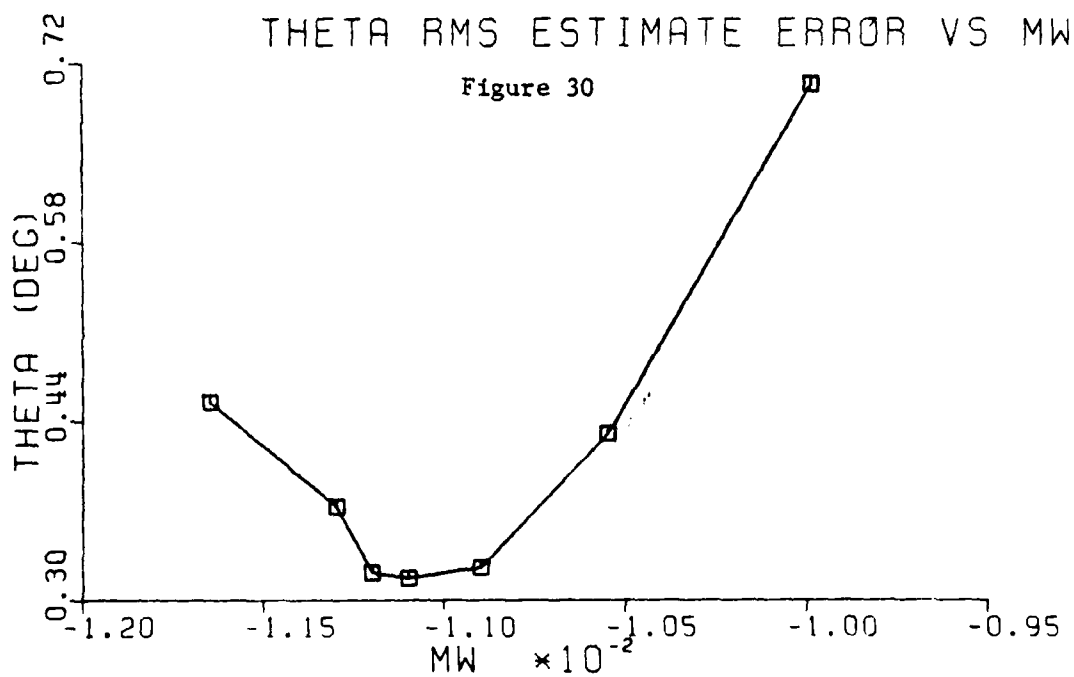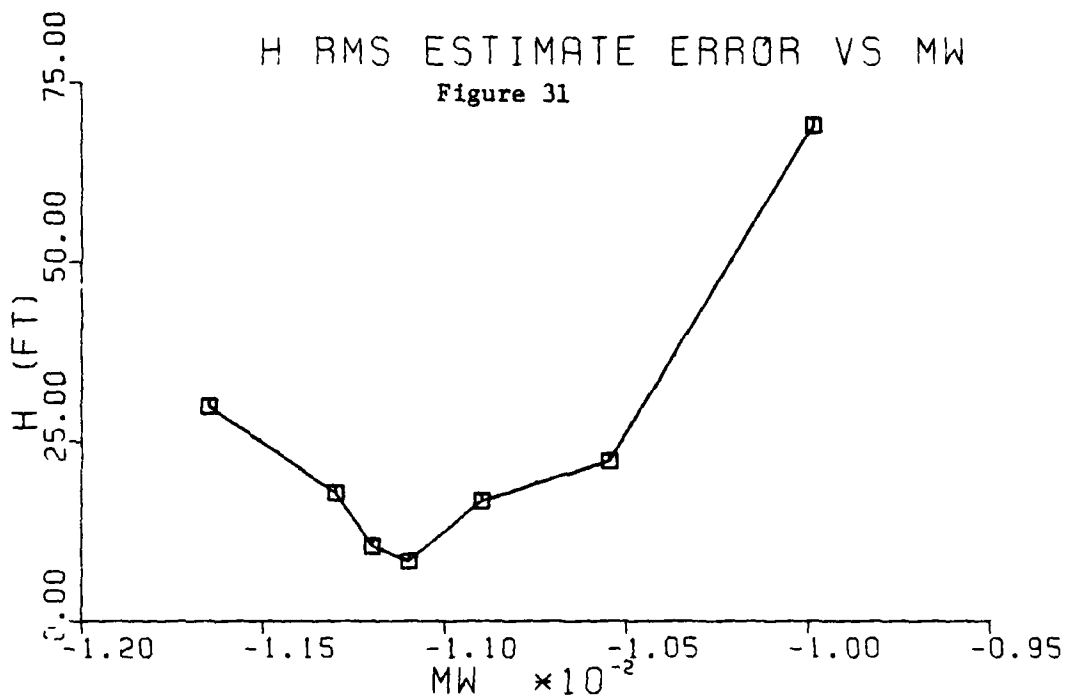
Figure 31

Figures 31 & 32. Sensitivity of $\bar{h}$ and $\bar{w}_g$ rms estimate errors vs variation in M_w stability derivative.

WG RMS ESTIMATE ERROR VS MW

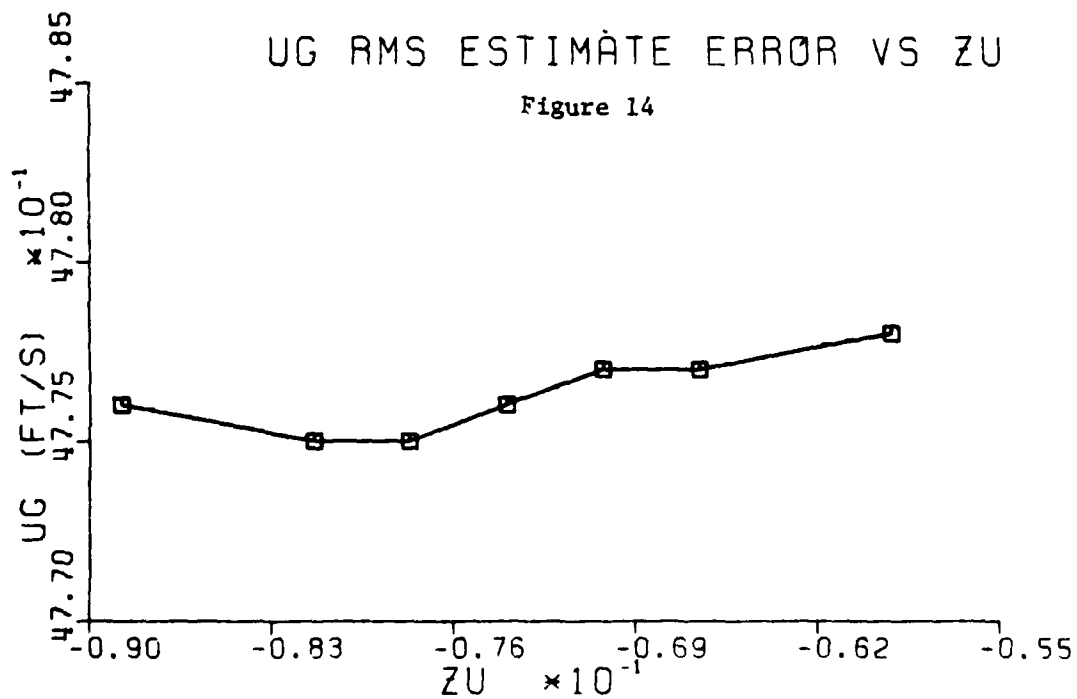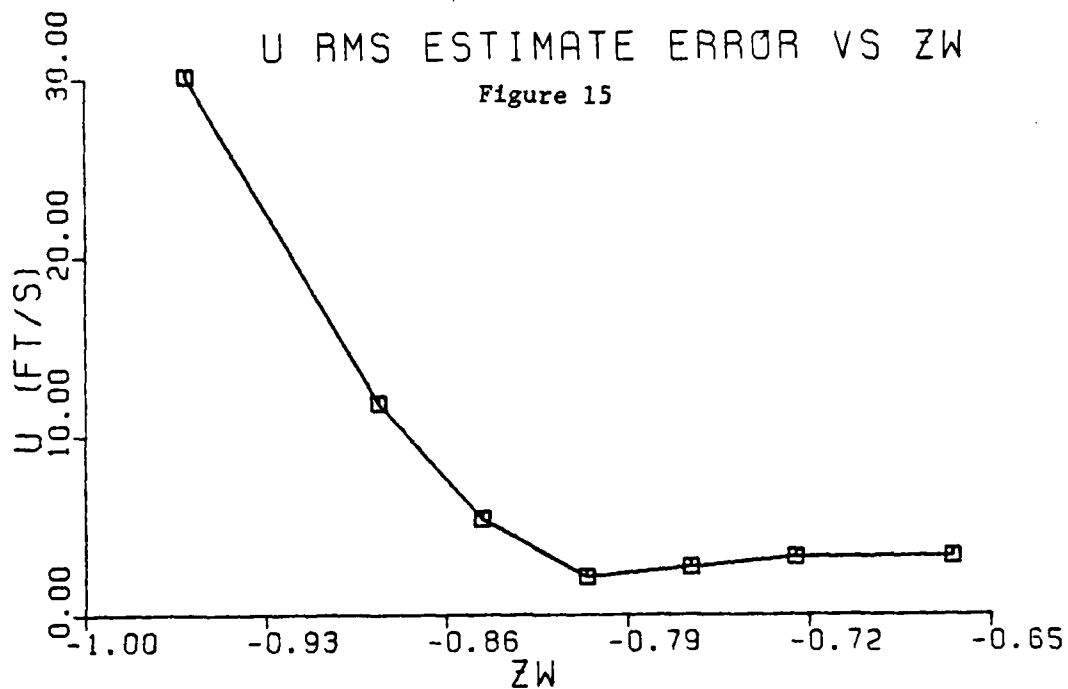### Figure 32
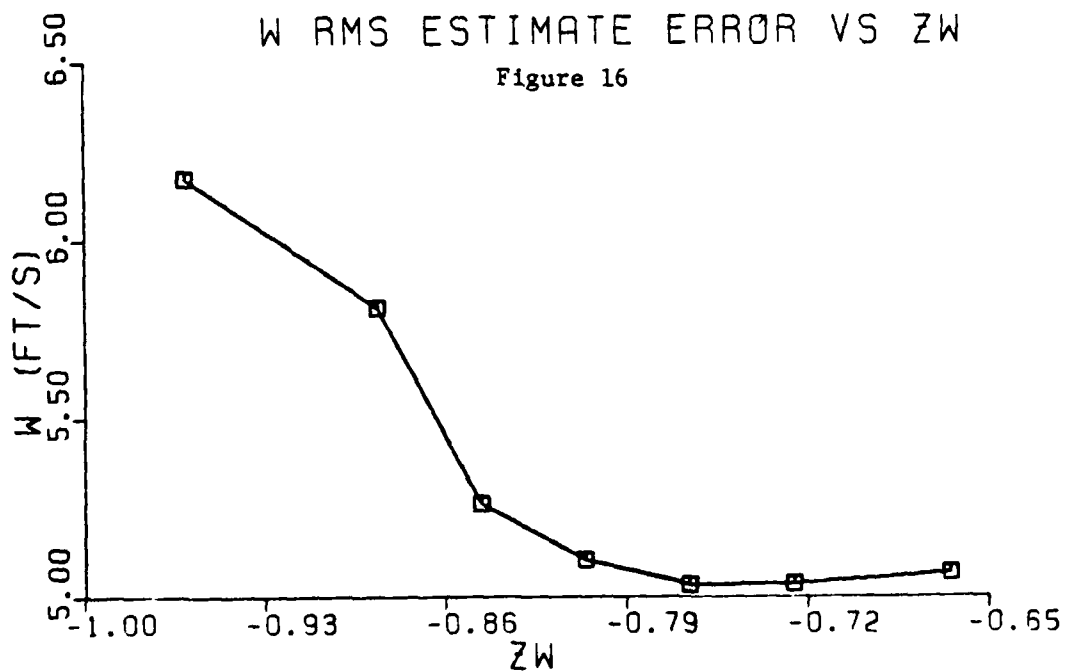

54

U RMS ESTIMATE ERROR VS MQ
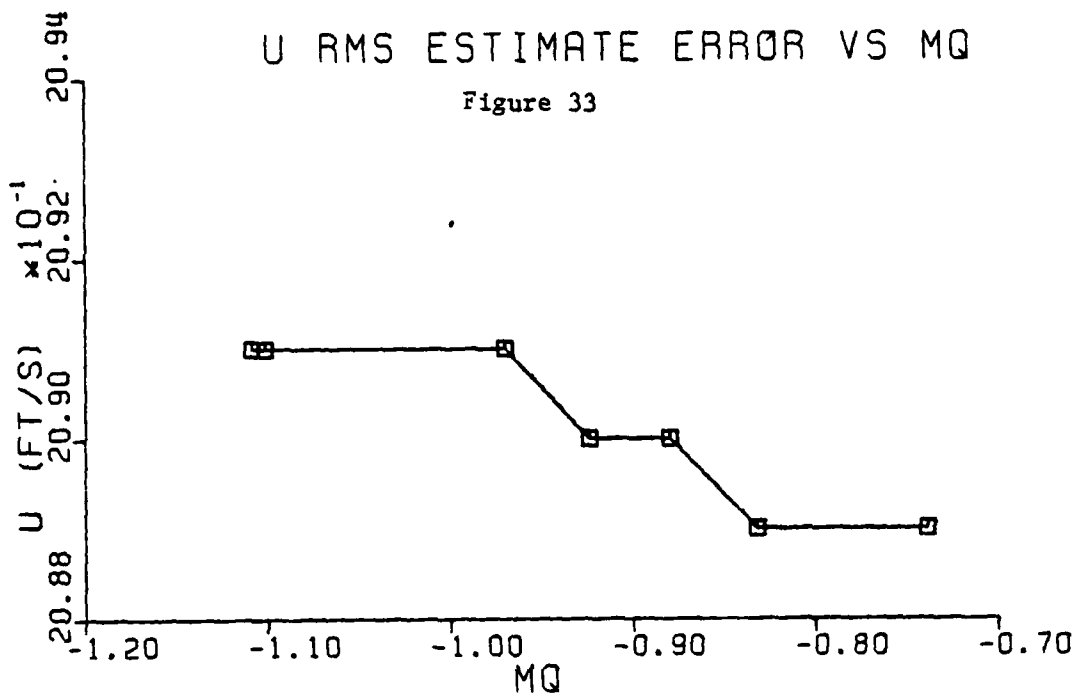
Figure 33

Figures 33 & 34. Sensitivity of $\bar{u}$ and $\bar{h}$ rms estimate errors vs variation in Mq stability derivative.

H RMS ESTIMATE ERROR VS MQ

Figure 34

55

U RMS ESTIMATE ERROR VS MWDOT
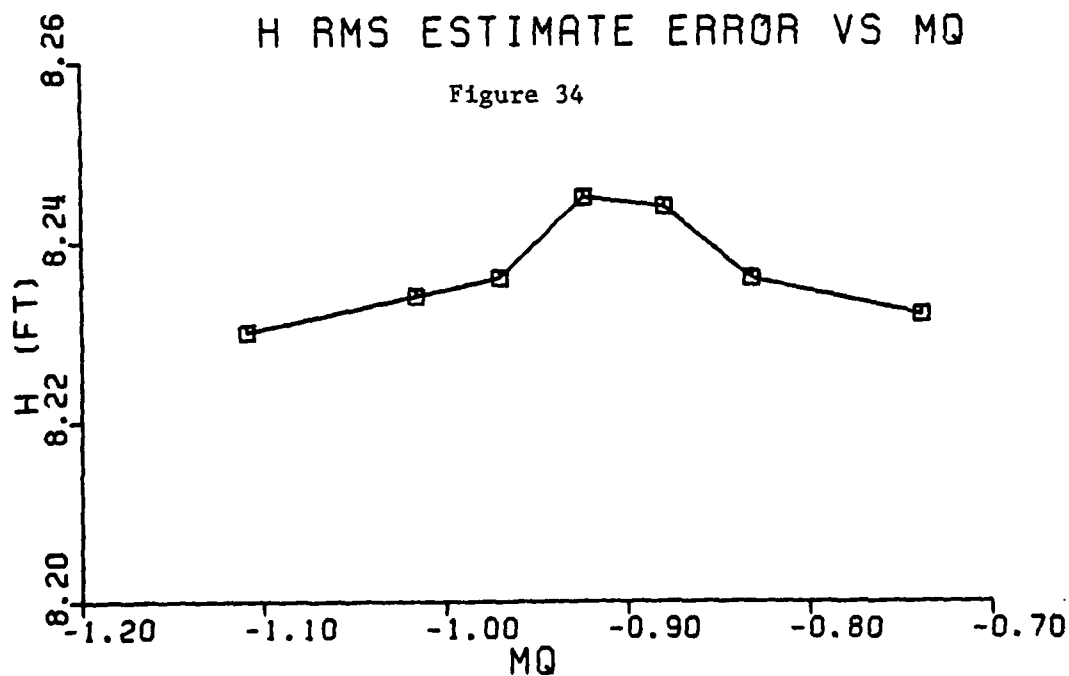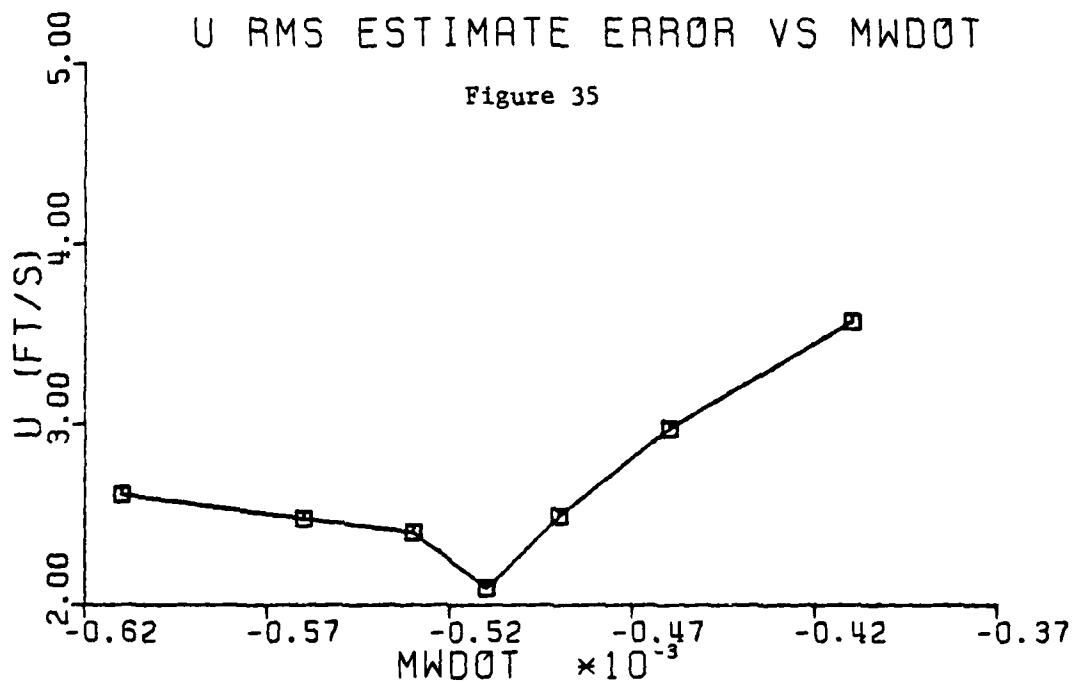
Figure 35

Figures 35 & 36.   Sensitivity of $\bar{u}$ and $\bar{w}$ rms estimate errors vs variation in $M_{\dot{w}}$ stability derivatives.

W RMS ESTIMATE ERROR VS MWDOT

Figure 36

56

Q RMS ESTIMATE ERROR VS MWDOT
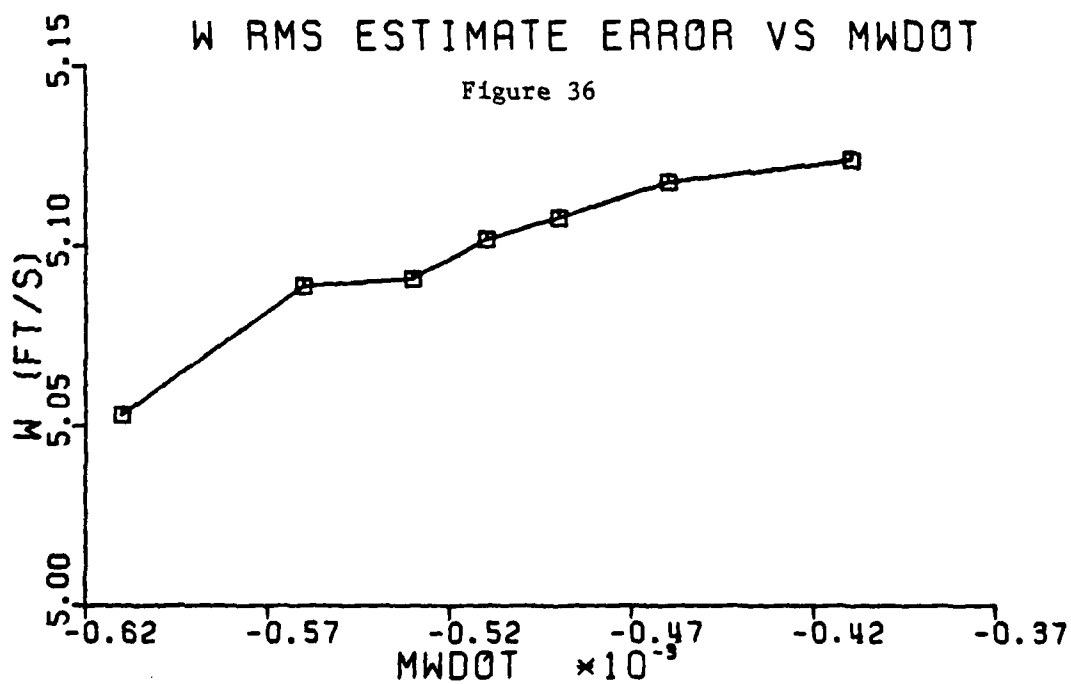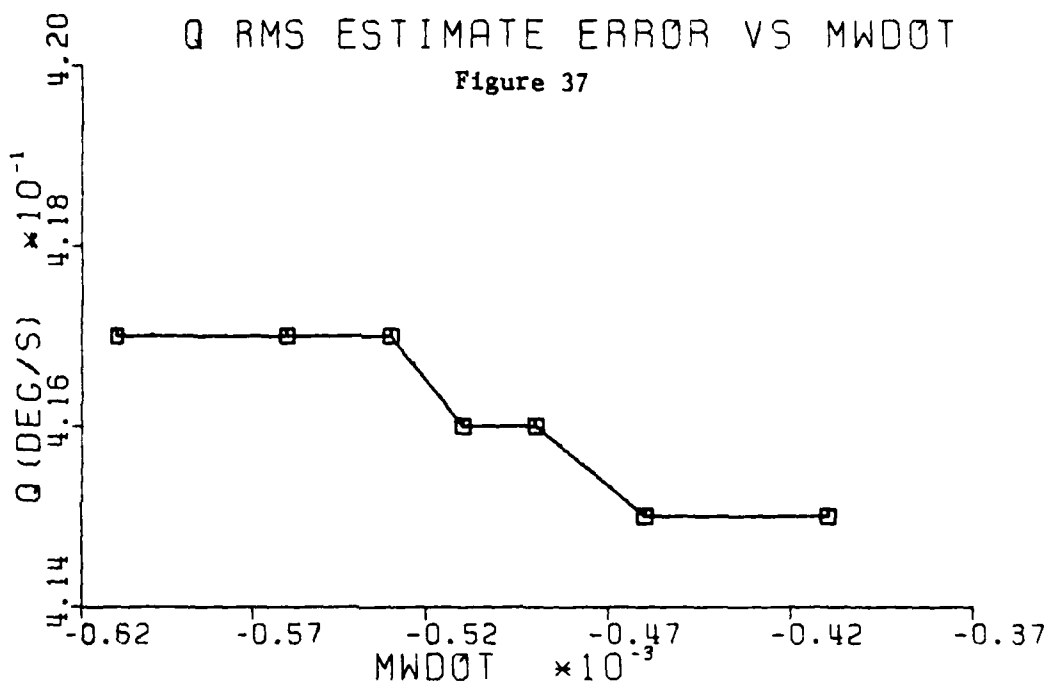
Figure 37

Figures 37 & 38. Sensitivity of $\bar{q}$ and $\bar{\theta}$ rms estimate errors vs variation in $M\dot{w}$ stability derivative.

THETA RMS ESTIMATE ERROR VS MWDOT

Figure 38

57

H RMS ESTIMATE ERROR VS MWDOT
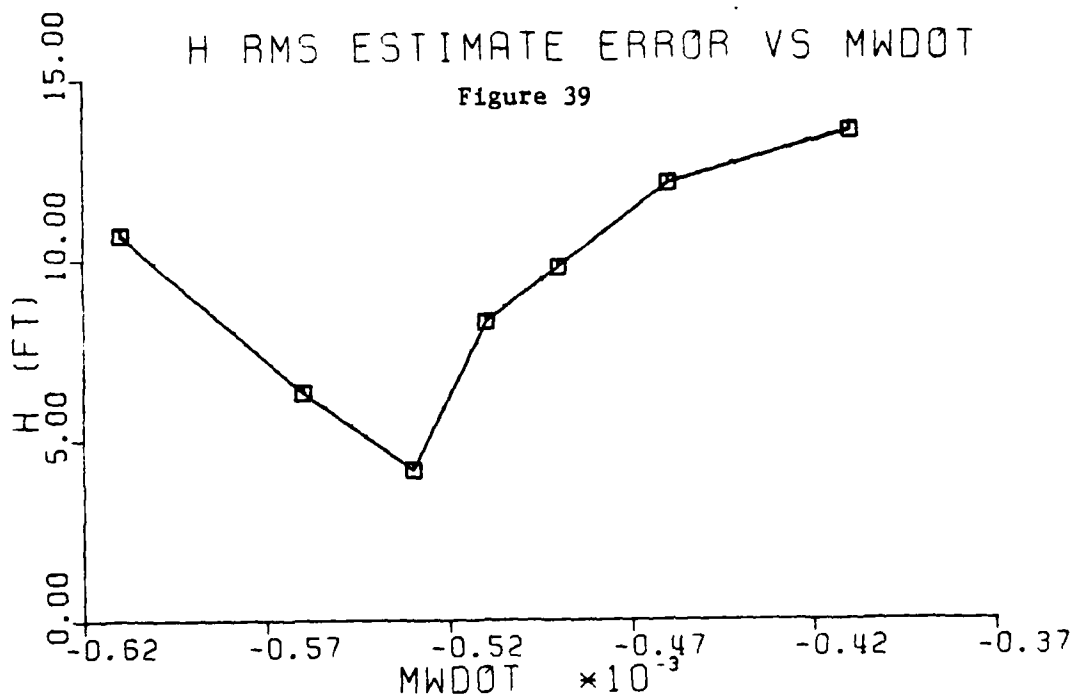
Figure 39

Figures 39 & 40.   Sensitivity of $\bar{h}$ and $\bar{w}_g$ rms estimate errors vs variation of $M\dot{w}$ stability derivative.

WG RMS ESTIMATE ERROR VS MWDOT

Figure 40

58

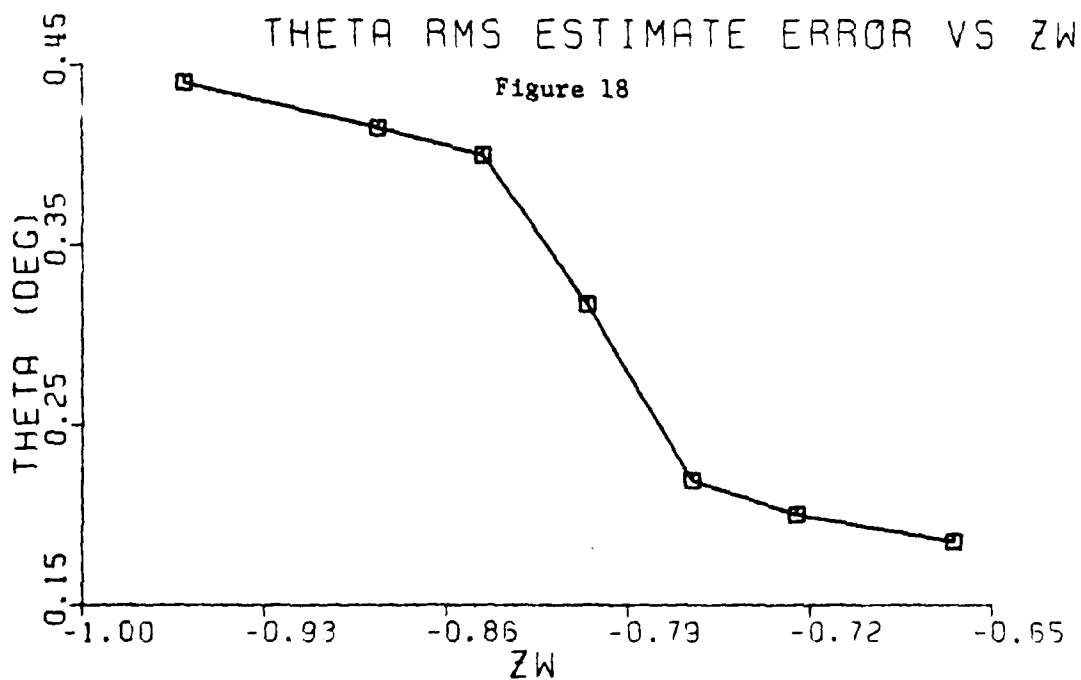# VB RMS ESTIMATE ERROR VS YV
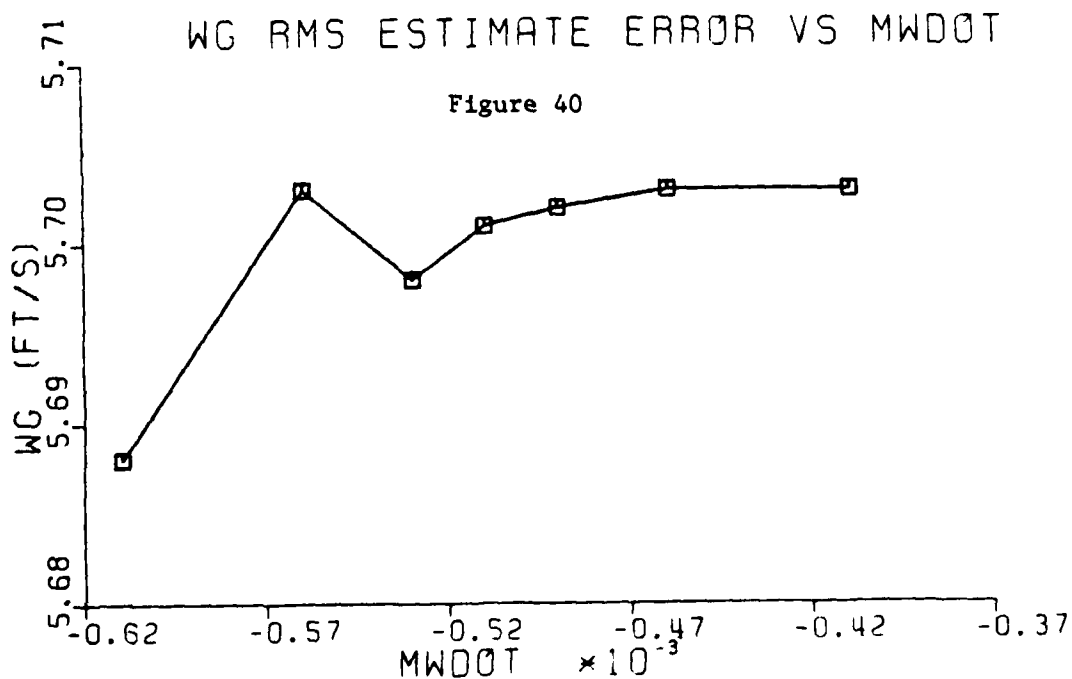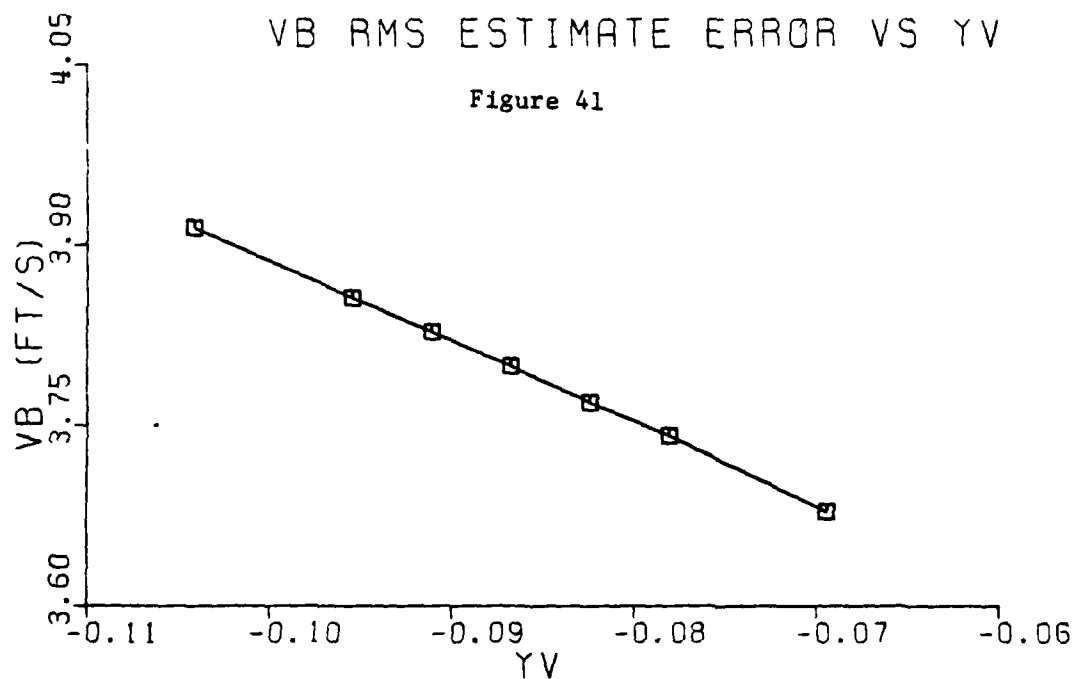
Figure 41

Figures 41 & 42. Sensitivity of $V\bar{\beta}$ and $\bar{p}$ rms estimate errors vs variation in Yv stability derivative.

P RMS ESTIMATE ERROR VS YV

Figure 42
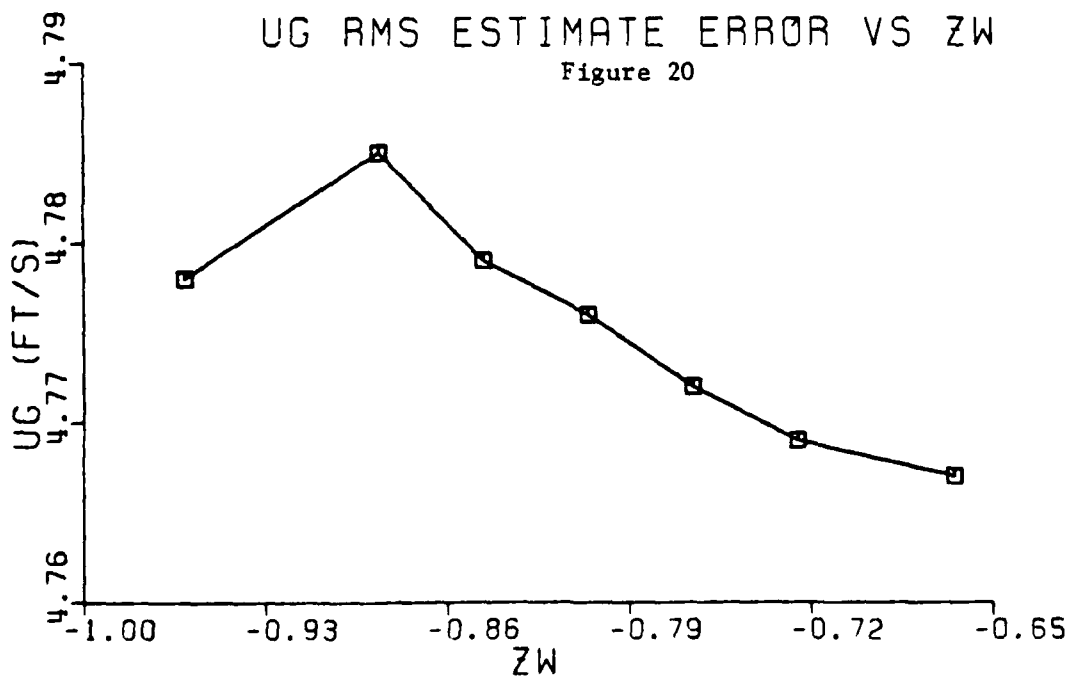
PHI RMS ESTIMATE ERROR VS YV
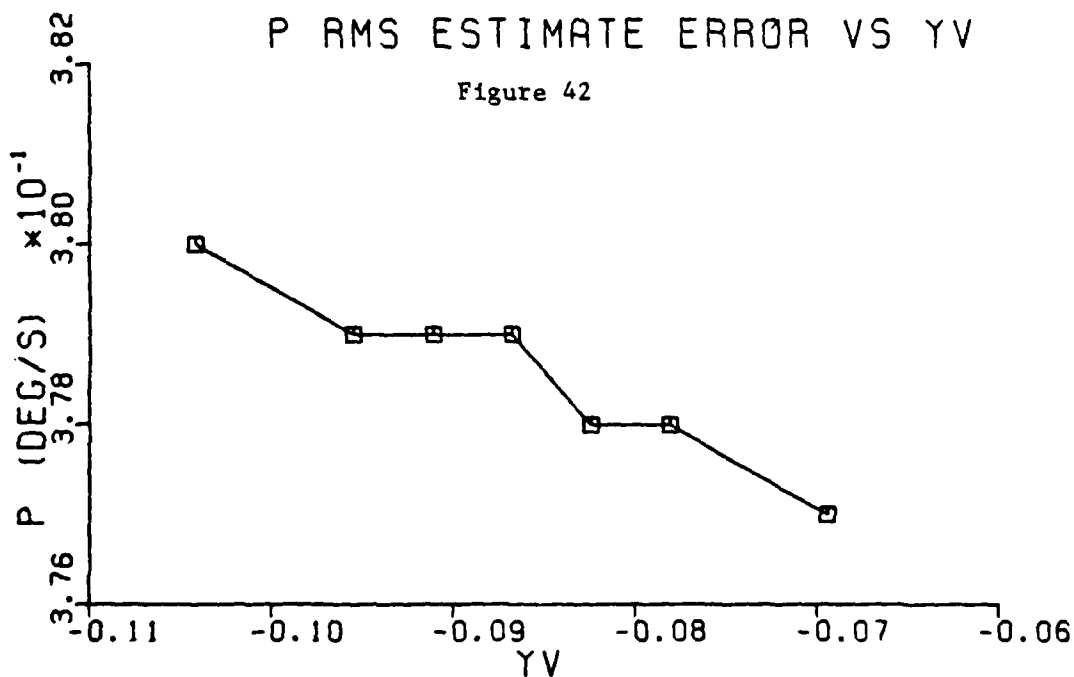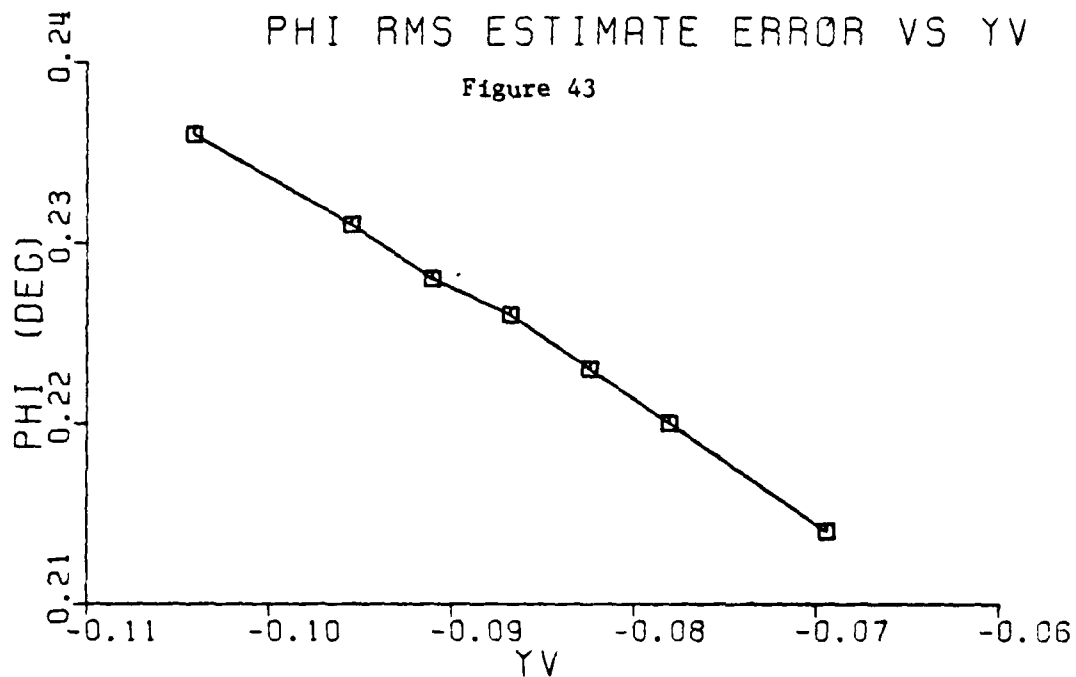
Figure 43

Figures 43 & 44. Sensitivity of $\bar{\theta}$ and $V\bar{\beta}_g$ rms estiamte errors vs variation in Yv stability derivative.

VBG RMS ESTIMATE ERROR VS YV

Figure 44

60

VB RMS ESTIMATE ERROR VS NB'
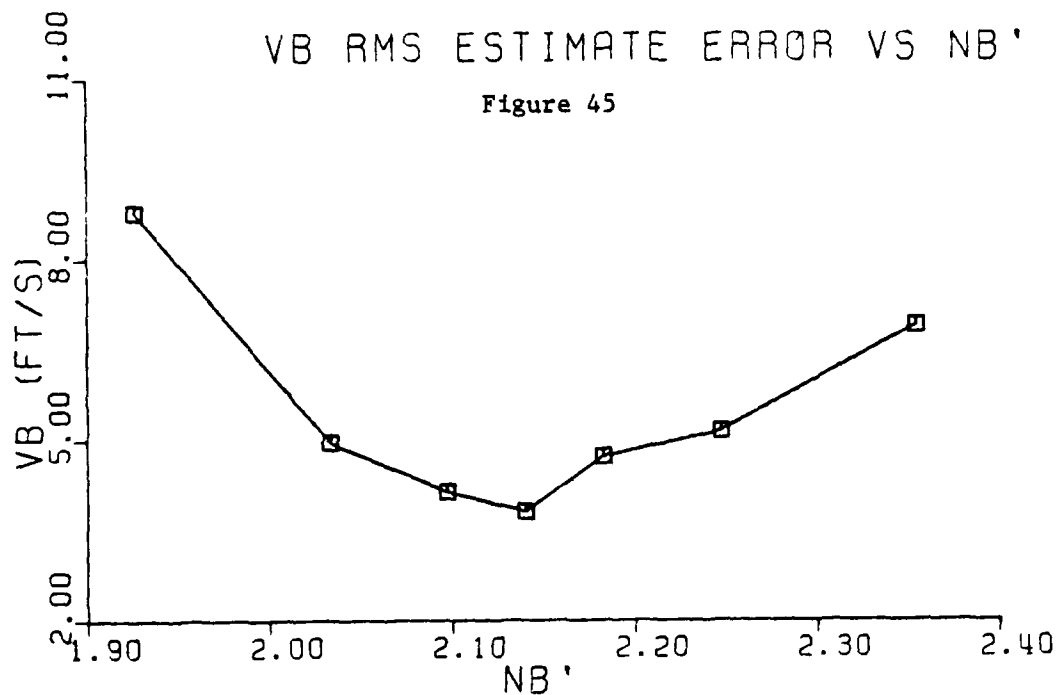
Figure 45

Figures 45 & 46. Sensitivity of $V\bar{\beta}$ and $\bar{r}$ rms estimate errors vs variation in N_β' stability derivative.

R RMS ESTIMATE ERROR VS NB'

Figure 46

P RMS ESTIMATE ERROR VS NB'
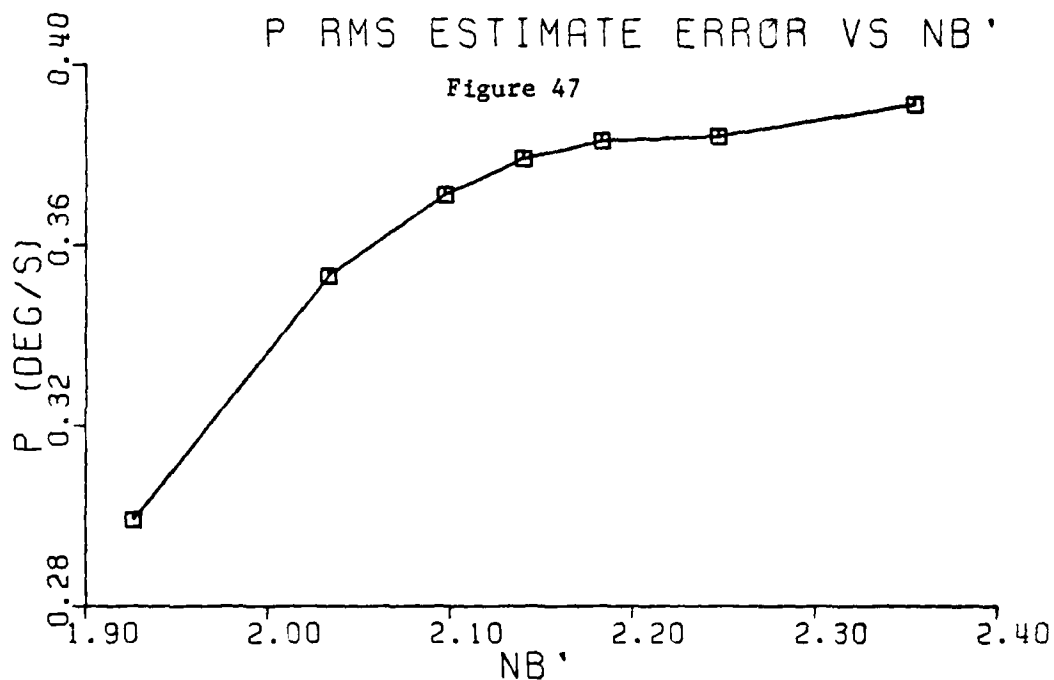
Figure 47

Figures 47 & 48. Sensitivity of $\bar{p}$ and $\bar{\theta}$ rms estimate errors vs variation of N'_β stability derivative.

PHI RMS ESTIMATE ERROR VS NB'

Figure 48

PSI RMS ESTIMATE ERROR VS NB'
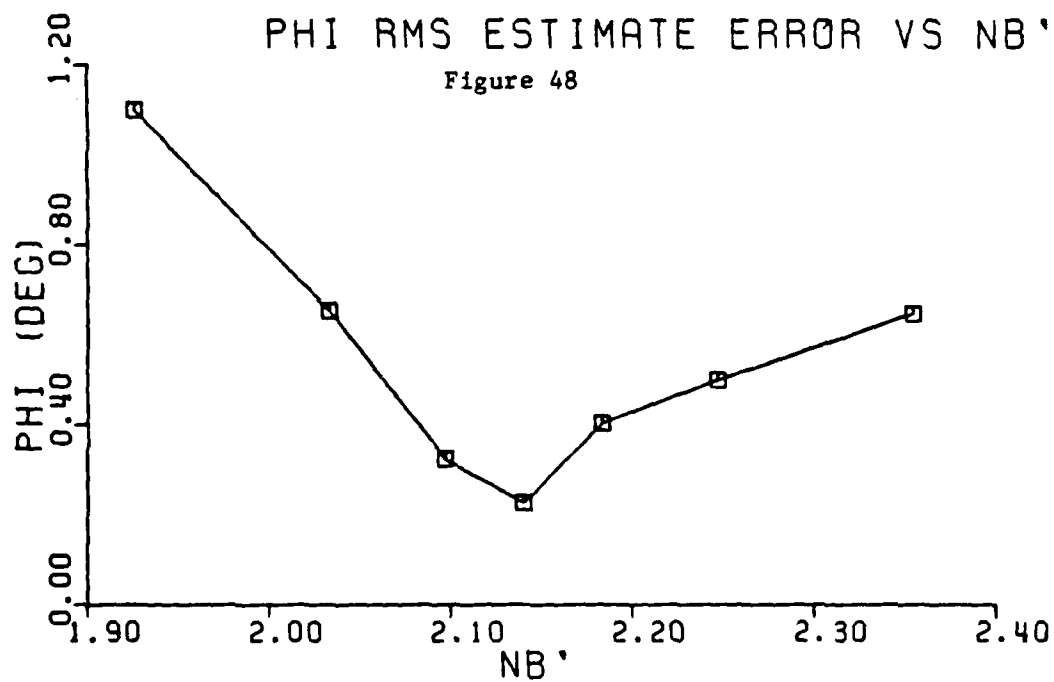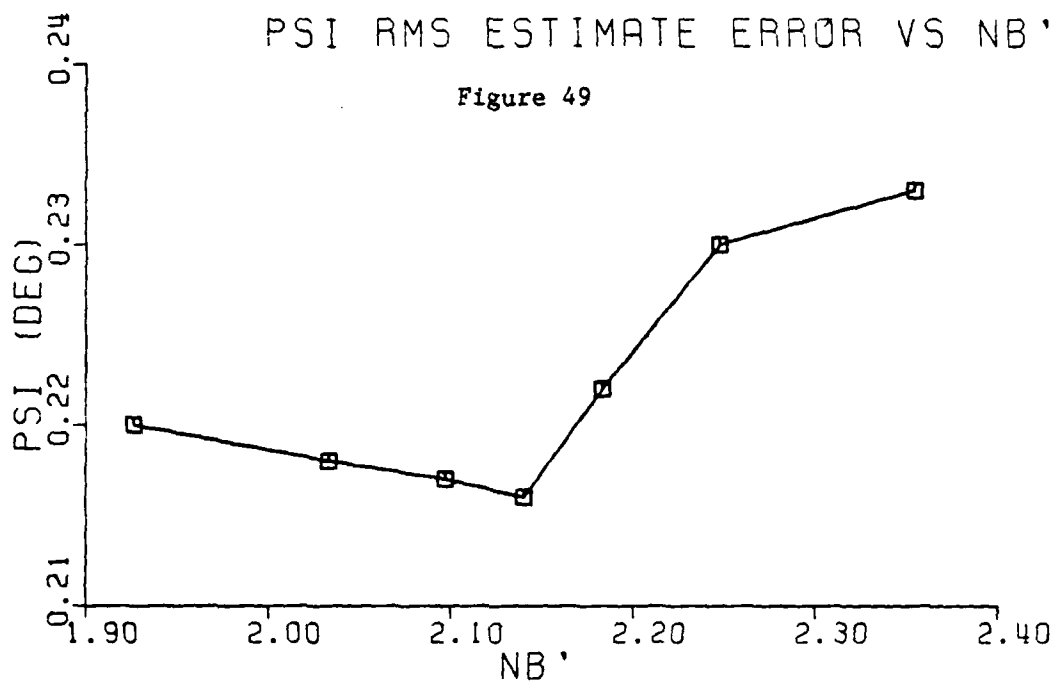
Figure 49

Figures 49 & 50. Sensitivity of $\bar{\psi}$ and $\overline{V\beta_g}$ rms estimate errors vs variation in N_β' stability derivative.

VBG RMS ESTIMATE ERROR VS NB'

Figure 50

63

VB RMS ESTIMATE ERROR VS NR'
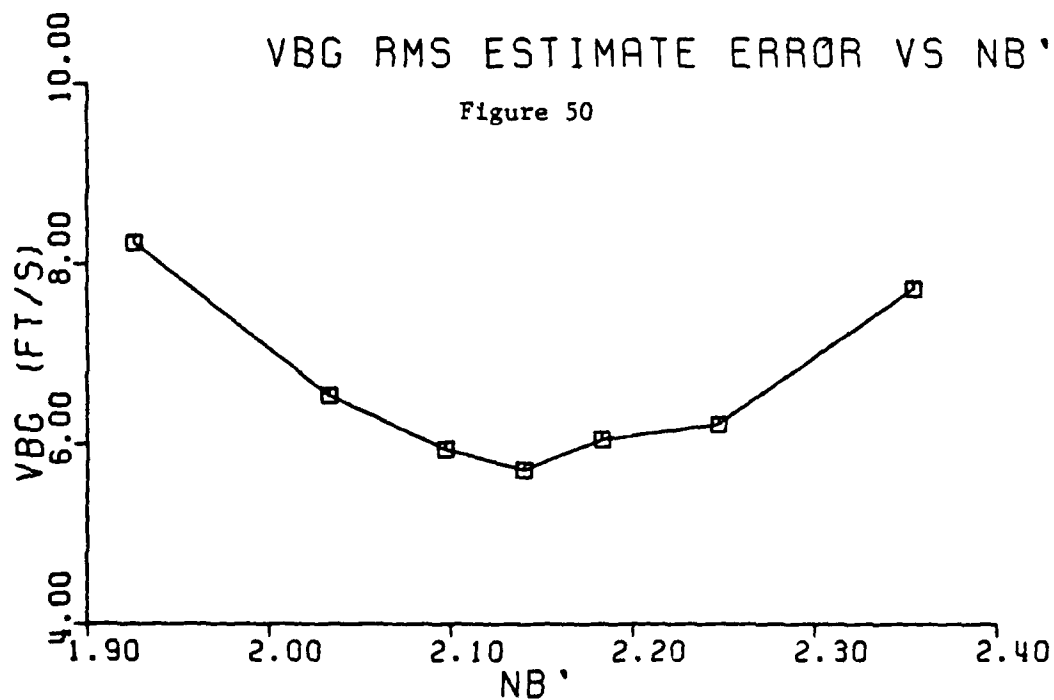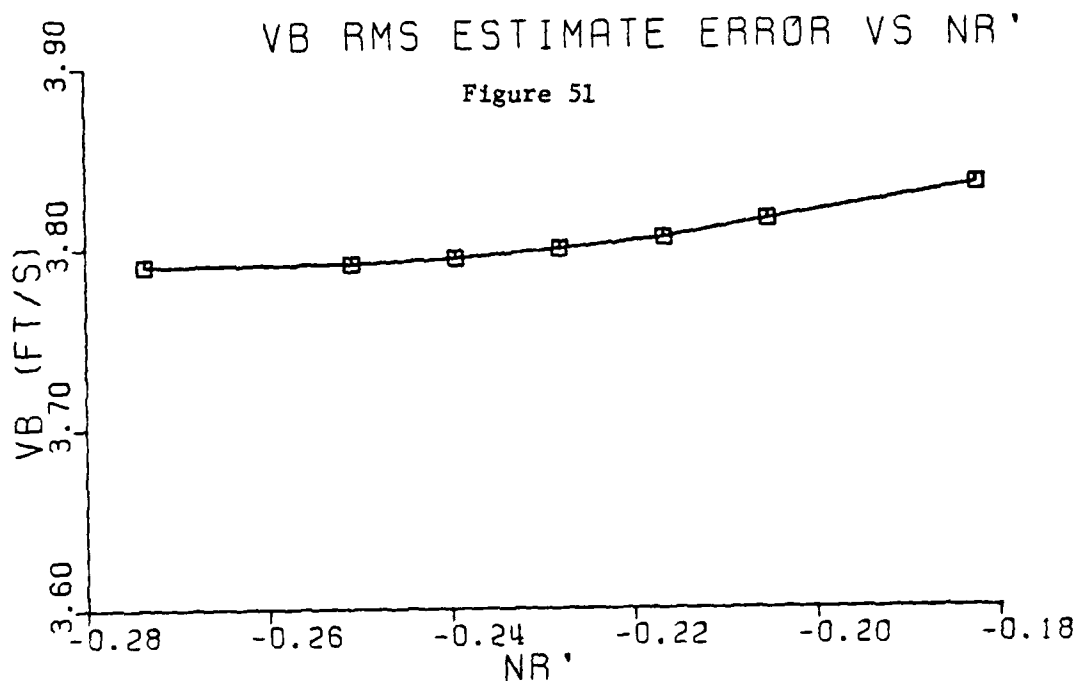
Figure 51

Figures 51 & 52. Sensitivity of V_{β}^{-} and $\bar{r}$ rms estimate errors vs variation in N_r' stability derivative.

R RMS ESTIMATE ERROR VS NR'

Figure 52

64

PHI RMS ESTIMATE ERROR VS NR'
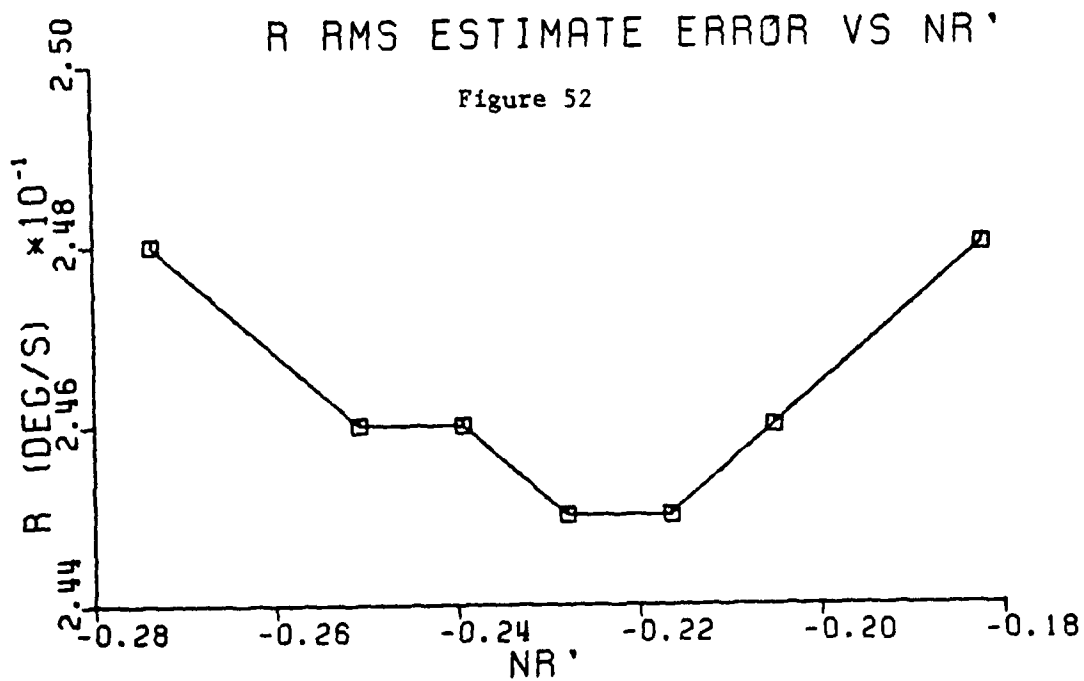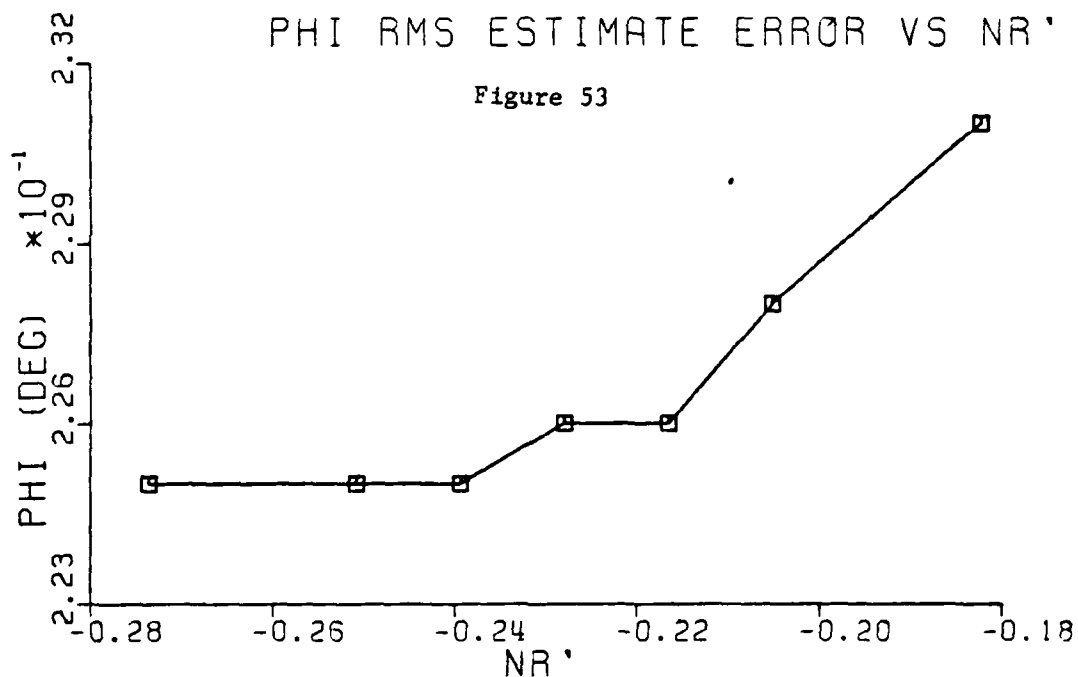
Figure 53

Figures 53 & 54. Sensitivity of $\bar{\theta}$ and $V_{\beta_g}^-$ rms estimate errors vs variation in N_r' stability derivative.

VBG RMS ESTIMATE ERROR VS NR'

Figure 54

65

VB RMS ESTIMATE ERROR VS NP'
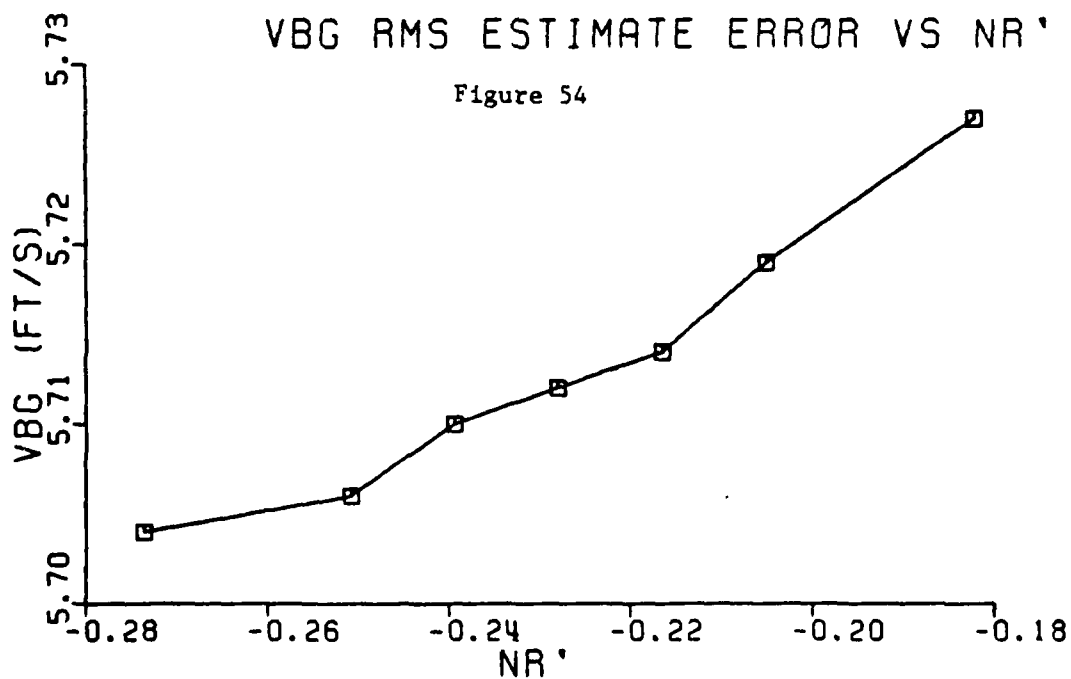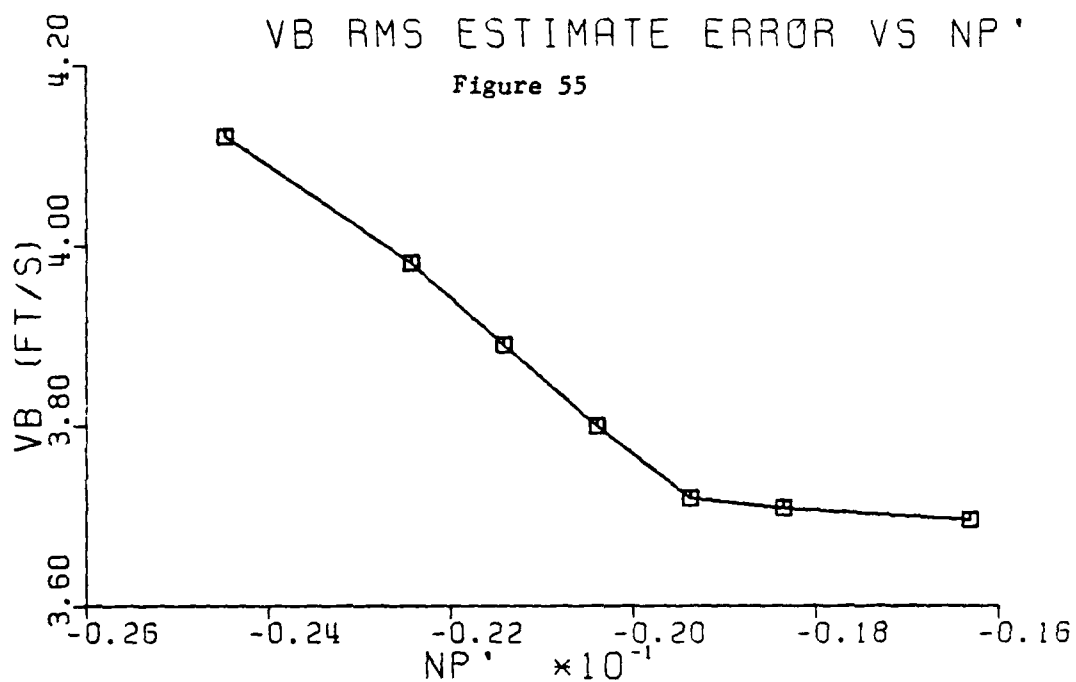
Figure 55

Figures 55 & 56. Sensitivity of $\bar{V}_\beta$ and $\bar{r}$ rms estimate errors vs variation in N_p' stability derivative.

R RMS ESTIMATE ERROR VS NP'

Figure 56

P RMS ESTIMATE ERROR VS NP'
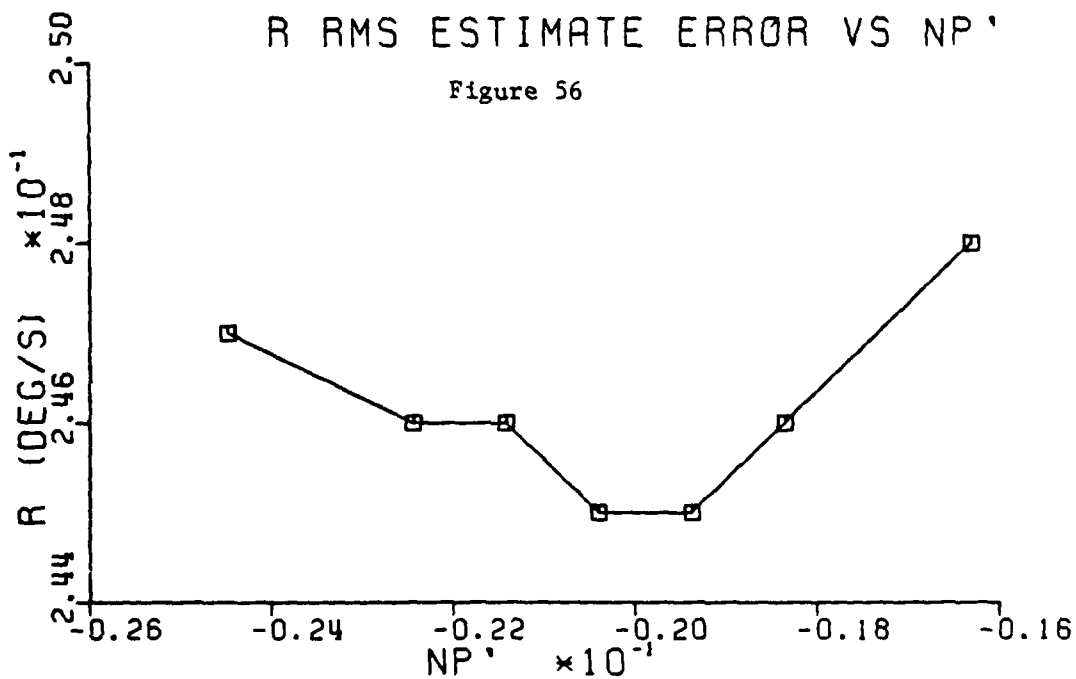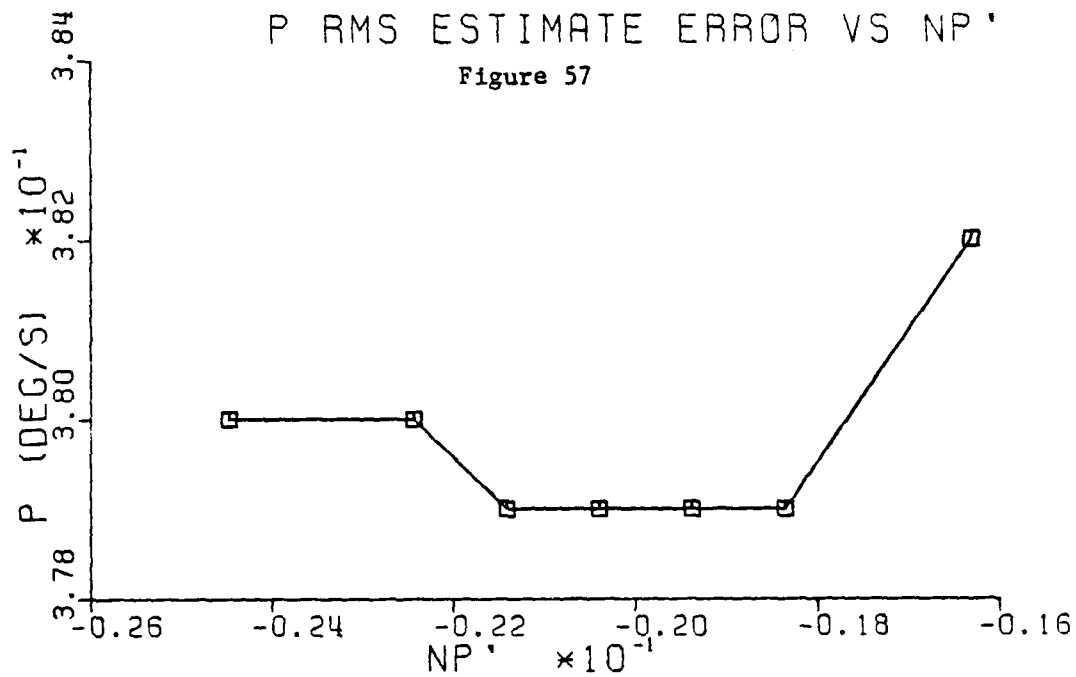
Figure 57

Figures 57 & 58. Sensitivity of $\bar{p}$ and $\bar{\theta}$ rms estimate errors vs variation of N_p' stability derivative.

PHI RMS ESTIMATE ERROR VS NP'

Figure 58

PSI RMS ESTIMATE ERROR VS NP'
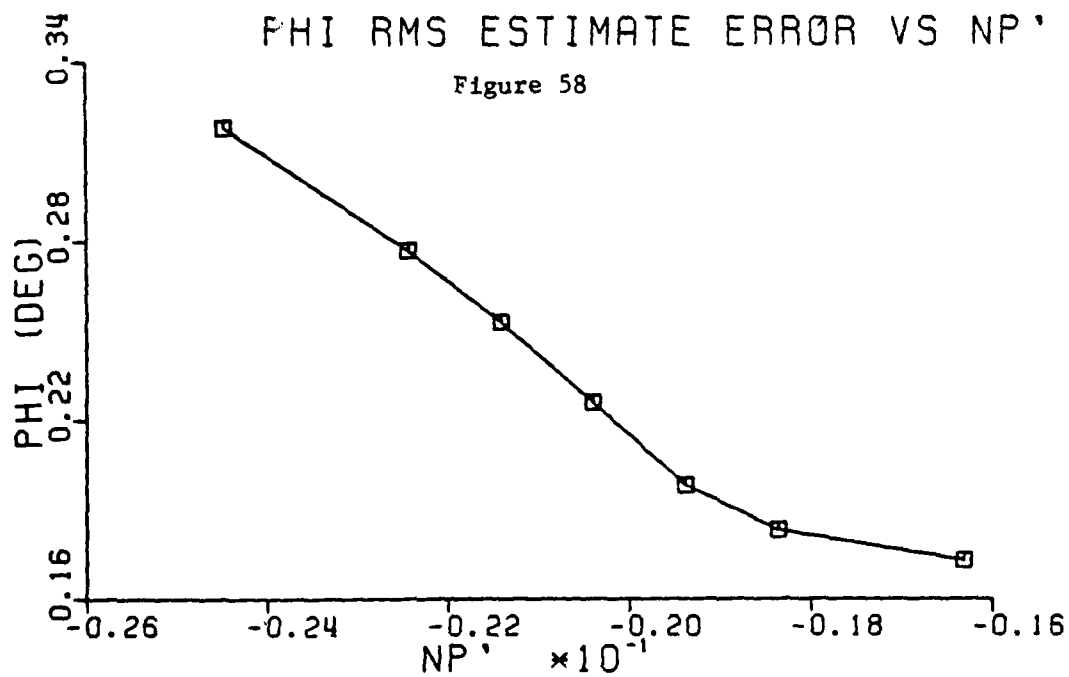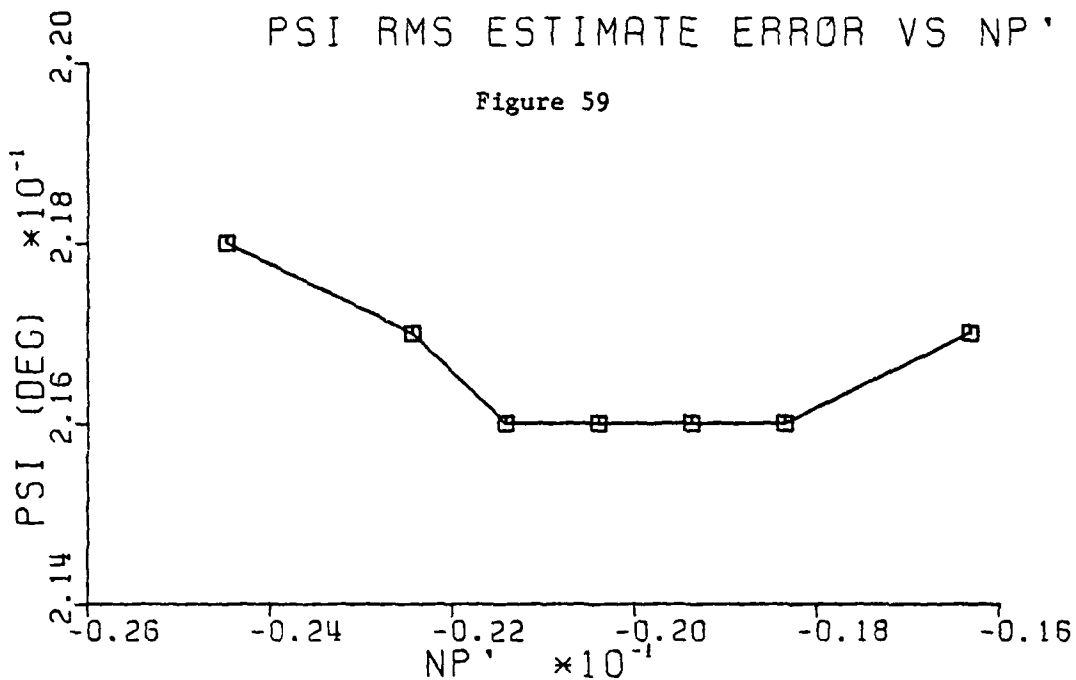
Figure 59

Figures 59 & 60. Sensitivity of $\bar{\psi}$ and $\bar{V}_{\beta_g}$ rms estimate errors vs variation in N'_p stability derivative.

VBG RMS ESTIMATE ERROR VS NP'

Figure 60

VB RMS ESTIMATE ERROR VS LB'
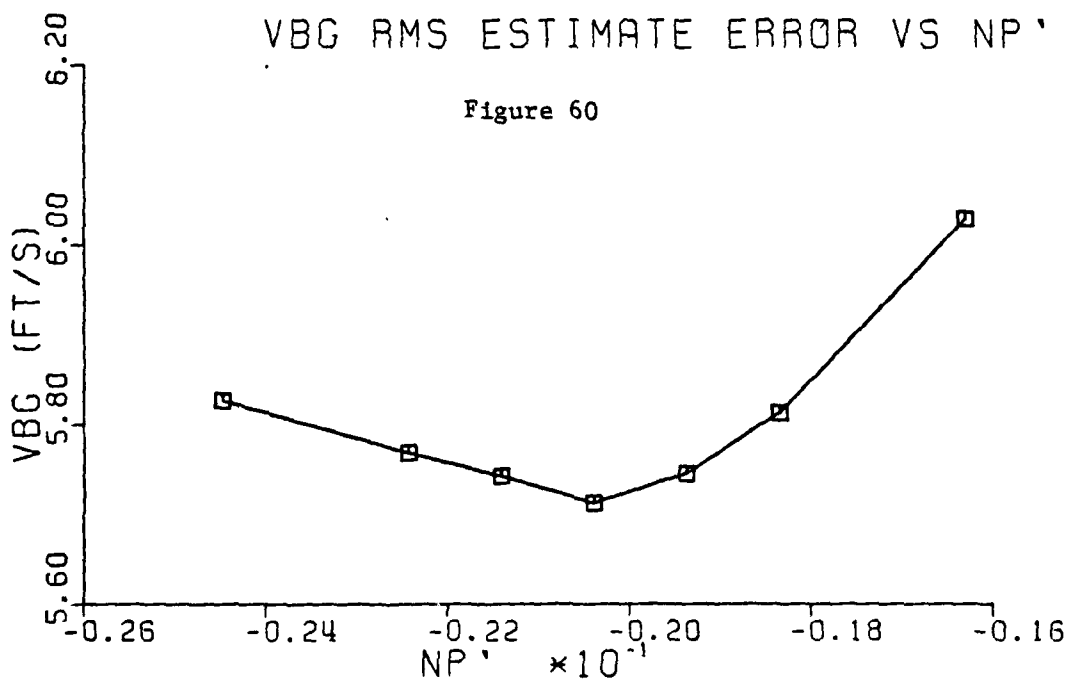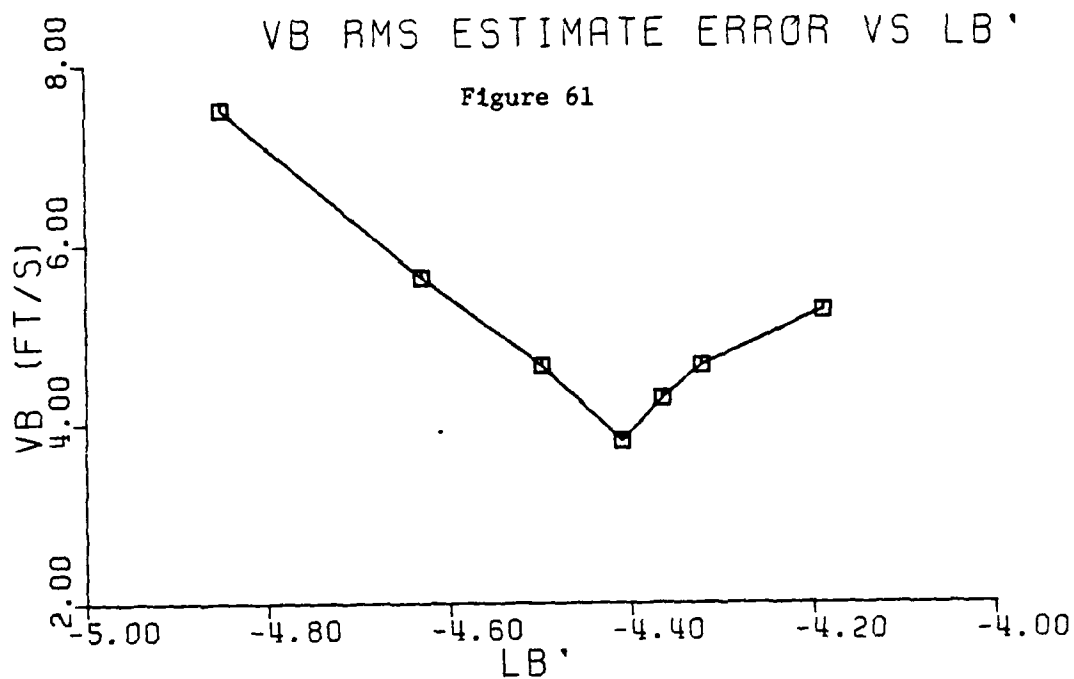
Figure 61

Figures 61 & 62.   Sensitivity of $\bar{V}_\beta$ and $\bar{r}$ rms estimate errors vs
variation L'_β stability derivative.

R RMS ESTIMATE ERROR VS LB'

Figure 62

69

P RMS ESTIMATE ERROR VS LB'
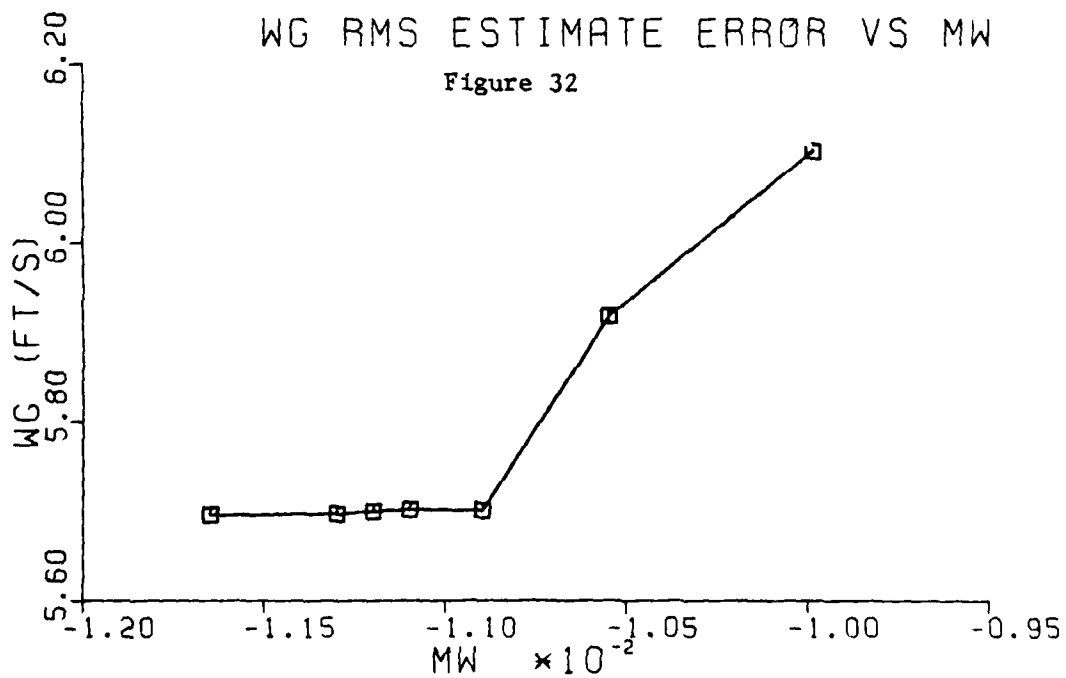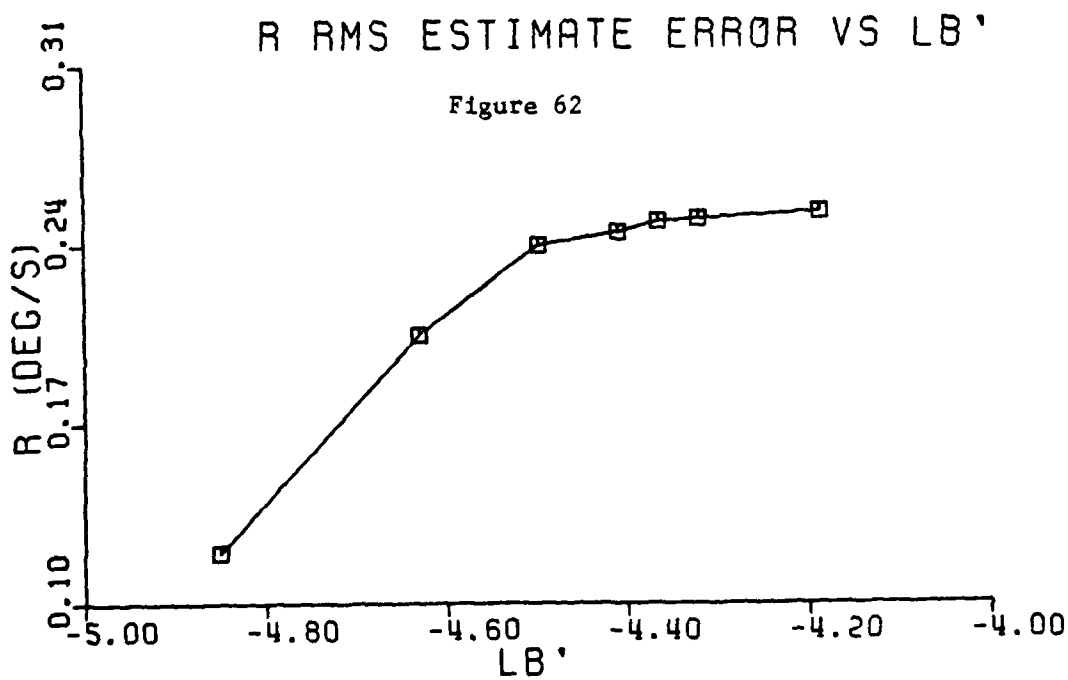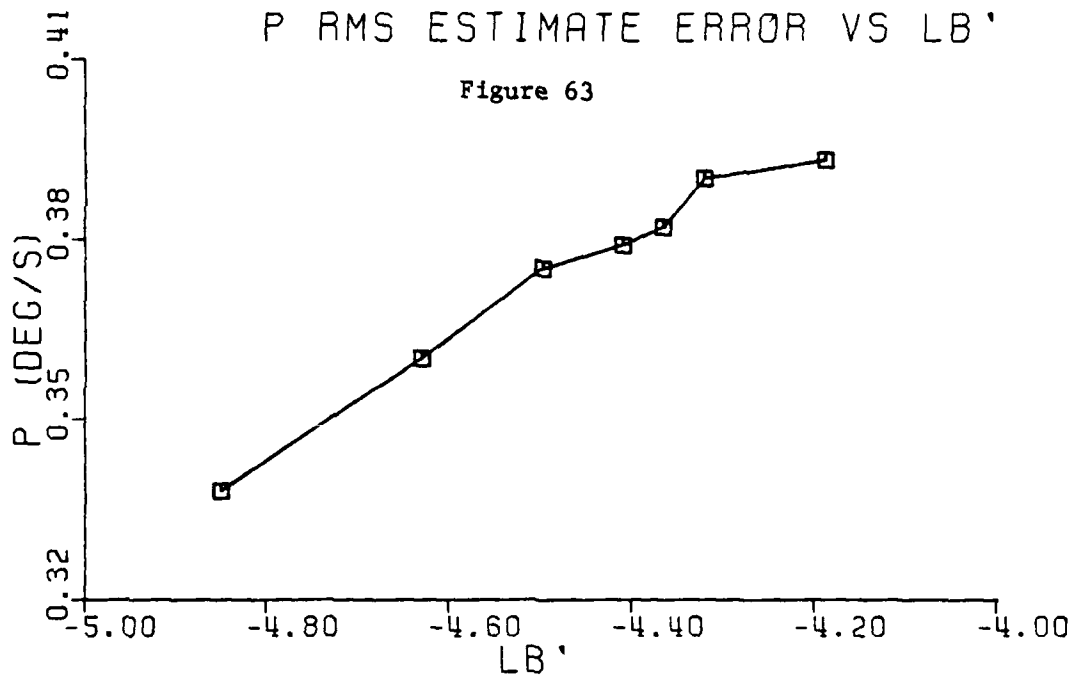
Figure 63

Figures 63 & 64. Sensitivity of $\bar{p}$ and $\bar{\theta}$ rms estimate errors vs variation in L_β' stability derivative.

PHI RMS ESTIMATE ERROR VS LB'

Figure 64

70

PSI RMS ESTIMATE ERROR VS LB'
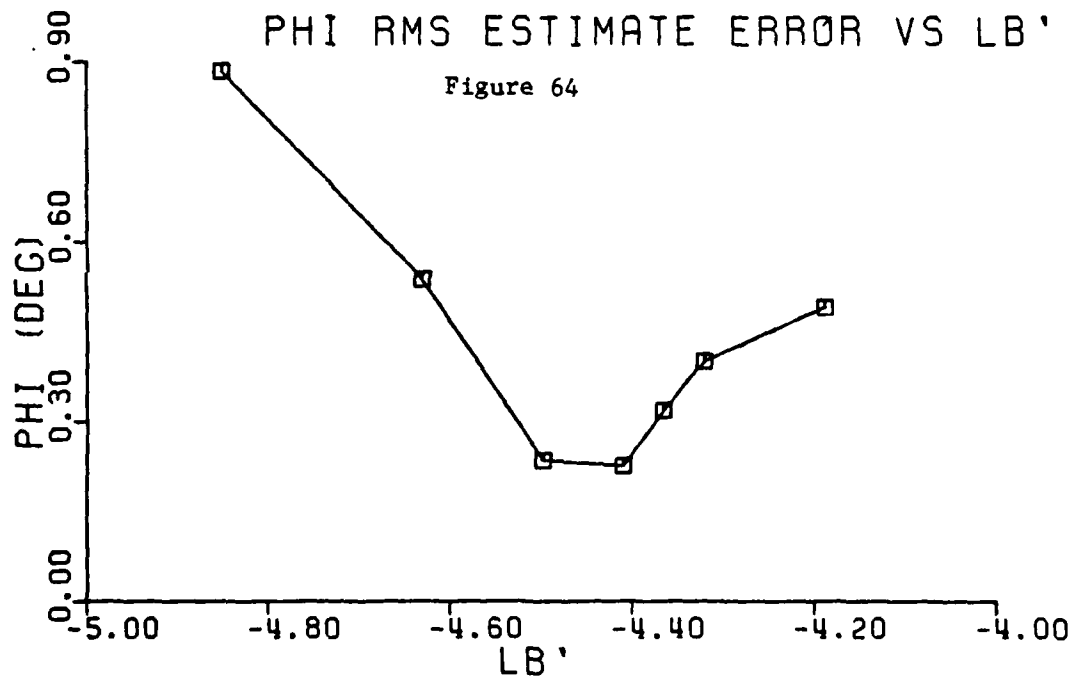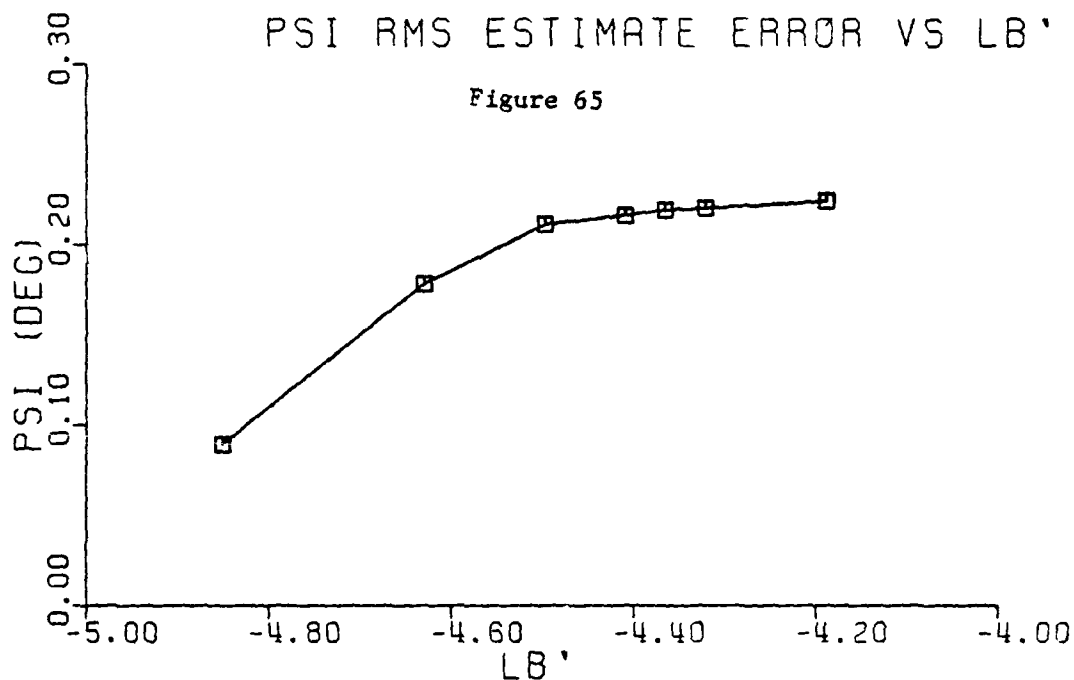
Figure 65

Figures 65 & 66. Sensitivity of $\bar{\psi}$ and $V\bar{\beta}_g$ rms estimate errors vs variation in L'_β stability derivative.

VBG RMS ESTIMATE ERROR VS LB'

Figure 66

71

VB RMS ESTIMATE ERROR VS LR'
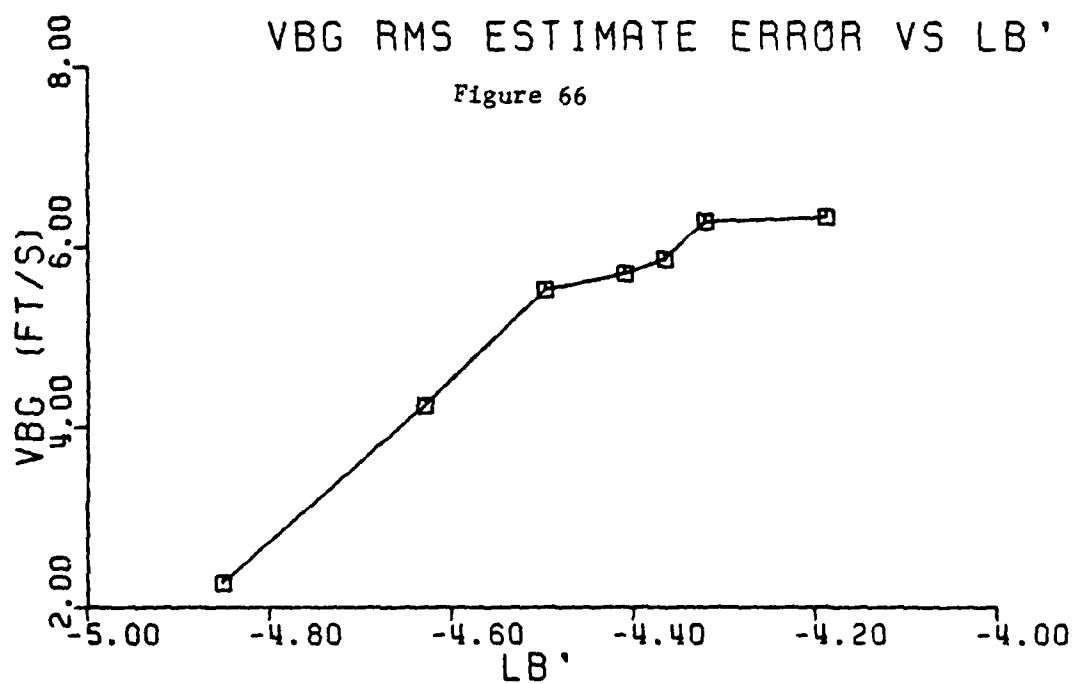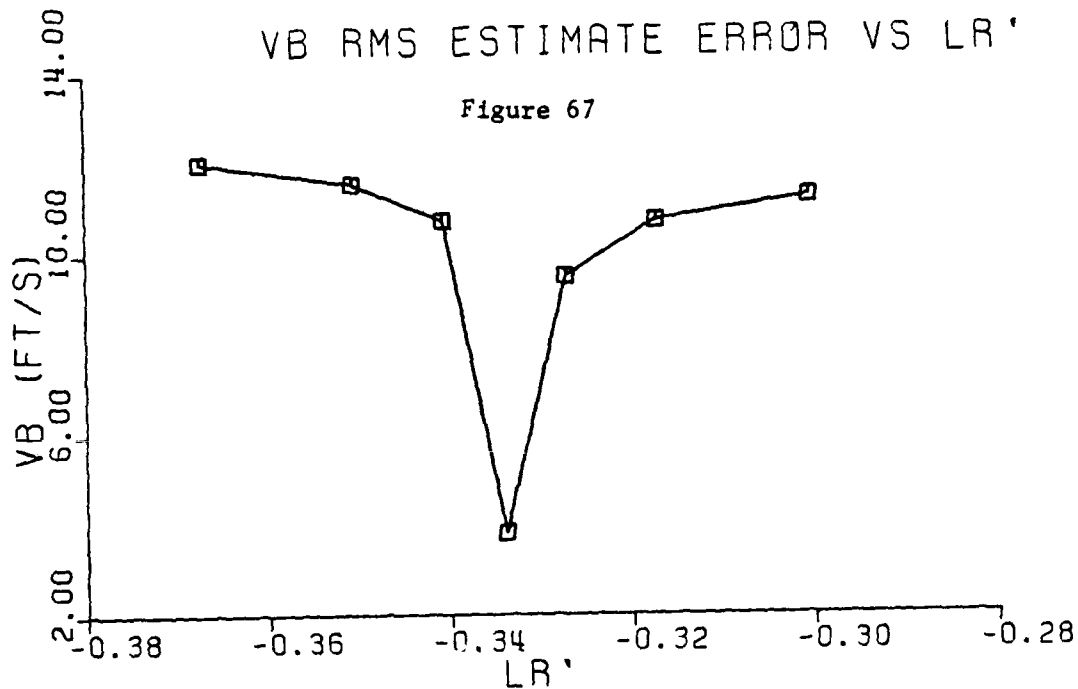
Figure 67

Figures 67 & 68. Sensitivity of $V\bar{\beta}$ and $\bar{r}$ rms estimate errors vs variation of L'_r stability derivative.

R RMS ESTIMATE ERROR VS LR'

Figure 68

72

P RMS ESTIMATE ERROR VS LR'
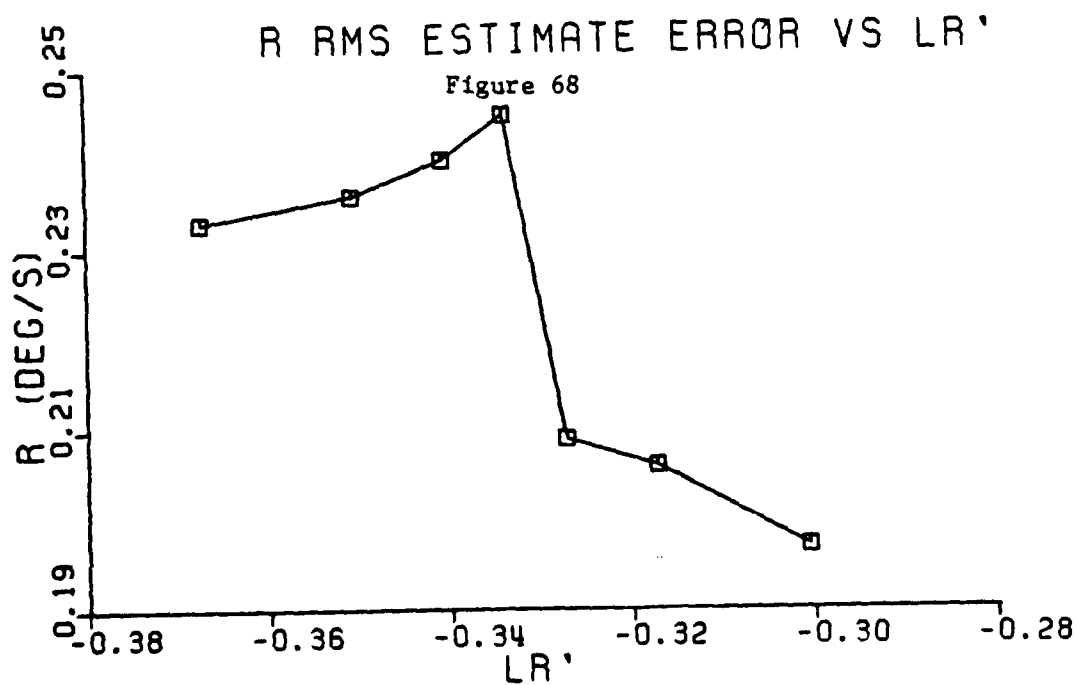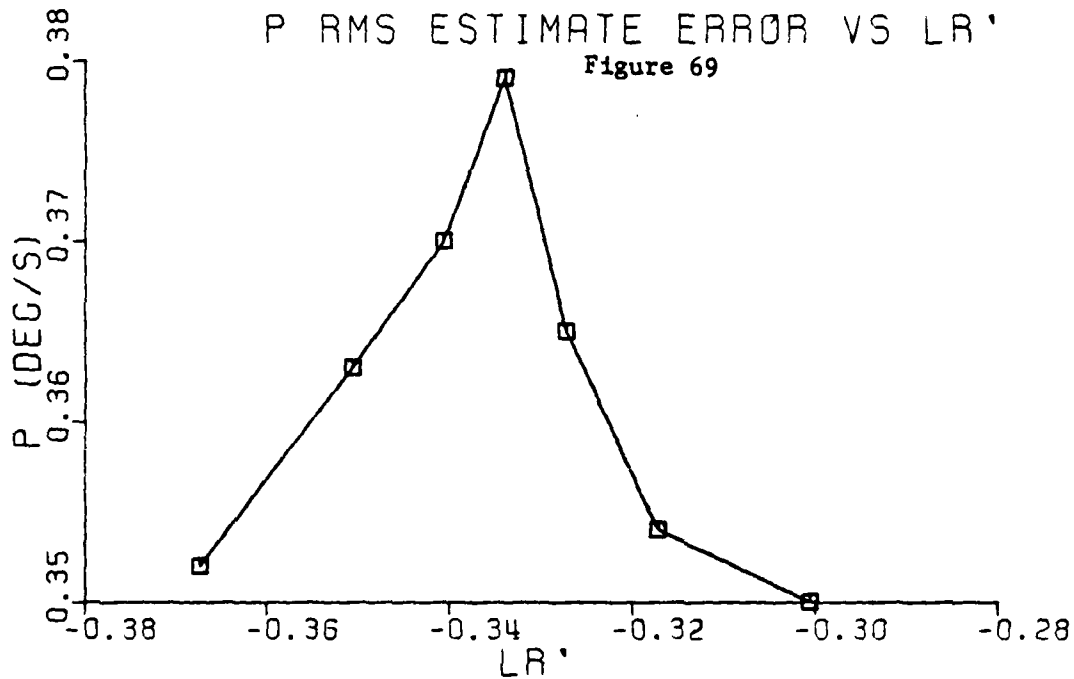
Figure 69

Figures 69 & 70. Sensitivity of $\bar{p}$ and $\bar{\theta}$ rms estimate errors vs variation of L_r' stability derivative.

PHI RMS ESTIMATE ERROR VS LR'

Figure 70

PSI RMS ESTIMATE ERROR VS LR'
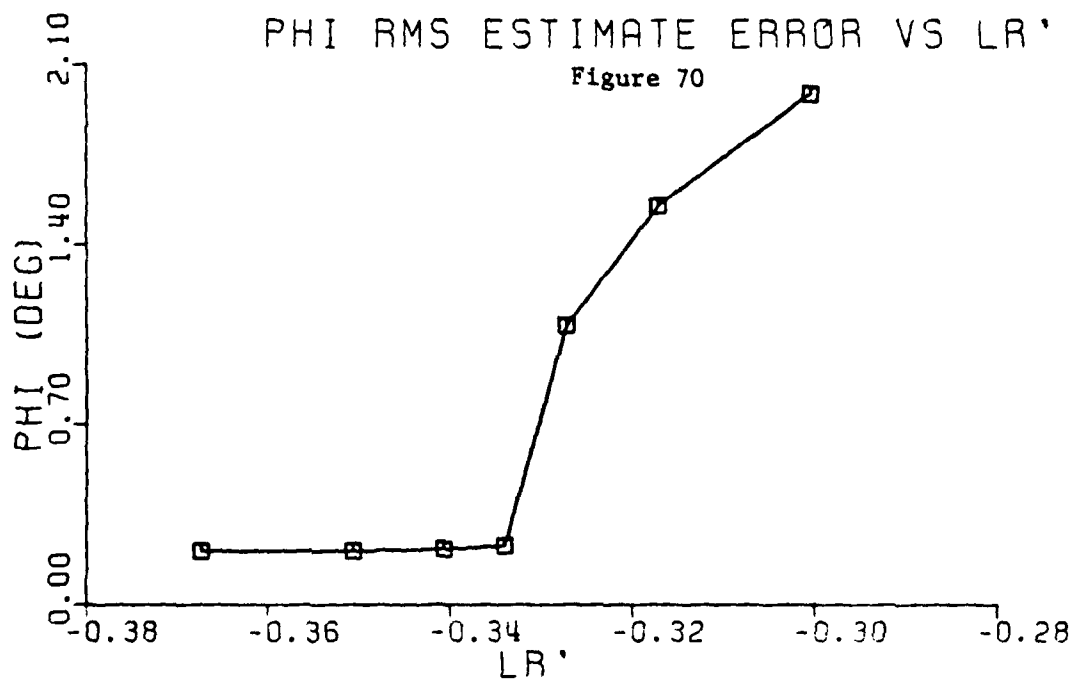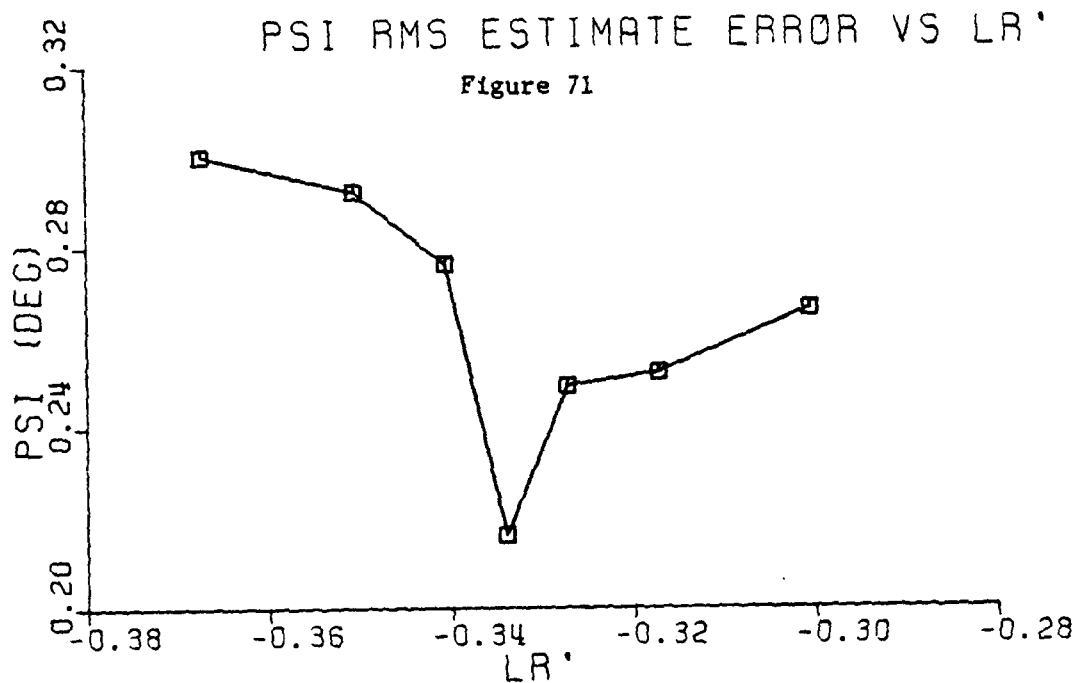
Figure 71

Figures 71 & 72. Sensitivity of $\bar{\psi}$ and $V\bar{g}_g$ rms estimate errors vs variation of L'_r stabiltiy derivative.

VBG RMS ESTIMATE ERROR VS LR'

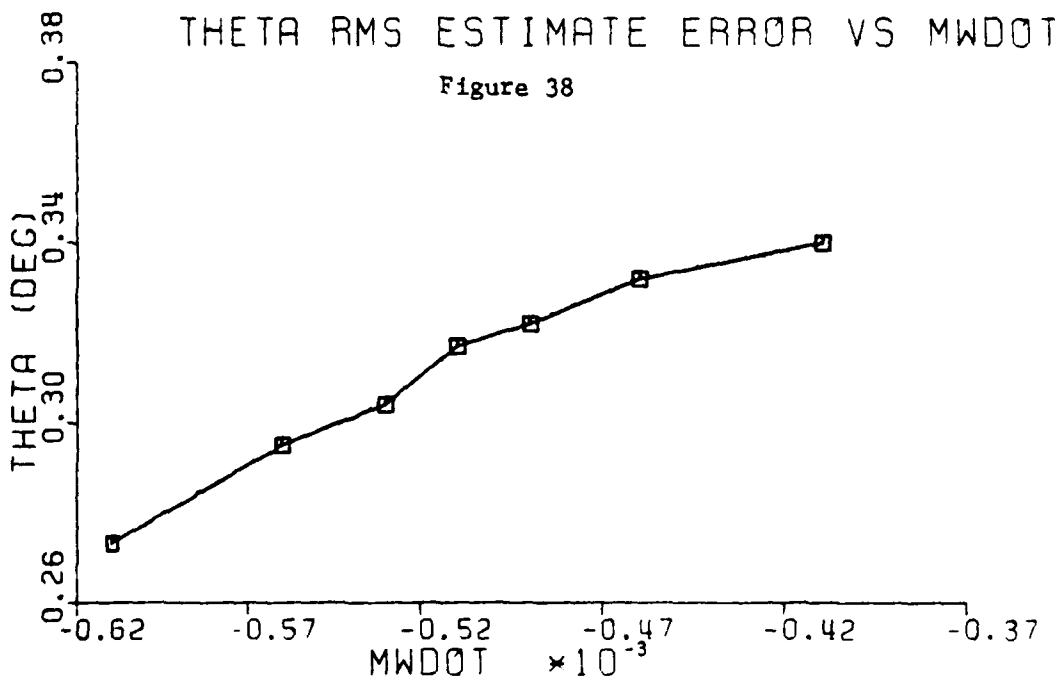## Figure 72

VB RMS ESTIMATE ERROR VS LP'
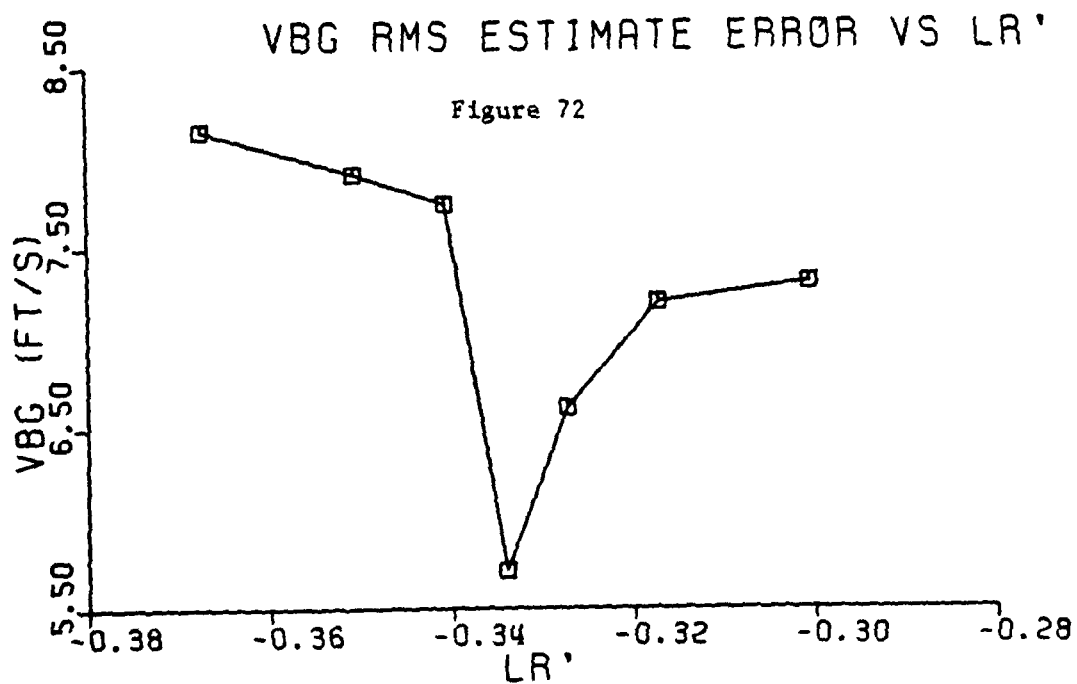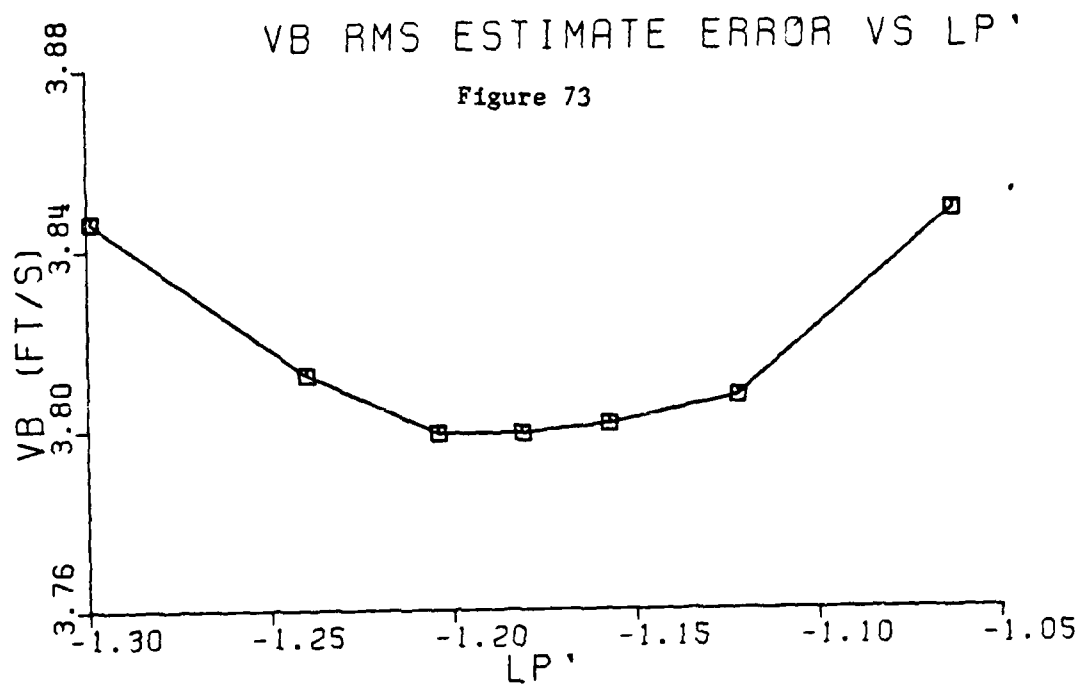
Figure 73

Figures 73 & 74. Sensitivity of $V\bar{\beta}$ and $\bar{r}$ rms estimate errors vs variation in L_p' stability derivative.

R RMS ESTIMATE ERROR VS LP'

Figure 74

75

PHI RMS ESTIMATE ERROR VS LP'
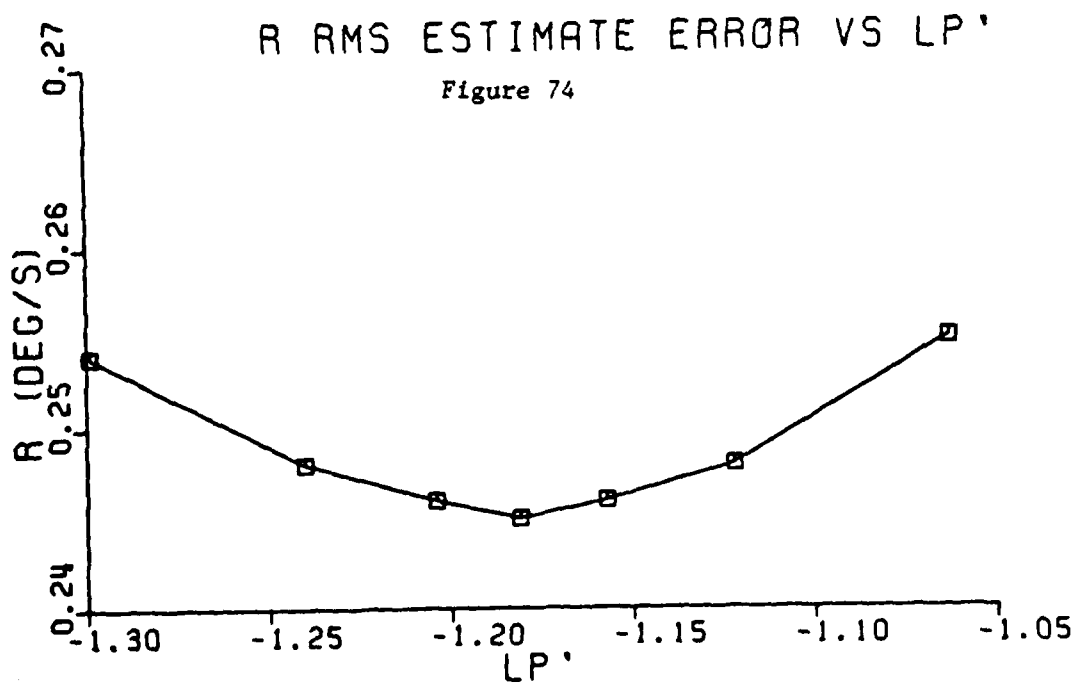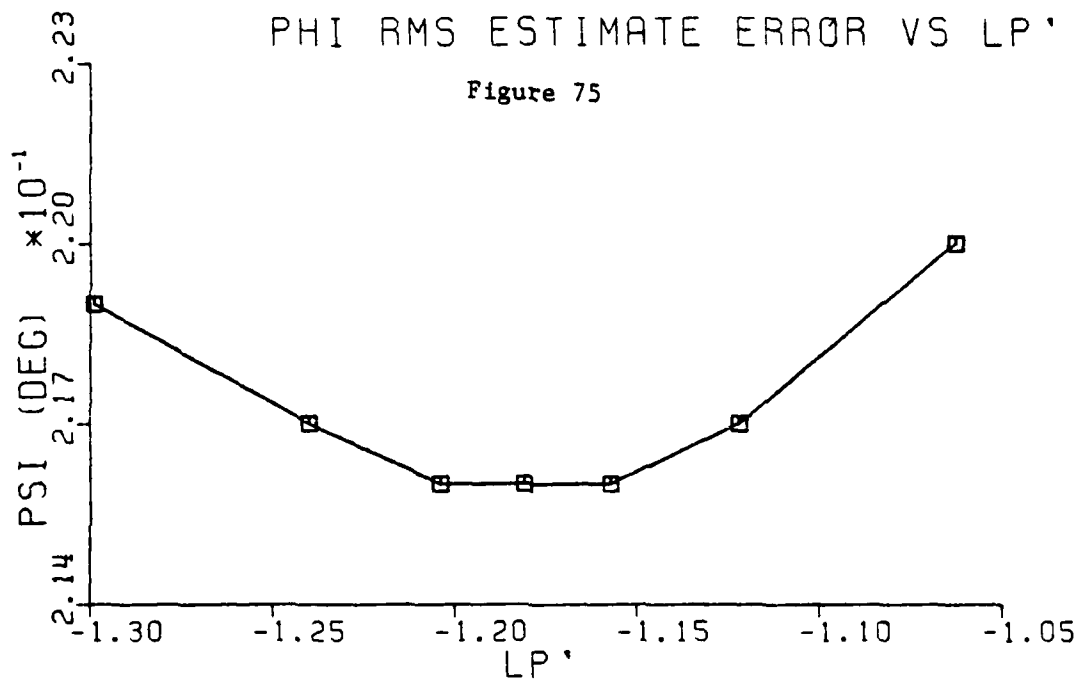
Figure 75

Figures 75 & 76. Sensitivity of $\bar{\theta}$ and $V\bar{\beta}_g$ rms estimate errors vs variation in L_p' stability derivative.

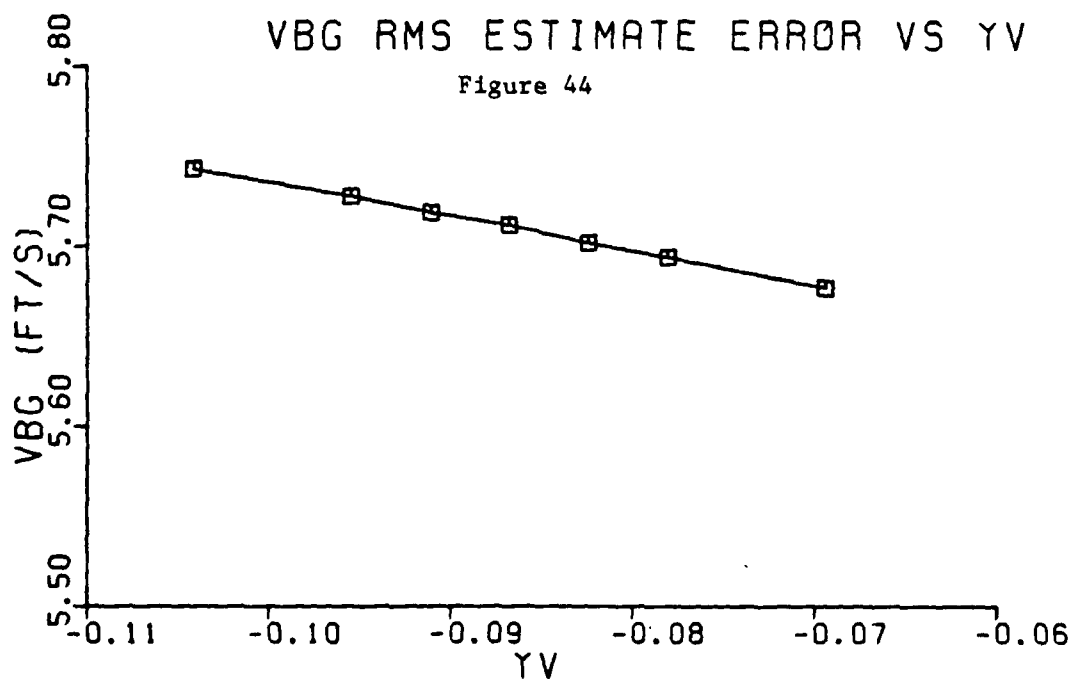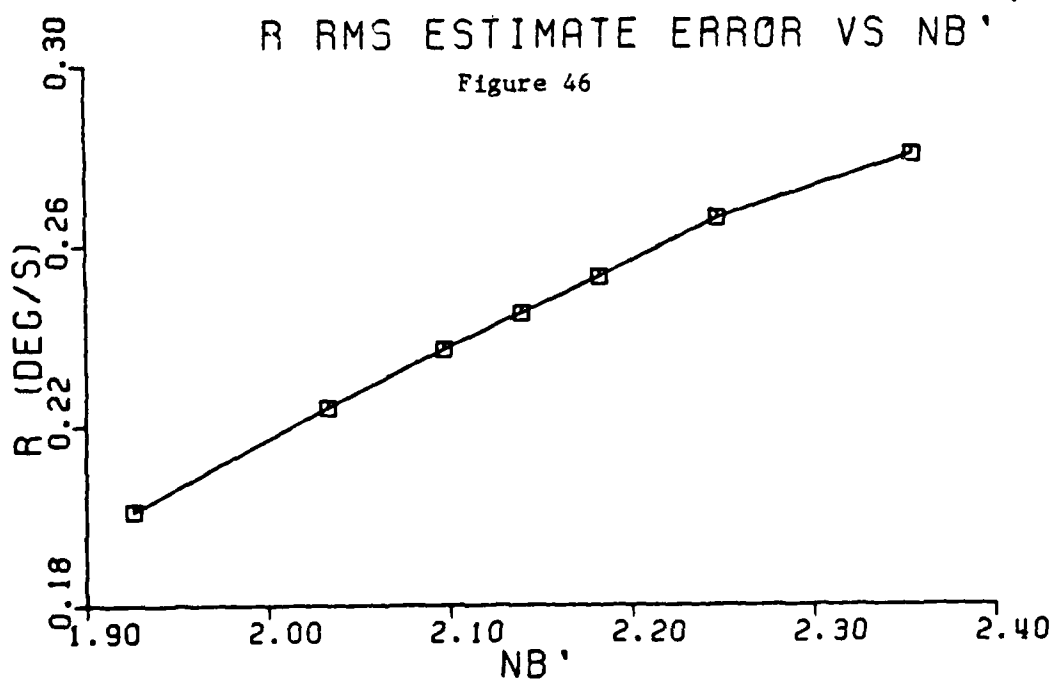# VBG RMS ESTIMATE ERROR VS LP'

Figure 76
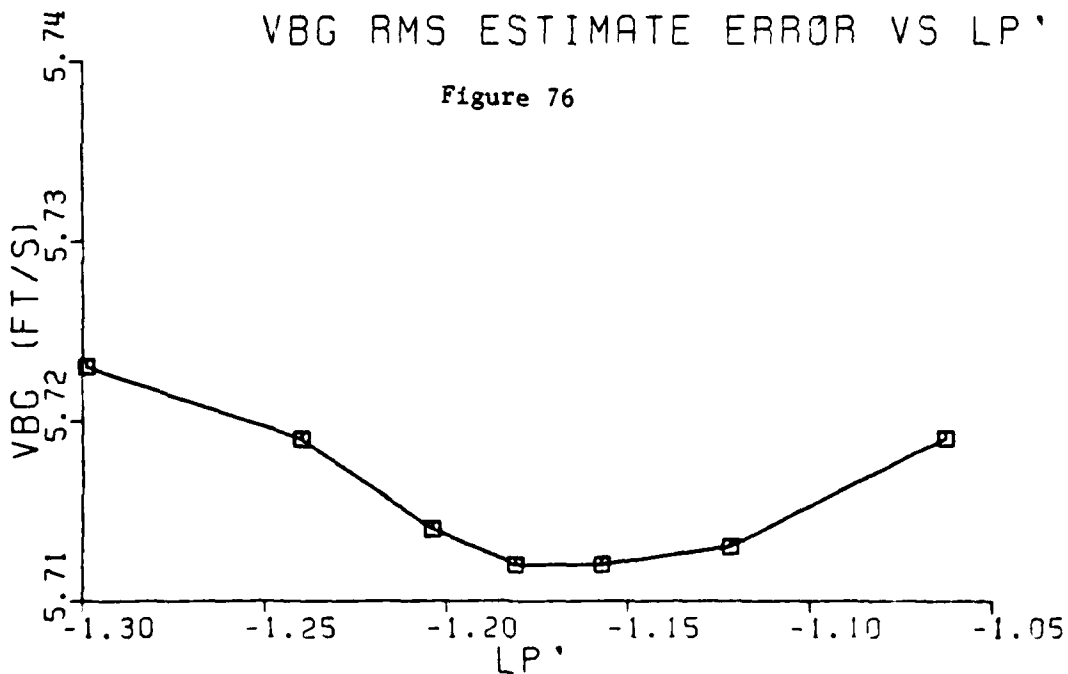
V. CONCLUSIONS AND RECOMMENDATIONS

A. CONCLUSIONS

Using steady-state Kalman Filters as observers in an inertial navigation system, the sensitivity of rms estimate errors to inaccuracies in the stability derivatives was studied. The conclusions reached at the end of this research are presented in two parts as they were analyzed.

1. Longitudinal Motion Estimator

a. Numerical variations in the dimensional derivatives; X_u, X_w and M_q do not show any important effect in the rms estimate errors. The value of these parameters as implemented in the filter can have large variations with respect to their nominal values (perhaps a tolerance of $\pm 20\%$).

b. Changes in the stability derivatives; Z_u, M_u and $M_{\dot{w}}$ are reflected with variation in almost all the rms estimate errors. In particular, large variations in $\bar{u}$ rms estimate error can begin to be important in terms of accuracy in the radial position. These parameters can be implemented in the dynamics of the filter with some degree of tolerance with respect to their true value (for the case under analysis no more than $\pm 5\%$).

c. The most important effects are found with the variations of the stability derivatives; Z_w and M_w. Z_w gives the strongest alterations in all the rms estimate errors and

77

small changes ($\pm 2\%$ the tolerance in the case under study) in this parameter are unacceptable in the filter. For Mw the situation is quite similar and the value of this derivative is very important. In general, Zw and Mw must be faithfully reproduced in the filter.

2. Lateral Motion Estimator

It is not possible to use the SKF as an observer under the particular configuration of the models given for lateral motion. The filter is stable but with a narrow margin of stability. The most minimum numerical variation (i.e., $\pm 1\%$) in the value of any stability derivative results in a failure of the filter due to divergence. This result complements the discussion given in Ref. [4]. Using a suboptimal filter (with modified gains), the effect of the numerical variation in each of the stability derivatives are:

a. Numerical variations in the dimensional derivatives; Yv, N_r' and L_p' do not cause important effects in any of the rms estimate errors. The reproduction of these parameters in the filter are not required to be too accurate (considering in this case a tolerance of $\pm 10\%$).

b. N_p' is a parameter that only accepts small variations in its value (in the problem discussed, 2% of tolerance) because it has strong effects in the estimation of $\bar{\phi}$ rms estimate error.

c. The stability derivative N_β' is one of the most
important in terms of faithful reproduction in the dynamics
of the filter. In general, it can be said that any numerical
variation in its true value is not allowed.

d. Finally, L_β' and L_r' present the most dramatic
situation, because a minimum change in its value is reflected
with very large changes in the estimation of rms errors and
it can result in divergence of the Kalman Filter. The lateral
motion estimator design requires that these stability deriva-
tives must be reproduced in the filter with the maximum of
accuracy, otherwise, the result can be failure of the filter.

Of the two estimators used in the implementation of
the INS, the lateral filter is more sensitive to variation in
its parameter value. It should be remembered that the con-
clusions reached in this analysis apply specifically to the
model being analyzed. Other models involving different
missiles may indicate different sensitivities.

Nevertheless, it is felt that the conclusions presented
in this thesis are of general validity.

B. SUGGESTIONS FOR FURTHER ANALYSIS

The most obvious extension of the work would be to test
the estimators using the real data for a missile.

Further study could be to consider the same problem de-
signing the estimators with a model that includes the addition
of the estimation in position in order to analyze the problem

79

in terms of miss distance in radial position for a missile
that at the end of the mid-course guidance phase must hit a
"basket" (terminal guidance phase).

VI. <u>SUMMARY</u>

The great advantage of the analysis in the sensitivity
of rms estimate errors to inaccuracies in the stability
derivatives is that it points out clearly which derivatives
are worthy of detailed accurate determination and which are
not.

The following table summarizes the level of importance of
each of the stability derivatives in the implementation of
the steady-state Kalman Filters to be used as estimators in
an INS.

	DERIVATIVE	NI	SI	PI
LONGITUDINAL MOTION ESTIMATION	X_u	X		
	X_w	X		
	Z_u		X	
	Z_w			X
	M_u		X	
	M_w			X
	M_q	X		
	$M_{\dot{w}}$		X	
LATERAL MOTION ESTIMATION	Y_v	X		
	N'_{β}			X
	N'_r	X		
	N'_p			X
	L'_{β}			X
	L'_r			X
	L'_p	X		

NI = Not Important

SI = Secondary (Relative) Importance

PI = Primary Importance

APPENDIX A
LIST OF SYMBOLS

Regular Symbols	Definition
A	Modal transformation of F matrix
B	Modal transofrmation of Γ matrix
C	Modal transformation of H matrix
D	Dutch roll mode
E	Destabilization matrix
F	System dynamics matrix
f	Subscript for filter
F'	Destabilized matrix
g	Subscript for wind speed
H	Measurement matrix
H	Heading Mode
h	Altitude
INS	Inertial Navigation System
K	Kalman Filter gain matrix
L	Rolling moment (about X axis)
M	Pitching moment (about Y axis)
MDS	Modal destabilization
N	Yawing moment (about Z axis)
n	Non-white gaussian noise
P	Covariance propagation of the estimate error matrix
p	Perturbed roll rate
Q	Covariance matrix of w
q	Perturbed pitch rate
R	Covariance matrix of v
r	Perturbed yaw rate
S	Spiral mode
SKF	Steady-state Kalman Filter
T	Transformation matrix

Regular Symbols	Definition
UNS	Undisturbed neutrally stable
u	Perturbed forward speed (along X axis)
v	Forward velocity
v	Perturbed side velocity
w	Driving white gaussian noise
w	Perturbed downward velocity
X	Reference axis
x	State vector of the system
$\hat{x}$	State estimate vector
$\tilde{x}$	Estimate error vector
Y	Reference axis
z	Measurement vector
Z	Reference axis

Greek Symbols	Definition
ψ	Heading Angle
θ	Perturbed pitch attitude angle
ϕ	Perturbed bank (roll) angle
β	Sideslip angle
Γ	Driving noise matrix
σ	Eigenvalue constrain
σ	Standard deviation
ξ	Transformed state vector

APPENDIX B
AERODYNAMIC DATA AND PROBABILISTIC INFORMATION

$$v = 820 \ ft/s$$

1. ## Longitudinal Model

   a. Dimensional Derivatives

      $X_u = -0.015$ 1/s

      $X_w = 0.004$ 1/s

      $Z_u = -0.074$ 1/s

      $Z_w = -0.0806$ 1/s

      $M_u = -0.0786$ 1/s-ft

      $M_w = -0.0111$ 1/s-ft

      $M_q = -0.924$ 1/s-rad.

      $M_{\dot{w}} = -0.00051$ 1/ft

   b. Disturbance Noise Standard Deviation

      $\sigma_u = \sigma_w = 1.15$ 1/s (10 ft/s)^2

      (7 ft/s rms gust with a 930-ft correlation distance).

   c. Observation Noise Standard Deviation

      $\sigma_q = 0.15$ s   (0.01 rad/s)

      $\sigma_h = 0.05$ s   (100 ft)^2

2. ## Lateral Models

   a. Dimensional Derivatives

      $Y_v = -0.0868$ 1/s

      $N_\beta' = 2.14$ 1/s^2

      $N_r' = -0.228$ 1/s

      $N_p' = -0.0204$ 1/s

85

$$L_\beta' = -4.41 \quad 1/s^2$$
$$L_r' = 0.034 \quad 1/s$$
$$L_p' = -1.181 \quad 1/s$$

b. Disturbance Noise Standard Deviation

$$\sigma = 1.63 \times 10^{-4} \quad 1/s \quad \text{(7 ft/s rms gust with a}$$
$$\text{930 ft correlation distance)}$$

c. Observation Noise Standard Deviation

$$\sigma_p = 1.5 \times 10^{-5} \text{ s}$$
$$\sigma_\psi = 1.5 \times 10^{-5} \text{ 1/s}$$

COMPUTER OUTPUT

Table 1. rms estimate errors for longitudinal motion estimator with variation in Xu derivative.

X_u	$\bar{u}$ ft/s	$\bar{w}$ ft/s	$\bar{q}$ deg/s	$\bar{\theta}$ deg	$\bar{h}$ ft	$\bar{u}_g$ ft/s	$\bar{w}_g$ ft/s
-0.018	2.096	5.102	0.416	0.317	8.248	4.776	5.701
-0.0165	2.094	5.102	0.416	0.317	8.246	4.776	5.701
-0.01575	2.091	5.102	0.416	0.317	8.240	4.776	5.701
-0.015 *	2.090	5.102	0.416	0.317	8.245	4.776	5.701
-0.01425	2.088	5.103	0.416	0.317	8.260	4.775	5.701
-0.0135	2.089	5.103	0.416	0.317	8.280	4.775	5.701
-0.012	2.092	5.103	0.416	0.317	8.340	4.775	5.701

Table 2. rms estimate errors for longitudinal motion estimator with variation in Xw derivative.

X_w	$\bar{u}$ ft/s	$\bar{w}$ ft/s	$\bar{q}$ deg/s	$\bar{\theta}$ deg	$\bar{h}$ ft	$\bar{u}_g$ ft/s	$\bar{w}_g$ ft/s
0.0048	2.070	5.102	0.416	0.317	8.319	4.776	5.701
0.0044	2.080	5.102	0.416	0.317	8.282	4.776	5.701
0.0042	2.086	5.102	0.416	0.317	8.257	4.776	5.701
0.004 *	2.090	5.102	0.416	0.317	8.245	4.776	5.701
0.0038	2.100	5.102	0.416	0.317	8.223	4.776	5.701
0.0036	2.103	5.102	0.416	0.316	8.215	4.776	5.701
0.0032	2.110	5.101	0.416	0.316	8.170	4.776	5.701

87

Table 3. rms estimate errors for longitudinal motion estimator with variation in Zu derivative.

Zu	$\bar{u}$ ft/s	$\bar{w}$ ft/s	$\bar{q}$ deg/s	$\bar{\theta}$ deg	$\bar{h}$ ft	$\bar{u}_g$ ft/s	$\bar{w}_g$ ft/s
-0.0888	1.885	5.106	0.416	0.322	9.310	4.776	5.707
-0.0814	1.974	5.104	0.416	0.319	8.808	4.775	5.703
-0.0777	2.026	5.194	0.416	0.318	8.579	4.775	5.702
-0.0740 *	2.090	5.102	0.416	0.317	8.245	4.776	5.701
-0.0703	2.122	5.100	0.416	0.315	7.800	4.777	5.700
-0.0666	2.270	5.095	0.416	0.313	7.101	4.777	5.697
-0.0592	2.32	5.094	0.416	0.311	7.000	4.778	5.695

Table 4. rms estimate errors for longitudinal motion estimator with variation in Zw derivative.

Zw	$\bar{u}$ ft/s	$\bar{w}$ ft/s	$\bar{q}$ deg/s	$\bar{\theta}$ deg	$\bar{h}$ ft	$\bar{u}_g$ ft/s	$\bar{w}_g$ ft/s
-0.9612	30.08	6.172	0.486	0.440	17.97	4.778	7.138
-0.8866	11.80	5.810	0.428	0.415	33.50	4.785	5.947
-0.8463	5/345	5/259	0.421	0.400	22.776	4.779	5.737
-0.806 *	2.090	5.102	0.416	0.317	8.245	4.776	5.701
-0.7657	2.668	5.032	0.412	0.219	16.903	4.772	5.710
-0.7256	3.188	5.035	0.407	0.200	21.026	4.769	5.746
-0.665	3.260	5.065	0.406	0.185	23.000	4.767	5.794

Table 5. rms estimate errors for longitudinal motion estimator with variation in M_u derivative.

$\bar{M}_u$	$\bar{u}$ ft/s	$\bar{w}$ ft/s	$\bar{q}$ deg/s	$\bar{\theta}$ deg	$\bar{h}$ ft	$\bar{u}_g$ ft/s	$\bar{w}_g$ ft/s
-0.000943	2.234	5.061	0.416	0.305	6.230	4.775	5.689
-0.000865	2.115	5.089	0.416	0.310	6.640	4.775	5.695
-0.000825	2.104	5.094	0.416	0.314	7.531	4.776	5.698
-0.000786*	2.090	5.102	0.416	0.317	8.245	4.776	5.701
-0.000747	1.993	5.105	0.416	0.318	8.595	4.777	5.703
-0.000707	1.866	5.108	0.416	0.319	8.832	4.779	5.705
-0.000629	1.566	5.111	0.416	0.322	9.178	4.783	5.708

Table 6. rms estimate errors for longitudinal motion estimator with variation in M_w derivative.

M_w	$\bar{u}$ ft/s	$\bar{w}$ ft/s	$\bar{q}$ deg/s	$\bar{\theta}$ deg	$\bar{h}$ ft	$\bar{u}_g$ ft/s	$\bar{w}_g$ ft/s
-0.01165	18.43	8.350	0.502	0.455	29.870	4.778	5.695
-0.0113	5.163	5.142	0.433	0.373	17.790	4.778	5.694
-0.0112	3.110	5.113	0.418	0.321	10.427	4.777	5.699
-0.0111*	2.090	51.102	0.416	0.317	8.245	4.776	5.701
-0.0109	5.206	5.018	0.419	0.325	16.650	4.776	5.700
-0.01055	13.652	5.342	0.447	0.430	12.204	4.776	5.918
-0.00999	19.13	18.95	0.475	0.704	68.98	4.756	6.102

Table 7. rms estimate errors for longitudinal motion estimator with variation in M_q derivative.

M_q	$\bar{u}$ ft/s	$\bar{w}$ ft/s	$\bar{q}$ deg/s	$\bar{\theta}$ deg	$\bar{h}$ ft	$\bar{u}_g$ ft/s	$\bar{w}_g$ ft/s
-1.109	2.091	5.102	0.416	0.316	8.230	4.776	5.701
-1.016	2.091	5.102	0.416	0.316	8.234	4.776	5.701
-0.970	2.091	5.102	0.416	0.317	8.236	4.776	5.701
-0.924*	2.090	5.102	0.416	0.317	8.245	4.776	5.701
-0.880	2.090	5.102	0.416	0.316	8.244	4.776	5.701
-0.832	2.089	5.102	0.416	0.316	8.236	4.776	5.701
-0.7392	2.089	5.102	0.416	0.316	8.232	4.776	5.701

Table 8. rms estimate errors for longitudinal motion estimator with variation in $M_{\dot{w}}$ derivative.

$M_{\dot{w}}$	$\bar{u}$ ft/s	$\bar{w}$ ft/s	$\bar{q}$ deg/s	$\bar{\theta}$ deg	$\bar{h}$ ft	$\bar{u}_g$ ft/s	$\bar{w}_g$ ft/s
-0.00061	2.610	5.053	0.417	0.273	10.665	4.775	5.688
-0.00056	2.476	5.089	0.417	0.295	6.301	4.776	5.703
-0.00053	2.398	5.091	0.417	0.304	4.150	4.776	5.698
-0.00051*	2.090	5.102	0.416	0.317	8.245	4.776	5.701
-0.00049	2.491	5.108	0.416	0.322	9.757	4.776	5.702
-0.00046	2.976	5.118	0.415	0.332	12.067	4.776	5.703
-0.00041	3.570	5.124	0.415	0.340	13.536	4.776	5.703

90

Table 9. rms estimate errors for lateral motion estimator with variation in Y derivate.

Y_v	$V\bar\beta$ ft/s	$\bar r$ deg/s	$\bar p$ deg/s	$\bar\theta$ deg	$\bar\psi$ deg	$V\bar\beta_g$ ft/s
-.10416	3.914	0.246	0.380	0.236	0.216	5.743
-.09548	3.856	0.246	0.379	0.231	0.216	5.728
-.09110	3.827	0.245	0.379	0.228	0.216	5.719
-.0868 *	3.799	0.245	0.379	0.226	0.216	5.719
-.08246	3.769	0.245	0.378	0.223	0.215	5.702
-.07812	3.741	0.245	0.378	0.220	0.215	5.694
-.06944	3.678	0.245	0.377	0.214	0.215	5.677

Table 10. rms estimate errors for lateral motion estimator with variation in N'_β derivative.

N'_β	$V\bar\beta$ ft/s	$\bar r$ deg/s	$\bar p$ deg/s	$\bar\theta$ deg	$\bar\psi$ deg	$V\bar\beta_g$ ft/s
2.354	6.889	0.280	0.391	0.649	0.233	7.719
2.247	5.129	0.266	0.384	0.501	0.230	6.220
2.1828	4.717	0.253	0.383	0.404	0.223	6.052
2.14 *	3.799	0.245	0.379	0.226	0.216	5.712
2.0972	4.125	0.237	0.371	0.325	0.217	5.938
2.033	4.956	0.224	0.353	0.655	0.218	6.543
1.926	8.781	0.201	0.299	1.101	0.220	8.240

Table 11. rms estimate errors for lateral motion estimator with variation in N_r' derivative.

N_r'	$\overline{V_\beta}$ ft/s	$\bar{r}$ deg/s	$\bar{p}$ deg/s	$\bar{\theta}$ deg	$\bar{\psi}$ deg	$\overline{V_{\beta g}}$ ft/s
−0.2736	3.790	0.248	0.380	0.225	0.217	5.704
−0.2508	3.791	0.246	0.379	0.225	0.216	5.706
−0.2394	3.794	0.246	0.379	0.225	0.216	5.710
−0.228 *	3.799	0.245	0.379	0.226	0.216	5.712
−0.2166	3.805	0.245	0.379	0.226	0.216	5.714
−0.2052	3.815	0.246	0.379	0.228	0.216	5.719
−0.1824	3.834	0.248	0.379	0.231	0.216	5.727

Table 12. rms estimate errors for lateral motion estimator with variation in N_p' derivative.

N_p'	$\overline{V_\beta}$ ft/s	$\bar{r}$ deg/s	$\bar{p}$ deg/s	$\bar{\theta}$ deg	$\bar{\psi}$ deg	$\overline{V_{\beta g}}$ ft/s
−0.02448	4.121	0.247	0.380	0.318	0.218	5.826
−0.02244	3.980	0.246	0.380	0.277	0.217	5.768
−0.02142	3.889	0.246	0.379	0.253	0.216	5.742
−0.0204 *	3.799	0.245	0.379	0.226	0.216	5.712
−0.01938	3.719	0.245	0.379	0.198	0.216	5.745
−0.01836	3.708	0.246	0.379	0.183	0.216	5.813
−0.01632	3.695	0.248	0.382	0.173	0.217	6.029

Table 13. rms estimate errors for lateral motion estimator with variation in L_β.

L_β	$v_{\bar\beta}$ ft/s	$\bar r$ deg/s	$\bar p$ deg/s	$\bar\theta$ deg	$\bar\psi$ deg	$v_{\bar\beta_g}$ ft/s
-4.8510	7.498	0.120	0.338	0.885	0.089	2.266
-4.6305	5.621	0.205	0.360	0.539	0.178	4.244
-4.4982	4.642	0.240	0.375	0.236	0.211	5.529
-4.41 *	3.799	0.245	0.379	0.226	0.216	5.712
-4.3659	4.268	0.249	0.382	0.319	0.219	5.875
-4.3218	4.640	0.250	0.390	0.402	0.220	6.295
-4.1895	5.246	0.253	0.393	0.492	0.224	6.238

Table 14. rms estimate errors for lateral motion estimator with variation in L_r'.

L_r'	$v_{\bar\beta}$ ft/s	$\bar r$ deg/s	$\bar p$ deg/s	$\bar\theta$ deg	$\bar\psi$ deg	$v_{\bar\beta_g}$ ft/s
-0.3674	12.030	0.233	0.352	0.205	0.300	8.149
-0.3507	11.538	0.236	0.363	0.208	0.292	7.910
-0.3407	10.712	0.240	0.370	0.213	0.276	7.746
-0.334 *	3.799	0.245	0.379	0.226	0.216	5.712
-0.3273	9.476	0.209	0.365	1.089	0.249	6.613
-0.3173	10.712	0.206	0.354	1.551	0.252	7.198
-0.3006	11.248	0.197	0.350	1.986	0.266	7.309

93

Table 15. rms estimate errors for lateral motion estimator with variation in L'_p.

L'_p	$\overline{V_\beta}$ ft/s	$\overline{r}$ deg/s	$\overline{p}$ deg/s	$\overline{\theta}$ deg	$\overline{\psi}$ deg	$\overline{V_{\beta_g}}$ ft/s
-1.299	3.846	0.254	0.380	0.228	0.219	5.723
-1.240	3.812	0.248	0.379	0.227	0.217	5.719
-1.204	3.799	0.246	0.379	0.226	0.216	5.714
-1.181 *	3.799	0.245	0.379	0.226	0.216	5.712
-1.1573	3.801	0.246	0.379	0.226	0.216	5.712
-1.122	3.807	0.248	0.379	0.226	0.217	5.713
-1.063	3.848	0.255	0.379	0.227	0.220	5.719

94

```
CCCCCCCCCCCCCCCCCCCCCCCCCCCCCCCCCCCCCCCCCCCCCCCCCCCCCCCCCCCC
C                                                          C
C               SENSITIVITY COVARIANCE PROGRAM             C
C                                                          C
C      THIS PROGRAM IS USED TO SOLVE THE ERROR SENSITIVITY C
C      EQUATIONS WHEN THERE IS AN INCORRECT IMPLEMENTATION C
C      OF DYNAMICS IN THE DESIGN OF THE KALMAN FILTER.THE  C
C      EQUATIONS BECOME                                    C
C                                                          C
C      PDOT=(F*-K*H)P+P(F*-K*H)T+DFV+VTDFT+GQGT+K*RK*T     C
C      VDOT=FV+V(F*-K*H)T+UDFT-GQGT                        C
C      UDOT=FU+UFT+GQGT                                    C
C                                                          C
C      THE PRINCIPAL PROGRAM INPUTS ARE THE FOLLOWING CO-  C
C      LLECTION OF SYSTEM AND FILTER MATRICES              C
C                                                          C
C      PO    THE INITIAL COVARIANCE MATRIX(NXN)            C
C      F     THE TRUTH MODEL DYNAMICS MATRIX(NXN)          C
C      F*    THE FILTER MODEL DYNAMICS MATRIX(NXN)         C
C      H     THE TRUTH MODEL MEASUREMENT MATRIX(LXN),WHERE C
C            L IS THE MEASUREMENT VECTOR DIMENSION         C
C      GQGT  THE INPUT NOISE COVARIANCE MATRIX(NX)         C
C      R     THE MEASUREMENT NOISE COVARIANCE MATRIX(LXL)  C
C      K*    FILTER GAIN(NXL)                              C
C                                                          C
CCCCCCCCCCCCCCCCCCCCCCCCCCCCCCCCCCCCCCCCCCCCCCCCCCCCCCCCCCCC
C
C      THIS PROGRAM HAS BEEN DEVELOPED USING THE IMSL LIBRARY
C      AVAILABLE IN THE COMPUTER CENTER OF THE NAVAL
C      POSTGRADUATE SCHOOL
C
C
       IMPLICIT REAL*8 (A-H,O-Z)
       COMMON F(7,7),FS(7,7),GQGT(7),AK(7,2),R(2,2),
      *AKRKT(7,7),DF(7,7),FT(7,7),FSMKHT(7,7),DFT(7,7),
      *FSMKH(7,7),H(2,7)
       COMMON/KTR/N,NS,NPD
       DIMENSION PFULL(7,7),PSQR(7)
       DIMENSION DDT(7)
       DIMENSION U(28),V(7,7),P(28),UD(28),VD(7,7),
      *VAR(105),DRV(105),C(24),WK(105,9),PD(28)
       DIMENSION TMP1(7,7),TMP2(7,7),TMP3(7,7)
       EQUIVALENCE (U(1),VAR(1)),(V(1,1),VAR(29)),(P(1),
      *VAR(78)),(UD(1),DRV(1)),(VD(1,1),DRV(29)),(PD(1),
      *DRV(78))
C
C      N=ORDER OF THE SYSTEM MODEL
C
C      NP=NUMBER OF POINTS
C
C      NPD=CONTROL OF INITIAL DIAGNOSTIC OUTPUT
C
C      DT=TIME INTERVAL
C
       EXTERNAL FUN
       CALL UGETIO(3,5,6)
C
C      THE FOLLOWING SECTION READS THE SPECIFIED INPUT
C      MATRICES,F,F*,GQGT,K*H AND R
C
       READ(5,98)N,NP,NPD,DT
   98  FORMAT(3I5,F10.5)
       WRITE(6,97)N,NP,NPD,DT
   97  FORMAT('1',3I5,1X,G18.10)
```

95

```fortran
      NS=N*(N+1)/2
      NI=NS+N**2+1
      NV=2*NS+N**2
   99 FORMAT(8F10.5)
C
      DO 1 I=1,N
    1 READ(5,99) (F(I,J),J=1,N)
      CALL USWFM('F',1,F,7,N,N,1)
C
      DO 2 I=1,N
    2 READ(5,99) (FS(I,J),J=1,N)
      CALL USWFM('FS',2,FS,7,N,N,1)
      READ(5,99) (GQGT(I),I=1,N)
      CALL USWFV('GQGT',4,GQGT,N,1,1)
C
      DO 3 I=1,N
    3 READ(5,99) (AK(I,J),J=1,2)
      CALL USWFM('K',1,AK,7,N,2,1)
C
      DO 4 I=1,2
    4 READ(5,99) (H(I,J),J=1,N)
      CALL USWFM('H',1,H,2,2,N,1)
C
      DO 5 I=1,2
    5 READ(5,99) (R(I,J),J=1,2)
      CALL USWFM('R',1,R,2,2,2,1)
C
      DO 6 I=1,105
    6 VAR(I)=0.
      DO 7 I=1,N
      DO 7 J=1,N
C
    7 DF(I,J)=FS(I,J)-F(I,J)
      CALL USWFM('DEL F',5,DF,7,N,N,1)
      CALL VMULFF(AK,R,N,2,2,7,2,TMP1,7,IER)
      CALL VMULFP(TMP1,AK,N,2,N,7,7,AKRKT,7,IER)
      CALL USWFM('KRKT',4,AKRKT,7,N,N,1)
C
C     CALCULATE THE DIFFERENCE BETWEEN THE DYNAMICS
C     IMPLEMENTED IN THE FILTER AND THE PLANT, DF=F*-F
C
      DO 20 I=1,N
      DO 20 J=1,N
      DFT(I,J)=DF(I,J)
   20 FT(I,J)=F(I,J)
      CALL VTRANX(DFT,N,N,7)
      CALL USWFM('DEL FT',6,DFT,7,N,N,1)
      CALL VTRANX(FT,N,N,7)
      CALL USWFM('FT',2,FT,7,N,N,1)
      CALL VMULFF(AK,H,N,2,N,7,2,TMP1,7,IER)
C
      DO 21 I=1,7
      DO 21 J=1,7
      FSMKH(I,J)=FS(I,J)-TMP1(I,J)
   21 FSMKHT(I,J)=FSMKH(I,J)
      CALL USWFM('FS-KH',5,FSMKH,7,N,N,1)
      CALL VTRANX(FSMKHT,N,N,7)
      CALL USWFM('(FS-KH)T',8,FSMKHT,7,N,N,1)
      T=0.
      TOL=1.D-5
      IND=1
      L=0
      IF(N.EQ.7) GO TO 11
C
      DO 31 I=1,NS
      L=L+1
   31 VAR(L)=U(I)
```

96

```
C
      DO 32 I=1,N
      DO 32 J=1,N
      L=L+1
   32 VAR(L)=V(I,J)
C
      DO 33 I=1,N
      L=L+1
   33 VAR(L)=P(I)
   11 DO 10 K=1,NP
C     TEND=FINAL TIME
C
      TEND=K*DT
C
C     DVERK SUBROUTINE FINDS THE SOLUTION OF THE SYSTEM OF
C     DIFFERENTIAL EQUATIONS
C
      CALL DVERK(NV,FUN,T,VAR,TEND,TOL,IND,C,105,WK,IER)
      IF(IND.LE.0.OR.IER.NE.0)STOP
      CALL VCVTSF(VAR(N1),N,PFULL,7)
C
C     CALCULATE AND PRINT THE RMS ESTIMATE ERRORS
C
      DO 30 I=1,N
   30 PSQR(I)=DSQRT(PFULL(I,I))
      WRITE(6,90)T,(PSQR(I),I=1,N)
   90 FORMAT('0T=',F10.5,' PSR=',7G15.7)
C
C     IF DESIRED PRINT THE  COVARIANCE MATRICES,P,U AND V
C     CALL USWSM('U',1,U,N,2)
C     CALL USWFM('V',1,VAR(NS+1),7,N,N,2)
C     CALL USWSM('P',1,VAR(N1),N,2)
   10 CONTINUE
      STOP
      END
```

```
      SUBROUTINE VTRANX(A,N,NC,IA)
      IMPLICIT REAL*8 (A-H,O-Z)
      DIMENSION A(IA,IA),B(7,7)
C
      DO 1 I=1,N
      DO 1 J=1,N
  1   B(I,J)=A(J,I)
C
      DO 2 I=1,N
      DO 2 J=1,N
  2   A(I,J)=B(I,J)
      RETURN
      END
```

```
      SUBROUTINE FUN(NV,T,VAR,DRV)
C
C
C     FCN SUBROUTINE IS USED FOR EVALUATING FUNCTIONS(INPUT)
C
      IMPLICIT REAL*8 (A-H,O-Z)
      COMMON F(7,7),FS(7,7),GQGT(7),AK(7,2),R(2,2),
     *AKRKT(7,7),DF(7,7),FT(7,7),FSMKHT(7,7),DFT(7,7),
     *FSMKH(7,7),H(2,7)
      COMMON/KTR/N,NS,NPD
      DIMENSION U(28),V(7,7),P(28),UD(28),VD(7,7),
     *VAR(105),DRV(105),C(24),WK(105,9),PD(28)
      DIMENSION TMP1(7,7),TMP2(7,7),TMP3(7,7)
C
      L=0
      DO 1 I=1,NS
      L=L+1
    1 U(I)=VAR(L)
C
      DO 2 I=1,N
      DO 2 J=1,N
      L=L+1
    2 V(I,J)=VAR(L)
C
      DO 3 I=1,NS
      L=L+1
    3 P(I)=VAR(L)
      IF(T.EQ.0)KT=NPD
      KT=KT+1
      IF (KT.GE.5) GO TO 15
      WRITE(6,99) T
   99 FORMAT('OT=',D25.15)
      CALL USWSM('U',1,U,N,2)
      CALL USWFM('V',1,V,7,N,N,2)
      CALL USWSM('P',1,V,N,2)
   15 CALL VMULFS(F,U,N,N,7,TMP1,7)
      IF(KT.LT.5) CALL USWFM('FU',2,TMP1,7,N,N,2)
      CALL VMULSF(U,N,FT,N,7,TMP2,7)
      IF(KT.LT.5) CALL USWFM('UFT',3,TMP2,7,N,N,2)
C
      DO 5 I=1,N
      DO 4 J=1,N
    4 TMP1(I,J)=TMP1(I,J)+TMP2(I,J)
    5 TMP1(I,I)=TMP1(I,I)+GQGT(I)
      CALL VCVTFS(TMP1,N,7,UD)
      IF(KT.LT.5) CALL USWSM('UDOT',4,UD,N,2)
      CALL VMULFF(F,V,N,N,N,7,7,TMP1,7,IER)
      IF(KT.LT.5) CALL USWFM('FV',2,TMP1,7,N,N,2)
      CALL VMULFF(V,FSMKHT,N,N,N,7,7,TMP2,7,IER)
      IF(KT.LT.5) CALL USWFM('V*(FS-KH)T',10,TMP2,7,N,N,2)
      CALL VMULSF(U,N,DFT,N,7,TMP3,7)
      IF(KT.LT.5) CALL USWFM('U*DFT',5,TMP3,7,N,N,2)
C
      DO 7 I=1,N
      DO 6 J=1,N
    6 VD(I,J)=TMP1(I,J)+TMP2(I,J)+TMP3(I,J)
    7 VD(I,I)=VD(I,I)-GQGT(I)
      IF(KT.LT.5) CALL USWFM('VDOT',4,VD,7,N,N,2)
      CALL VMULFS(FSMKH,P,N,N,7,TMP1,7)
      IF(KT.LT.5) CALL USWFM('(FS-KH)P',8,TMP1,7,N,N,2)
      CALL VMULSF(P,N,FSMKHT,N,7,TMP2,7)
      IF(KT.LT.5) CALL USWFM('P(FS-KH)T',9,TMP2,7,N,N,2)
      CALL VMULFF(DF,V,N,N,N,7,7,TMP3,7,IER)
      IF(KT.LT.5) CALL USWFM('DF*V',4,TMP3,7,N,N,2)
C
      DO 8 I=1,N
```

```
      DO 8 J=1,N
  8   TMP1(I,J)=TMP1(I,J)+TMP2(I,J)+TMP3(I,J)
      CALL VMULFM(V,DF,N,N,N,7,7,TMP3,7,IER)
      IF(KT.LT.5) CALL USWFM('VT*DF',5,TMP3,7,N,N,2)
C
      DO 10 I=1,N
      DO 9 J=1,N
  9   TMP3(I,J)=TMP1(I,J)+TMP3(I,J)+AKRKT(I,J)
 10   TMP3(I,I)=TMP3(I,I)+GQGT(I)
      IF(KT.LT.5) CALL USWFM('PDOT',4,TMP3,7,N,N,2)
      CALL VCVTFS(TMP3,N,7,PD)
      IF(KT.LT.5) CALL USWFV('PDOT(SYM)',9,PD,N,1,2)
      L=0
C
      DO 11 I=1,NS
      L=L+1
 11   DRV(L)=UD(I)
C
      DO 12 I=1,N
      DO 12 J=1,N
      L=L+1
 12   DRV(L)=VD(I,J)
C
      DO 13 I=1,NS
      L=L+1
 13   DRV(L)=PD(I)
      IF(KT.LT.5) CALL USWFV('DRV',3,DRV,NV,1,2)
      RETURN
      END
```

LIST OF REFERENCES

1. Gelb, A. and others, <u>Applied Optimal Estimation</u>, M.I.T. Press, 1974.

2. Maybeck, P. S., <u>Stochastic Models, Estimation and Control</u>, Vol. 1, Academic Press, 1979.

3. Franklin, G. F. and Powell, J. D., <u>Digital Control of Dynamic Systems</u>, Addison-Wesley, 1980.

4. Bryson, A. E., Jr., <u>Kalman Filter Divergence and Aircraft Motion Estimators</u>, Vol. I, No. I, AIAA Journal, January 1978.

5. Anderson, B. D. O., and Moore, J. B., <u>Linear System Optimization with Prescribed Degree of Stability</u>, Proc. IEE, Vol. 116, No. 12, December 1969.

6. Garnell, P. and East, D. J., <u>Guided Weapon Control Systems</u>, 1st ed., Pergamon Press, 1977.

7. Collins, D. J., <u>Missiles, Navigation and Avionic Systems</u>, Class Notes, Naval Postgraduate School, April 1980.

8. McRuer, D., and others, <u>Aircraft Dynamics and Automatic Control</u>, Princeton University Press, 1973.

9. Holley, W. E., and Bryson, A. E., Jr., <u>Wind Modeling and Lateral Control for Automatic Landings</u>, Vol. 14, No. 2, AIAA Journal, February 1977.

10. Sandell, N. R., and Athans, M., <u>Modern Control Theory, Manual of Fortran Computer, Subroutines for Linear, Quadrotic, Gaussian Designs</u>, Massachusetts Institute of Technology.

11. Walker, R., <u>OPTSYS 4 at SCIP Computer Program</u>, Stanford University, Aero/Astro Dept., December 1979.

INITIAL DISTRIBUTION LIST

		No. Copies
1.	Defense Technical Information Center Cameron Station Alexandria, Virginia 22314	2
2.	Library, Code 0142 Naval Postgraduate School Monterey, California 93940	2
3.	Department Chairman, Code 62 Department of Electrical Engineering Naval Postgraduate School Monterey, California 93940	1
4.	Professor D. J. Collins, Code 67Co Department of Aeronautics Naval Postgraduate School Monterey, California 93940	3
5.	Professor A. Gerba, Jr., Code 626Z Department of Electrical Engineering Naval Postgraduate School Monterey, California 93940	1
6.	Sr. Almirante Comandante Armada Nacional Ministerio de Defensa C.A.N. Bogota, Colombia S.A.	1
7.	Sr. Vicealmirante Segundo Comandante Armada Nacional Ministerio de Defensa C.A.N. Bogota, Colombia S.A.	1
8.	Sr Vicealmirante G. Uribe Comando Armada Nacional Ministerio de Defensa S.A.	1
9.	Sr. Contralmirante Director Escuela Naval de Cadetes Cartagena, Colombia S.A.	2
10.	Sr. Teniente de Navio M. Soto G. Escuela Naval de Cadetes Cartagena, Colombia S.A.	1
11.	Sr. Teniente de Navio J. Matallana R. Escuela Naval de Cadetes Cartagena, Colombia S.A.	3